A Propagation Simulator for Land Mobile Satellite Communications

Seong-Youp Suh

Thesis submitted to the Faculty of the
Virginia Polytechnic Institute and State University
in partial fulfillment of the requirements for the degree of

Master of Science
in
Electrical Engineering

Warren L. Stutzman, Chair
Gary S. Brown
Timothy Pratt

April 24, 1998
Blacksburg, Virginia

Keywords: LMSS, Propagation Model, Rayleigh, Rician, Lognormal, Shadowing,
Cumulative Fade Statistics, Average Fade Duration, Level Crossing Rate

A Propagation Simulator for Land Mobile Satellite Communications

Seong-Youp Suh

(ABSTRACT)

The performance of a mobile satellite communications link can be determined by the propagation path between a satellite and mobile users. Some of the most important factors are multipath propagation and vegetative shadowing. System designers should have the most reliable information about the statistics of fade duration in order to determine fade margin or to compensate for the fades using modulation and coding scheme.

This report describes a simulator, PROSIM, developed at Virginia Tech for simulating a propagation model in land mobile satellite communications. The simulator is based on a random number generator that generates data sets to compute statistics of the propagation channel. Performance of the simulator was evaluated by comparing statistics from an analytical model and experimental data provided by W. Vogel of Univ. of Texas at Austin and J. Goldhirsh of the Applied Physics Laboratory. New expressions for phasor plot and its mathematical expression for lognormal channel were derived and were simulated. Finally, the advantages of the simulator using random number generator in simulating the propagation model are described.

Acknowledgements

I would like to thank all those who gave help for finishing my thesis research. I would especially like to thank my advisor, Dr. Warren Stutzman, for his continuous encouragement and his helpful suggestions. I would also like to thank the other members on my advisory committee, Drs. Brown and Pratt for their sincere advice.

In addition, I would like to thank to Michael Barts for his help in sharing his idea and in correcting my thesis. And I also would like to thank to members of Satellite Communications Group for their concern about my thesis. I would like to thank Dr. W. J. Vogel and Dr. J. Goldhirsh for supporting their experimental data.

Finally, I wish to thank my family, specially my mother, Jeong-Jee Kweon and parents-in-law, Doo-Ok Kim and Jeong-Soon Yoon in Korea for their continuous encouragement and prayer. In particular, I want to thank Hyunhee, my lovely wife for her self-sacrificing support and her counseling with me when I was depressed. I would like to dedicate my thesis to God because He makes my thesis initiate and possible.

Table of Contents

List of Figures

List of Tables

Chapter 1. Introduction

A land mobile satellite system (LMSS) is a satellite-based communications system that provides voice and data communications to terrestrial mobile users. The first mobile satellite experiment named MSAT-X was initiated by the National Aeronautics and Space Administration (NASA) in 1984 and was managed by the Jet Propulsion Laboratory (JPL). MSAT-X propagation research was aimed at characterizing the land mobile satellite channel between a satellite and a mobile user. Since the feasibility of mobile satellite communication system was demonstrated at NASA, a lot of experimental mobile satellites have been launched in the world. In January 1985, the US Federal Communication Commission (FCC) proposed to allocate spectrum in both the UHF band (806 to 890 MHz) and L-band (1.53 to 1.6605 GHz) for a North American Mobile Satellite Service (MSS). In 1986, the proposed allocation spectrum was modified to only L-band [14].

Channel characteristics of communications systems determine the modulation and coding scheme in the communications system. The channel characteristics are also dependent on propagation effects through the channel. The propagation effects on LMSS are quite severe due to fading caused by roadside vegetation and structures. An experiment in phase 1 of the PROSAT mobile satellite program (initiated by the

European Space Agency) revealed that even in open sites, shadowing effects from vegetation and other structures produce fades of 15 dB. Hence, allowing a 15 dB fade margin in the system will only produce 80 percent circuit continuity [10].

The Virginia Tech Satellite Communications Group has been concerned with the problem of modeling and simulating the propagation effects of LMSS channels. Several versions of a VT simulator were developed and were used to predict propagation effects. However, the VT simulator has some problems to be resolved. 1) The possible operating frequency band of the VT simulator is restricted to UHF and L band. 2) The simulation results are not identical when different universal data sets were used. 3) The secondary statistics from the VT simulator are not matched with measurement data; that is, it does not provide proper simulated data sets to satisfy the dynamics of the propagation channel [2],[21],[22].

These problems in the VT simulator were resolved by author's efforts through the development of a new propagation simulator, called PROSIM, using a random number generator. PROSIM uses random number to generate the simulated output data set, rather than measured data used in the VT simulator. PROSIM is based on the fundamentals of random phasor sum theory and its performance was evaluated with an analytical model and measured data. In evaluating the performance, we examined several statistics such as Cumulative Fade Distribution (CFD), Average Fade Duration (AFD), Level Crossing Rate (LCR), and phase Probability Density Function (PDF).

Chapter 2 describes background for designing and evaluating PROSIM. Chapter 3 reviews the VT simulator and propagation experiment data used in this study. Chapter 4 introduces details of a new simulator, PROSIM, and shows several simulation results compared with analytical models and experimental data. Finally, the conclusions and recommendation for future work are discussed in Chapter 5.

Chapter 2. Physics and Statistics of Mobile Satellite Propagation

2.1 Introduction

This chapter describes the physics occurring along the path between a satellite and land mobile vehicles. Land mobile systems experience multi-path fading and shadowing (signal blockage) by terrain obstacles. This is quite different from the fixed service satellite system in that a fixed system is free from multi-path and shadowing. We can classify the received signal at the land mobile vehicle into two types of signal, the unshadowed signal and the shadowed signal. The unshadowed signal consists of the direct component, the specular component, and the diffuse component. The shadowed signal consists of the shadowed direct component and the diffuse component. The details of these components will be introduced and used to model propagation effects including the statistics of these components [2].

2.2 Physics of Mobile Satellite Propagation [2],[21],[22],[24]

2.2.1 Unshadowed Propagation

Unshadowed propagation occurs when the path between a stationary source and a mobile vehicle has a clear line-of-sight (LOS). There are three components in the propagation: the direct component, the specular component, and the diffuse component. These three components are illustrated in Figure 2.2-1.

2.2.1.1 The Direct Component

The unshadowed direct signal is the one along the clear LOS. However, it is affected by atmospheric effects such as an ionospheric effect and a tropospheric effect. These effects include Faraday rotation, scintillation, and absorption by atmospheric gases, etc. All of them are caused by interaction with the earth's magnetic field and the ambient electron content in ionosphere.

Faraday rotation is rotation of the orientation of the polarization angle of a polarized electric field. The Faraday rotation angle is inversely proportional to frequency squared, and it is significant at UHF and L-band, which are widely used in land mobile satellite communication. Faraday rotation can be minimized by employing circular polarization, and in fact, some satellite communication systems use circular polarization to avoid the problem [23]. Hence the effects of Faraday rotation are ignored in this study.

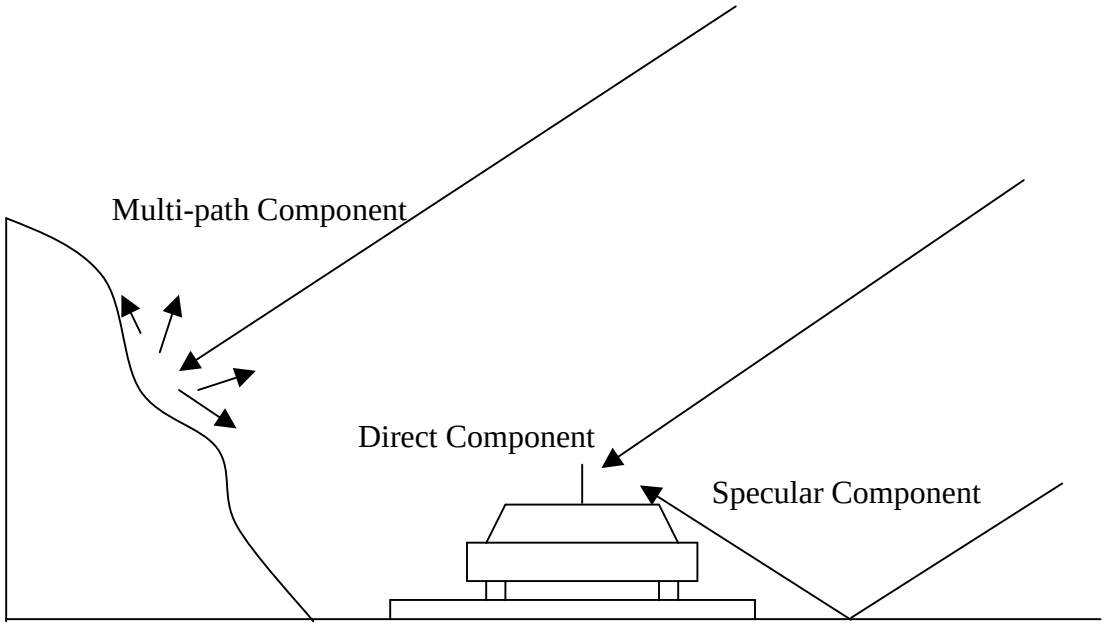

Figure 2.2-1 Illustration of signal components for unshadowed propagation

Ionospheric scintillation results from variations of the electron density as a wave passes through the ionosphere. The effect is not significant in our region of interest. Scintillation is severe at low latitudes (about 9 degrees North to 21 degrees South) and a auroral latitudes (above 59 degrees North for North America) [24]. Hence the scintillation effects are also ignored in our analysis.

Absorption by atmospheric gases is severe with extremely low elevation angles and high frequencies. The elevation angle is relatively large for most North American mobile satellite users, and the operating frequency band is relatively low for satellite communications. The amount of atmospheric absorption expected is very small in land mobile satellite systems [13]. Hence the absorption by atmospheric gases is ignored in our analysis.

2.2.1.2 The Specular Component

The specular component is a phase coherent ground reflected wave from points on the first Fresnel zone of the mobile vehicle. It may cause deep fades of the received signal if its amplitude is comparable to that of the direct component, and its phase is opposite. Beckmann [4] and Jamnejad [13] analyzed each the Fresnel zone ellipses and specular reflections of a circularly polarized wave. Polarization status of the ground reflected wave for an incident circularly polarized wave is illustrated in Figure 2.2-2 for several incident angles. Except for grazing angle 0° and 90°, the reflected wave is elliptically polarized. For grazing angles less than the Brewster angle, the reflected wave is of the same sense as the incident pure circularly polarized wave, but for grazing angles greater than the Brewster angle, the wave is of opposite sense. The Brewster angle is considered to be between 6°and 27°, but the elevation angle for most land mobile satellite system will be between 20° and 60°. Hence, the specular component will be of opposite sense to the incident wave in most cases.

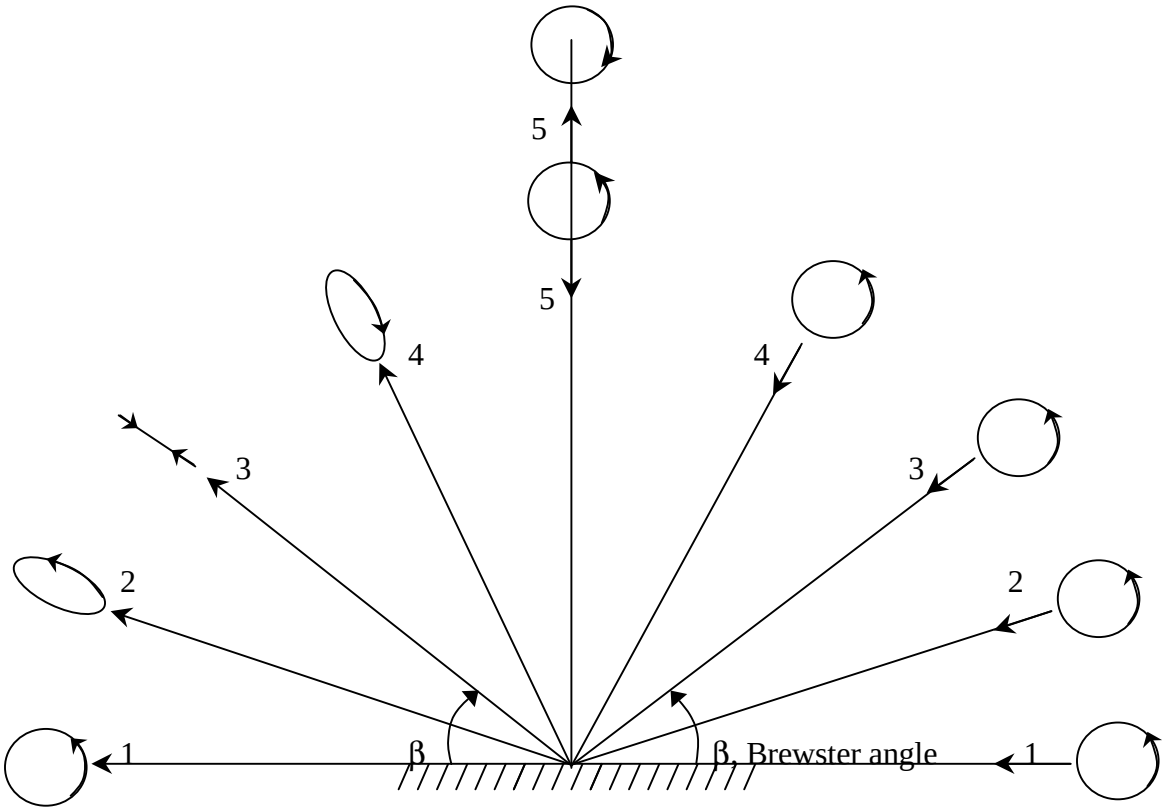

Figure 2.2-2 Polarization of a reflected wave from the ground for an incident circularly polarized wave for several incident angle [13].

2.2.1.3 The Diffuse Component

The diffuse component is a phase incoherent multi-path wave due to reflections and scattering from outside the first Fresnel zone of the vehicle [4]. The diffuse component has little directivity. Campbell verified it in his experiments [7]. The diffuse component is the phasor sum of a number of individual scattered signals from the terrain surrounding the mobile vehicle. The magnitude of the component is assumed to be Rayleigh distributed while its phase is uniformly distributed. The statistics of the diffuse component are explained in Section 2.3.1. Interference with the direct component causes rapid fading of the received signal [4].

2.2.1.4 The Total Unshadowed Signal

The total received signal for unshadowed propagation is the phasor sum of the three components discussed above.

$$R_{total\ unshadowed} = R_{direct} + R_{specular} + R_{diffuse} \tag{2.2-1}$$

The sum of the received signals is based on the implicit assumption of incoherence of the components. For the reason, the specular component is considered negligible. Thus the total unshadowed signal is simplified to

$$R_{total\ unshadowed} @ R_{direct} + R_{diffuse} \tag{2.2-2}$$

The direct component is essentially a constant for the analysis of propagation effects. The total unshadowed signal has a Rician distribution, which is a phasor sum of constant and Rayleigh phasor. The statistics of the total unshadowed signal is explained in Section 2.3.2.

2.2.2 Vegetatively Shadowed Propagation

Vegetatively shadowed propagation is defined along a path between a stationary source and a mobile vehicle with a blocked line-of-sight (LOS). There are mainly two components: the shadowed direct component, and the diffuse component. These two components are illustrated in Figure 2.2-3.

2.2.2.1 The Shadowed Direct Component

When the mobile vehicle drives along roadside trees, the direct component from satellite passes through the roadside vegetation where it is attenuated and scattered by the leaves, branches, and limbs. The amount of attenuation and scattering depends on the path length through the vegetation. The attenuation causes a degradation of the power of the direct component, and the scattering causes deep fades and degrades its phase coherency by interfering with the direct component. The shadowed direct component can be expressed by a phasor sum of two components discussed above.

$$R_{shadowed\_direct} = A \cdot R_{direct} + R_{scattered} \tag{2.2-3}$$

where A is the attenuation factor of the direct component by the vegetation and $R_{scattered}$ is the forward scattered signal from the vegetation. The shadowed direct component can be modeled by a lognormally distributed signal, the statistics of which are explained in Section 2.3.3.

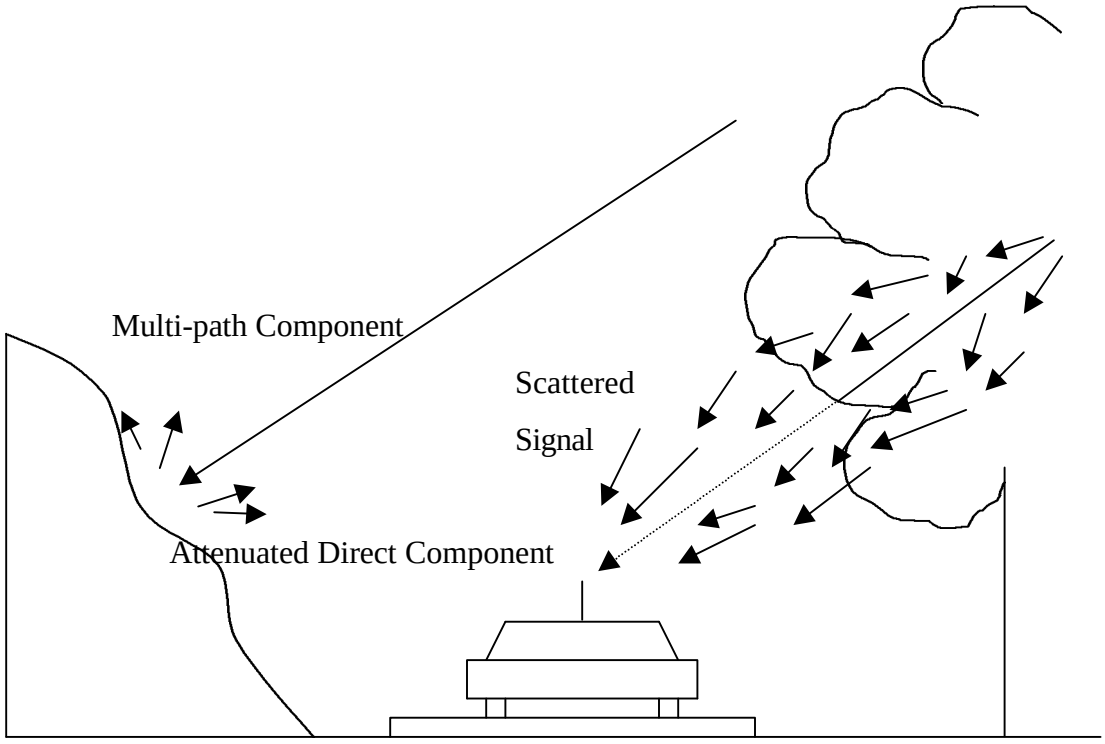

Figure 2.2-3 Illustration of signal components for vegetatively shadowed propagation

2.2.2.2 The Diffuse Component

The diffuse component is an incoherent ground scattered signal like one for unshadowed propagation and is also assumed to have Rayleigh distribution in magnitude and uniform distribution in phase. The carrier-to-multipath ratio, $\overline{K}$, for vegetatively shadowed propagation tends to be lower than one, K, for unshadowed propagation. The reason is that the vegetatively scattered signal is added in multi-path power for shadowed propagation. The vegetatively forward scattered signal is assumed to be received from approximately the same angular direction as one of the direct component in our analysis, while the diffuse component is assumed to be received from all angular directions. Hence, the vegetatively forward scattered signal is included in the shadowed direct component in our analysis.

2.2.2.3 The Total Shadowed Signal

The total received signal for vegetatively shadowed propagation is the phasor sum of the shadowed direct component and the diffuse component.

$$R_{total\ shadowed} = R_{shadowed\ direct} + R_{diffuse} \tag{2.2-4}$$

The total shadowed signal can be modeled by a Vegetatively Shadowed (VS) distribution, which is the sum of a lognormally distributed signal and a Rayleigh distributed signal, the statistics of which are explained in Section 2.3.4.

2.3 Statistical Representations for Mobile Satellite Propagation

Some statistical representations are employed in modeling mobile satellite propagation and in evaluating the propagation link. The physics of mobile satellite propagation can be modeled by four statistics distributions such as Rayleigh, Rician, lognormal , and VS distribution. When we evaluate the propagation link in our analysis, we use the primary statistics, called Probability Density Function (PDF), Cumulative Fade Distribution (CFD) and the secondary statistics, called Average Fade Duration (AFD) and Level Crossing Rate (LCR). An analytical model is used to derive these parameters. This section describes these statistical representations for mobile satellite propagation.

2.3.1 Primary Statistics

2.3.1.1 The Rayleigh Distribution

The Rayleigh Distribution is a model used to describe the diffuse component. The diffuse component can be expressed as a phasor sum of a number of scattering point sources.

$$R_{diffuse} = r \cdot e^{jq} = \sum_{j=1}^{n} A_j \cdot e^{j f_j} \qquad (2.3\text{-}1)$$

where r is the amplitude of the diffuse component, θ is the phase of the diffuse component, ϕ_j is the phase of the j^{th} diffuse component with respect to the direct component, A_j is the random amplitude of j^{th} scattered wave with respect to the direct component. If the scattered signals are sufficiently random and the phases are uniformly

distributed over 2π, Beckmann shows that the diffuse component can be modeled by the Rayleigh density function defined by [3].

$$\begin{aligned} p(r) &= \frac{2r}{a} e^{-r^2/a} , \qquad r \geq 0 \\ p(r) &= 0 , \qquad r < 0 \end{aligned} \tag{2.3-2}$$

where α is the mean square value of r. Beckmann also shows that the mean square value of r is [3]

$$\left\langle r^2 \right\rangle = 2s^2 = a \tag{2.3-3}$$

where σ^2 is a variance of the real (X) and the imaginary (Y) component of R (=X+jY).

In our analysis we will specify the Rayleigh density function by the parameter $\overline{K}$, in dB, which is given by

$$\overline{K} = 10 \log \frac{1}{a} \qquad \text{[dB]} \tag{2.3-4}$$

$\overline{K}$ is physically interpreted to be the ratio of carrier-to-multipath power with unity carrier power assumed. If we express the Rayleigh density function in terms of $\overline{K}$, equation (2.3-2) becomes

$$\begin{aligned} p(r) &= \frac{2r}{10^{-\overline{K}/10}} \exp\left[-\frac{r^2}{10^{-\overline{K}/10}} \right] , \qquad r \geq 0 \\ p(r) &= 0 , \qquad r < 0 \end{aligned} \tag{2.3-5}$$

The complement of the Rayleigh distribution function is given by [3]

$$P_{Rayleigh}(R) = \int_{R}^{\infty} p_{Rayleigh}(r)dr = e^{-R^2/a} = \exp\left[-\frac{R^2}{10^{-\bar{K}/10}}\right] \tag{2.3-6}$$

which is the probability that the Rayleigh distributed signal amplitude is greater than R.

2.3.1.2 The Rician Distribution

The Rician Distribution is a model used to describe the unshadowed component. It can be expressed as a phasor sum of a constant and a number of scattering point sources.

$$R_{unshadowed} = r \cdot e^{jq} = C + \sum_{j=1}^{n} A_j \cdot e^{jf_j} \tag{2.3-7}$$

where C is a constant coherent signal with clear LOS and the rest of the symbols are as defined for the Rayleigh distribution. Beckmann shows that the unshadowed component can be modeled by a Rician probability density function defined by [3]

$$p(r) = \frac{2r}{b}\exp\left[-\frac{\left(r^2 + C^2\right)}{b}\right]\mathrm{I}_0\left(\frac{2rC}{b}\right), \quad r \geq 0$$

$$p(r) = 0\ , \qquad r < 0 \tag{2.3-8}$$

where β is the mean square value of the Rayleigh distributed component of r and I_0 is the modified Bessel function of order zero. The phase distribution is no longer uniform like a

Rayleigh distribution. The phase distribution of Rician distribution is derived by Beckmann [3].

$$p(q) = \frac{1}{2p} e^{-C^2/a} \left[1 + G\sqrt{p}\, e^{G^2} (1 + erf(G))\right] \tag{2.3-9}$$

where $G = \frac{C \cos q}{\sqrt{a}}$, $0 \le q \le 2p$ (2.3-10)

and

$$erf(G) = \frac{2}{\sqrt{p}} \int_0^G e^{-y^2} dy \tag{2.3-11}$$

The Rician distribution can be completely specified by the parameter K in dB which is given by

$$K = 10 \log\left(\frac{C^2}{b}\right) \quad \text{[dB]} \tag{2.3-12}$$

K is physically interpreted to be the ratio of carrier-to-multipath power. We assumed C is unity power in our analysis. Hence we can rewrite (2.3-8) expressed in K as

$$p(r) = 2r10^{-K/10} \exp\left[-10^{-K/10}\left(r^2 + 1\right)\right] \mathrm{I}_0\left(2r10^{-K/10}\right) \tag{2.3-13}$$

The complement of Rician distribution function, which models unshadowed propagation, is given by [3]

$$G\left(R \mid \overline{VS}\right) = \int_R^\infty p_{unshadowed}(r) dr \tag{2.3-14}$$

where $\overline{VS}$ indicates no vegetative shadowing. $G\left(R \mid \overline{VS}\right)$ is the probability that the signal amplitude is greater than R.

2.3.1.3 The Lognormal Distribution

The lognormal distribution is a part of a model used to describe vegetatively shadowed propagation. The lognormal distribution arises from a theory of random variables in which the variables are combined by a multiplicative process just as a normal distribution arises from a theory of random variables in which the variables are combined by an additive process [1],[3],[15].

$$R_{\log normal} = r \cdot e^{jq} = \prod_{j=1}^{n} B_j \cdot \exp\left[j \sum_{j=1}^{n} \Phi_j \right] \tag{2.3-15}$$

where the B_j are a sequence of independent positive random variables and the phase Φ_j is uniformly distributed between 0 and 2π.

The lognormal probability density fuction is given by [3]

$$p(r) = \frac{1}{\sqrt{2p}\, sr} \exp\left[-\frac{(\ln r - m)^2}{2 s^2} \right], \qquad r > 0$$

$$p(r) = 0, \qquad r \le 0 \tag{2.3-16}$$

where r is the signal amplitude, μ is the mean of $\ln r$, and σ is the standard deviation of $\ln r$. The lognormal density function is completely specified by μ_{dB} and σ_{dB} in dB which are given by

$$\log r = (\log e) \ln r \tag{2.3-17}$$

$$m_{dB} = (20 \log e) m \tag{2.3-18}$$

$$s_{dB} = (20 \log e) s \tag{2.3-19}$$

Hence we can rewrite (2.3-17) expressed in $\log r$, m_{dB}, and s_{dB}.

$$p(r) = \frac{20\log e}{\sqrt{2p}\, s_{dB} r} \exp\left[- \frac{(20\log r - m_{dB})^2}{2 s^2_{dB}} \right], \qquad r > 0 \qquad (2.3\text{-}20)$$

The complement of the lognormal distribution function, which models the shadowed direct component, is given by [3]

$$G(R) = \int_R^\infty p_{\log normal}(r) dr \qquad (2.3\text{-}21)$$

which is the probability that the lognormal signal amplitude is greater than R.

2.3.1.4 The VS Distribution

The VS distribution is a model to describe shadowed propagation, which is a phasor sum of a lognormally distributed direct component and a Rayleigh distributed diffuse component. The expression for the VS density function was derived by Loo and is given by [15]

$$p(r) = \frac{2r}{\sqrt{2p}\, a\, s} \int_0^\infty \frac{1}{z} \mathrm{I}_0\left(\frac{2rz}{a} \right) \exp\left[- \frac{(\ln z - m)^2}{2 s^2} - \frac{(r^2 + z^2)}{a} \right] dz \qquad (2.3\text{-}22)$$

The symbols used in (2.3-21) are same as defined for the previous sections. The VS distribution function is given by

$$G(R \mid VS) = \int_{R}^{\infty} p_{VS}(r) dr \tag{2.3-23}$$

where VS indicates vegetative shadowing and $G(R \mid VS)$ is the probability that the signal amplitude is greater than R. The evaluation of (2.3-22) can be achieved only by numerical calculation.

2.3.1.5 The Total Distribution

We considered the propagation path consist of two separate parts, as an unshadowed part and a shadowed portion; these were discussed in Section 2.3.2 and Section 2.3.4. A typical path for a mobile vehicle will include both unshadowed and shadowed propagation conditions, but the fractional mix varies. The total distribution is the mixed distribution, which is the sum of the shadowed and unshadowed distribution weighted by the fraction of shadowing path and unshadowing path respectively:

$$G(R) = G(R \mid VS) \cdot S + G\left(R \mid \overline{VS}\right) \cdot (1 - S) \tag{2.3-24}$$

which is the probability for a total signal that the signal amplitude is greater than R. This approach was developed by Smith and Stutzman [22] but was also apparently developed by Lutz, et al. independently, as well [16]. The total distribution (2.3-23) can be rewriten as a function of fade F instead of signal R to work with fade exceedance distributions rather than signal exceedance distribution.

$$CFD(R) = 1 - G(R) \tag{2.3-25}$$

$$F = -R \tag{2.3-26}$$

$$CFD(F) = 1 - G(F) \tag{2.3-27}$$

Referencing all signals to the clear LOS power level, positive signal levels correspond to negative fade levels. Likewise, negative signal levels correspond to positive fade levels. The fade exceedance distribution, $CFD(F)$ is the probability that the fade is greater than F dB while $G(F)$ is the probability that the fade will be less than F dB. The fade exceedance distribution, $CFD(F)$ will be used as a primary statistic in evaluating the satellite propagation link. Figure 2.3-1 illustrates the concept of the CFD. The plot shows the probability P% that the fade F dB will be greater than a given level.

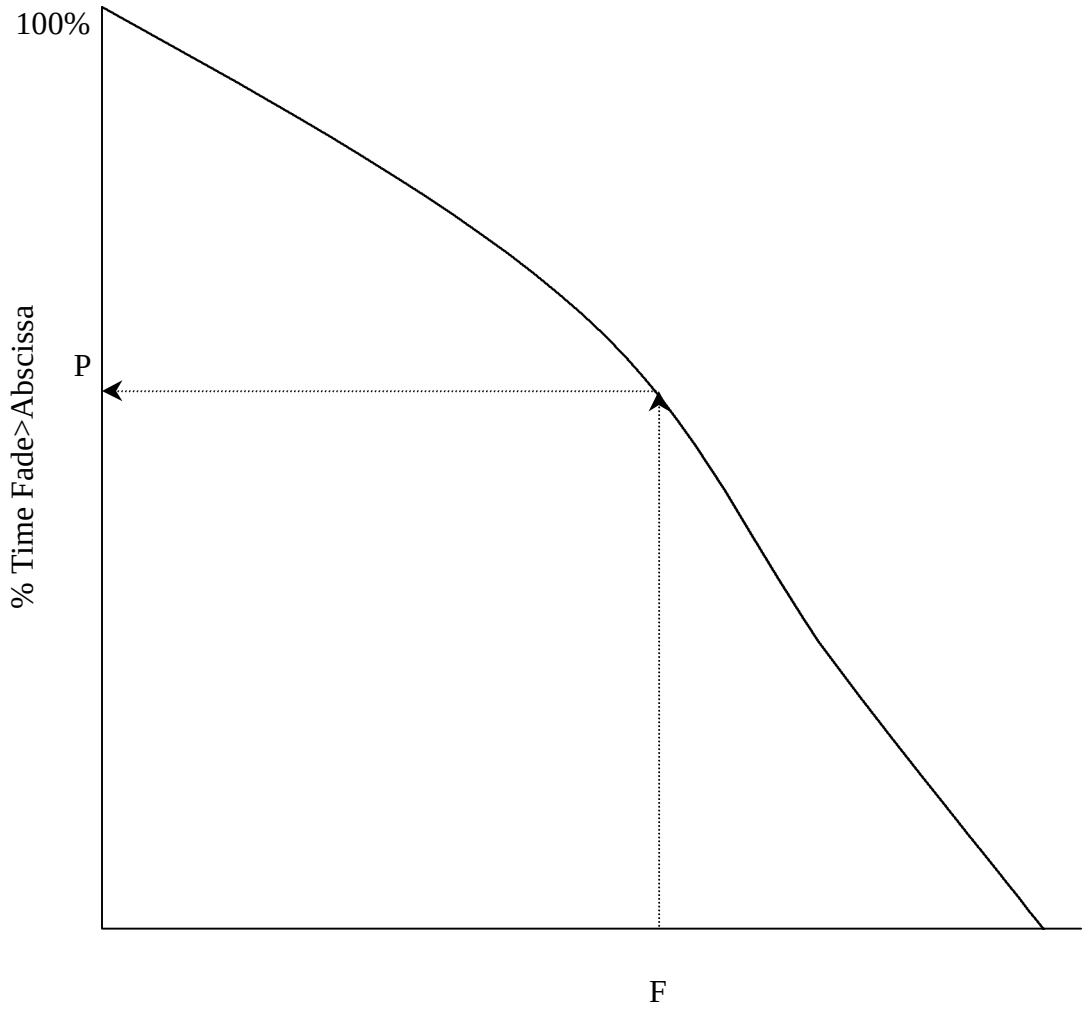

Figure 2.3-1 Fade distribution plot to illustrate the concept of CFD. A fade of level F dB is equalled or exceeded P % of the time

2.3.2 Secondary Statistics

The secondary statistics, Level Crossing Rate (LCR) and Average Fade Duration (AFD), are used to represent dynamic, time-varying characteristics of the propagation channel for the mobile. We will also consider AFD and LCR to evaluate the propagation link in the same manner as for the primary statistics in our analysis. They depend on presence of shadowing, speed of the mobile vehicle, relative direction of the source, and the antenna pattern [5]. We will describe the concept and its importance in the following section.

2.3.2.1 Level Crossing Rate (LCR)

The level crossing rate is the expected rate at which the envelope crosses a specified signal level R with positive slope in a given time period as illustrated in Figure 2.3-2. The analytical expression for the LCR is given by [15]

$$LCR(R) = \int_0^\infty \dot{r} p(R, \dot{r}) d\dot{r} \qquad \text{[crossings per second]} \qquad (2.3\text{-}28)$$

where r is the received signal level, $\dot{r}$ is the time rate of change of the envelope, and $p(R, \dot{r})$ is the joint probability density function of $\dot{r}$ and r at $r = R$. Figure 2.3-2 illustrates the concept of LCR. There are three positive crossings (at points 1, 2, 3) in T seconds. Hence the LCR for the signal level R in the illustration is

$$LCR(R) = \frac{3}{T} \qquad \text{[crossings per second]} \qquad (2.3\text{-}29)$$

The LCR can be normalized by maximum Doppler-shift frequency to eliminate the dependence on vehicle speed. The normalized LCR is given by [15]

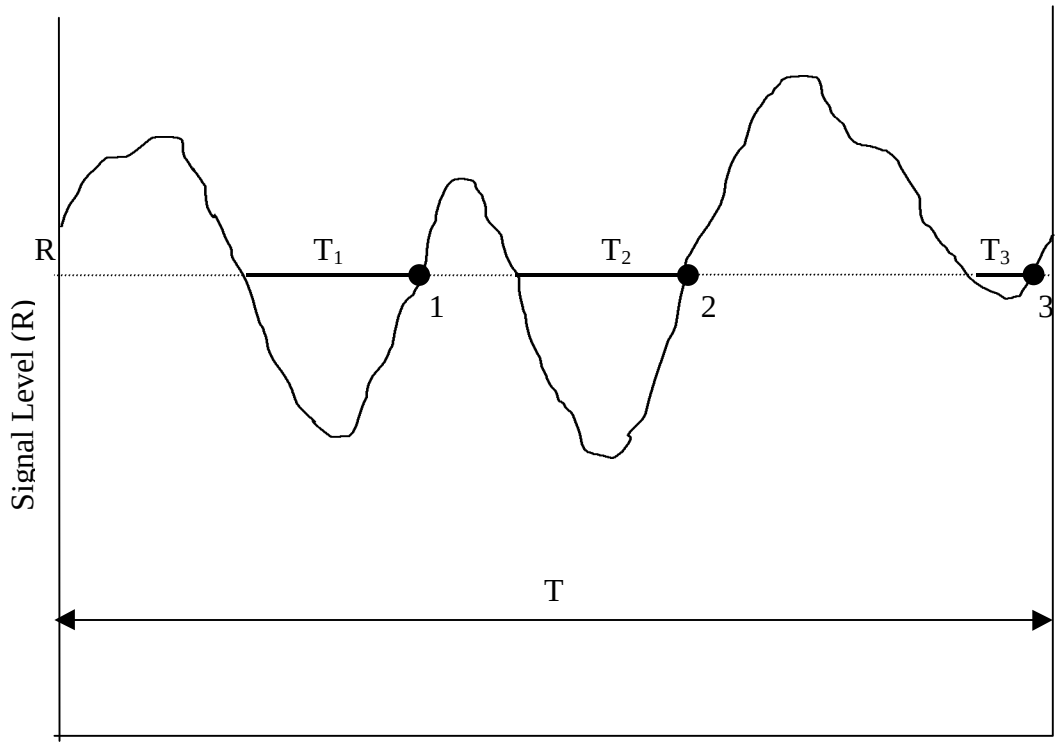

Figure 2.3-2 Signal level plot to illustrate level crossing rate and average fade duration.
LCR=3/T, AFD=$(T_1+T_2+T_3)/3$ in this example

$$LCR'(R) = \frac{LCR(R)}{f_m} \qquad \text{[crossings per wavelength]} \qquad (2.3\text{-}30)$$

where maximum Doppler-shift frequency, f_m is defined by

$$f_m = \frac{V}{l} \qquad \text{[Hz]} \qquad (2.3\text{-}31)$$

where V is the vehicle velocity and l is the wavelength.

2.3.2.2 Average Fade Duration (AFD)

The average fade duration is the average length of a fade for a given threshold. The analytical expression for the AFD is given by [12]

$$AFD(R) = \frac{CFD(R)}{LCR(R)} = \frac{1}{LCR(R)} \int_0^R p(r)dr \qquad \text{[second]} \qquad (2.3\text{-}32)$$

where $CFD(R) = \int_0^R p(r)dr$ is the probability that the signal envelope is less than a signal level R as in (2.3-24) and $LCR(R)$ is the LCR from (2.3-28). As you find in (2.3-32), the product of AFD and LCR becomes CFD. The AFD can also be normalized to eliminate the vehicle speed dependence. The normalized AFD is given by [15]

$$AFD'(R) = AFD(R) \cdot f_m \qquad \text{[wavelength]} \qquad (2.3\text{-}33)$$

where f_m is as defined in (2.3-31).

Figure 2.3-2 illustrates the concept of the AFD. There are three fade duration (T_1, T_2, T_3) in T second. Hence the AFD for the signal level R in the illustration is

$$AFD(R) = \frac{\sum_{i=1}^{N} T_i}{N} = \frac{T_1 + T_2 + T_3}{3} \qquad \text{[second]} \qquad (2.3\text{-}34)$$

where N is the number of fade duration in T second.

2.4 Analytical Model

Several statistics were presented in Section 2.3. The expressions for PDF and CFD require integration and evaluation of non-analytic functions. They can be evaluated only by numerical computation. The author developed a numerical evaluation tool for PDF and CFD described in Section 2.3. A numerical evaluation of CFD was also developed by Smith and Stutzman [22]. It is a program called LMSSMOD.

LMSSMOD can output the CFD and the PDF corresponding to the input parameters used in the statistical models of Section 2.3. The inputs to the LMSSMOD are the fraction of shadowing, S, the Rician carrier-to-multipath power ratio, K, for unshadowed propagation, the Rayleigh carrier-to-multipath power ratio, $\overline{K}$, the lognormal mean, m_{dB}, and the lognormal standard deviation, s_{dB}, for shadowed propagation. The output of LMSSMOD, CFD, can be interpreted as the fraction of either time or distance traveled that the fade will be greater than a given fade level. There can be computing error if the integration interval is not sufficiently small (ideally close to zero) and the upper bound for integration is not sufficiently large (ideally infinity). Employing a proper value is highly recommended to minimize the error and to save computing time.

LMSSMOD was used to evaluate the reliability of the simulator. The outputs of LMSSMOD were compared with those from the simulator using the CFD and PDF of each density function, Rayleigh, Rician, lognormal, and shadowed density function. This allows us to rate the quality of the simulator. LMSSMOD was also used to fit the fade distribution of LMSS experiments. We can estimate the model parameters for experimental propagation conditions by adjusting the input parameters of LMSSMOD until the fade distributions are matched with the experimental distribution. The parameters, however, are not deterministic; several different sets of input parameters can produce similar statistics. Hence determinination of fraction of shadowing and threshold level of the shadowing and unshadowing is the most important to estimate the proper

values. Some comparisons between fade distributions predicted by LMSSMOD and ones measured from samples of the helicopter data from Vogel that were analyzed by the author are shown in Figure 4.7-1 through Figure 4.7-4 in chapter 4.

Chapter 3. Review of Propagation Experimental Efforts and VT Simulator

3.1 Introduction

Since Hess of Motorola conducted propagation measurements for the land mobile satellite communications in 1978, many propagation experiments have been performed by several researchers including Vogel, Goldhirsh, Campbell, and Butterworth, etc. We will use Goldhirsh and Vogel's measured data in our study. The data samples were collected in October 1985 and March 1986 in Central Maryland using a helicopter to provide a moving platform and a receiver in a moving van. The experimenter kindly supplied to Virginia Tech their measured data which was used to verify the author's simulator.

Several versions of the simulator were developed at Virginia Tech based on Goldhirsh and Vogel's experimental data. This chapter reviews the details of the 1985 and 1986 their experiments and the VT simulator.

3.2 Goldhirsh and Vogel's Helicopter Experiment

Vogel and Goldhirsh performed several propagation experiments. They employed several kinds of equipment such as a transmitter mounted under a balloon, on a tower, in a helicopter, and also a satellite. They used a van with a receiver and data acquisition instrumentation. The details are discussed in [6], [8], [11], and [19].

3.2.1 Description of the Helicopter Experiment [11]

Vogel and Goldhirsh conducted roadside tree attenuation experiments at 870 MHz in October 1985 and March 1986 in Central Maryland. They performed the experiments twice in the same area to compare the fade distribution in bare deciduous roadside trees (March 1986) and in full foliage roadside trees (October 1985). They attempted to determine the effect of elevation angle and the difference between driving along the left side and right side of a four lane highway with trees along side.

They employed a Bell Jet Ranger Helicopter (single engine with front and rear seat) carrying a transmitting source, instead of satellite for same of these experiments. A helical antenna was mounted on the helicopter side door as a transmitting source and pointed at a depression angle of 45° relative to the horizontal. The transmitter was operated at a frequency of 870 MHz. The helical antenna had a 60° beamwidth and transmitted a right hand circularly polarized signal. They used a van equipped with a receiver as the mobile vehicle and mounted a receiving antenna, which consisted of a drooping crossed dipole, on the roof of the van. The van was equipped with the receiver system and data acquisition instrumentation. Measurement data were sampled and stored at a rate of 1024 samples per second. A total of 88 records of high rate data made up a file. Each record contains a header with recording time and vehicle speed information. The amplitude and phase information was stored in the same file. The measurement was

performed along three stretches of roads in Central Maryland; namely Route 295 (north and south between Routes 175 and 450, a distance of 24 km), Route 108 (southwest and northeast between Routes 32 and 97, a distance of 15 km), and Route 32 (north and south between Routes 108 and 70, a distance of 15 km). We will use the experimental data measured along Route 108 in this analysis. Route 108 is a two-lane secondary road but is a well traveled one. There are some utility poles and trees along long stretches. Vogel and Goldhirsh measured Percentage of Optical Shadowing (POS) to assess the population of trees along the road. For Route 108, the POS was found to be approximately 55 percent for the southwest right side and the northeast right side.

3.2.2 Results of the Experiment [11]

The measurement data along Route 108 was stored in seven files. Each file contains 88 seconds of recorded data. Average vehicle speed was 55 miles per hour. The cumulative fade distribution for Route 108 southwest was generated by Goldhirsh and Vogel. The fade distribution is reproduced using concatenated measured data in Figure 3.2-1. We note that fade levels of 7 dB and 15 dB are exceeded 10% and 1% of the time. The percentage of shadowing extracted from the data is about 60%, which is similar to the POS, 55%, measured by Goldhirsh and Vogel. The rest of the extracted parameter values are also shown in Table 3.2-1.

Table. 3.2-1 Value of the Parameters for measurement data along Route 108 in Central Maryland

	S	K	$\overline{K}$	m_{dB}	s_{dB}
Value	60 %	12 dB	0.2 dB	-2 dB	1 dB

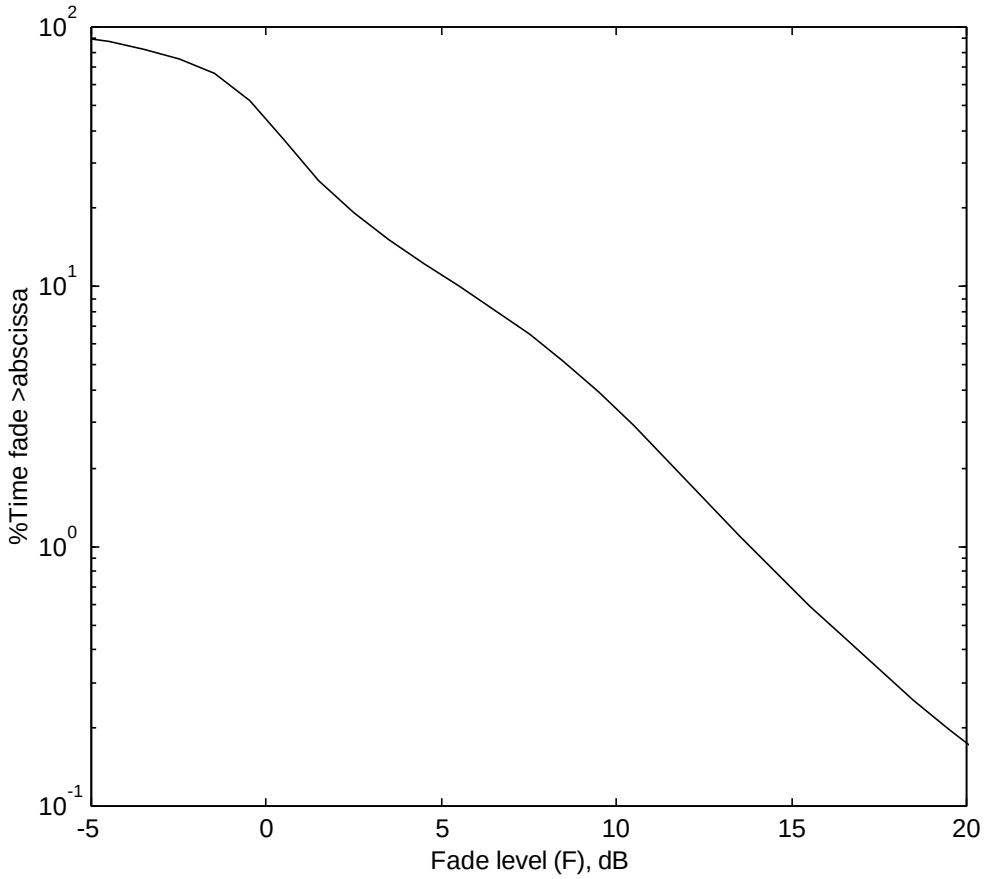

Figure 3.2-1 Cumulative Fade Distribution for measured data in Central Maryland, Route 108 (S=60%, K=12 dB, $\overline{K}$ =0.2 dB, m_{dB} =-2 dB, s_{dB} =1 dB)

Volgel and Goldhirsh demonstrated several important features in their study: 1) The dominant attenuation effects are caused by branches on the trees and not the leaves. 2) There could be a great fade reduction in traveling on the lane of the road corresponding to minimum shadowing. 3) Elevation angle to satellite is a very important factor to minimize fade due to shadowing. 4) Four-lane roads having roadside trees are much more likely to attenuate the signal than two-lane roads lined with trees.

3.3 VT Propagation Simulator [2]

VT propagation simulator simulates the primary statistics and the secondary statistics using a universal data set, which is generated by experimental data in the simulator. By using measured data as a basis for the simulation, the time (or distance) behavior of the signal is preserved.

The input of the VT simulator is the same as LMSSMOD (S, K, $\overline{K}, m_{dB,} s_{dB}$) plus the number of data points to be generated. The simulator output is the sample of a simulated propagation model sampled every 0.1 wavelength. The simulated output data samples are processed using spatially sequential data rather than temporally sequential data in order to be independent of the vehicle speed. The simulation results, however, are not identical when different measured data are used as an input of the universal data set generation routine. Some simulation results of the VT simulator are very close to those of the analytical model, but other simulation results do not render satisfactory agreement. That is, the universal data set, which is generated in a routine of the VT propagation simulator is not consistent for each input measured data. Moreover, simulator results are restricted to UHF band and L-band Land Mobile Satellite System because the frequency band of the universal data set is in these bands. Figure 3.3-1 is the block diagram of the VT propagation simulator. Barts and Stutzman described the details of the VT simulator in [2]. Figure 3.3-2, 3.3-3, and 3.3-4 shows the outputs of VT simulator. The outputs are compared with ones generated by another universal dataset and LMSSMOD.

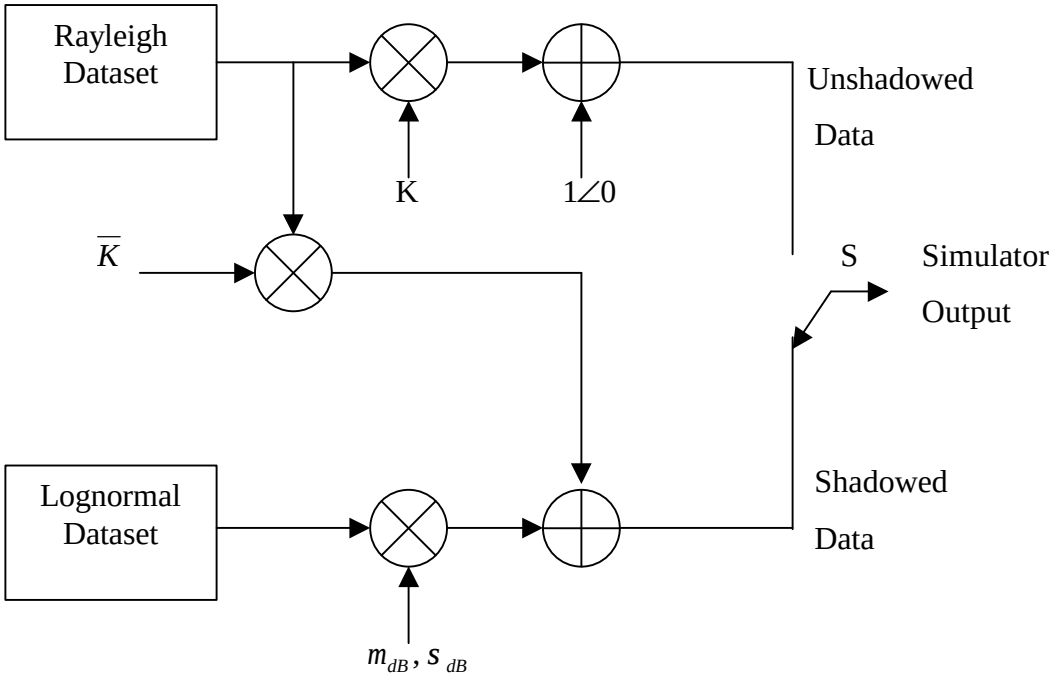

Figure 3.3-1 Block diagram of VT propagation simulator [2]

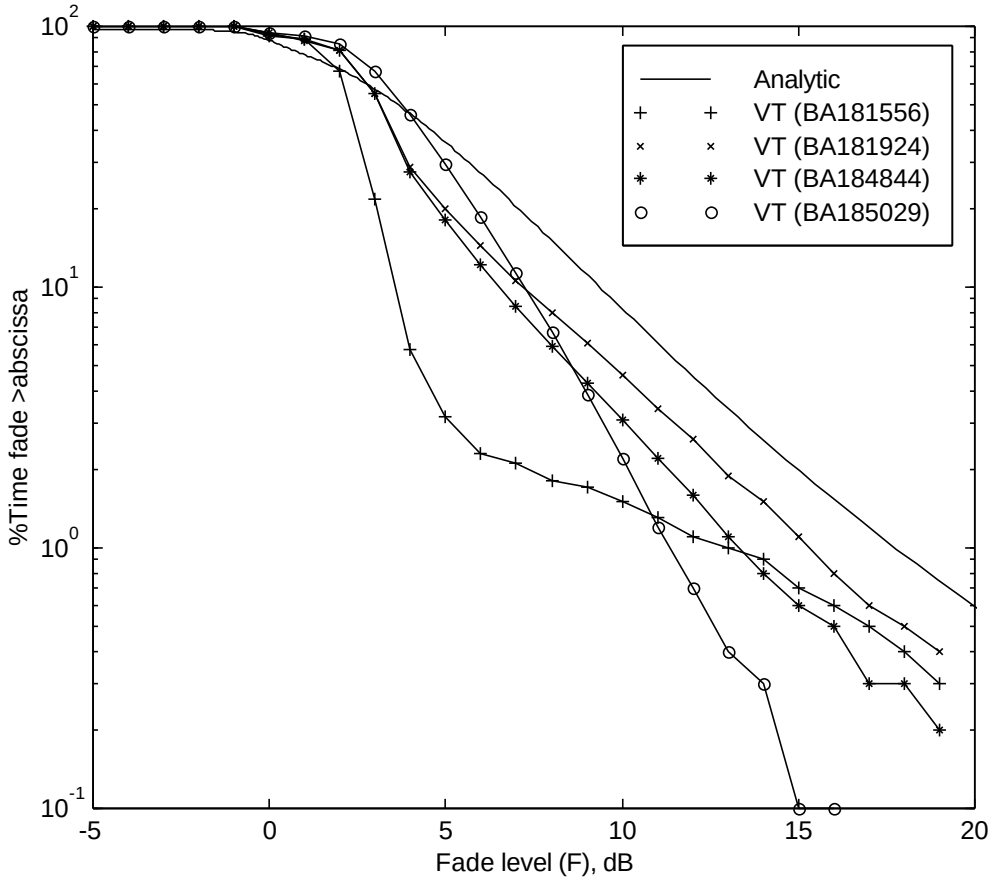

Figure 3.3-2 Comparison of fade distributions from VT simulator using the following parameters (S=92.5 %, K=21.5 dB, $\overline{K}$ =9.9 dB, m_{dB} =-4.8 dB, s_{dB} =1.7 dB)

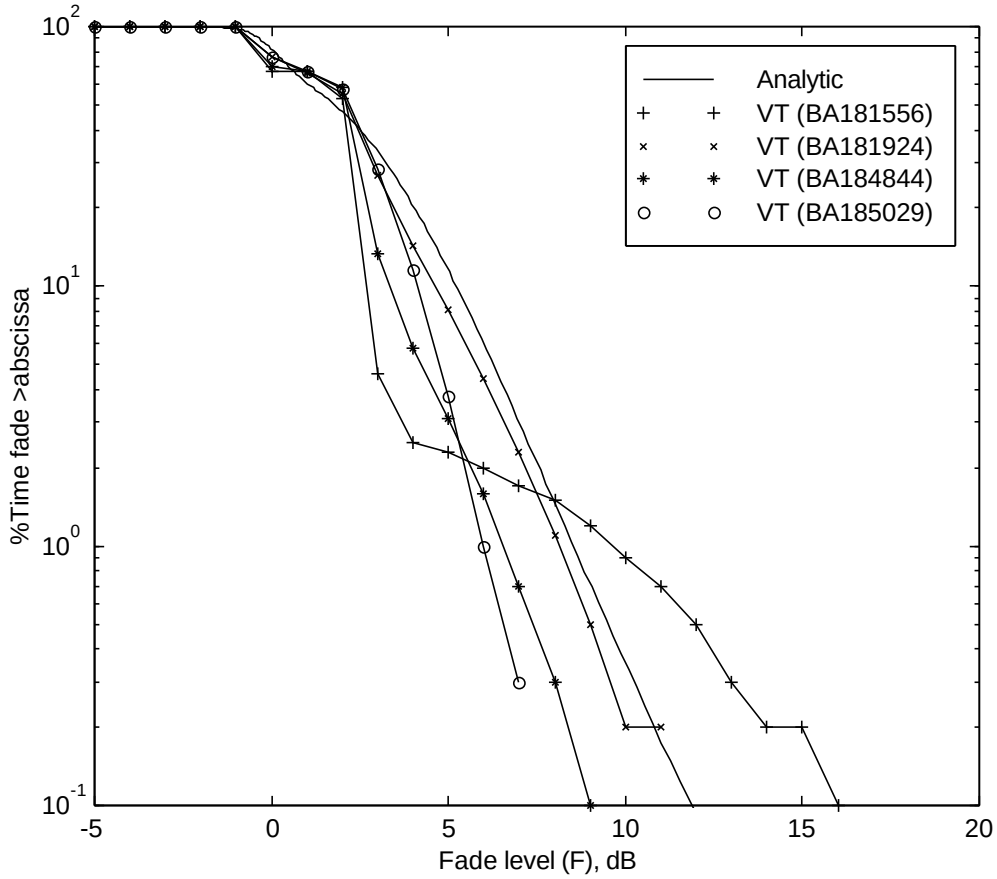

Figure 3.3-3 Comparison of fade distributions from VT simulator using the following parameters (S=67 %, K=20 dB, $\overline{K}$ =14 dB, m_{dB} =-3.1 dB, s_{dB} =0.9 dB)

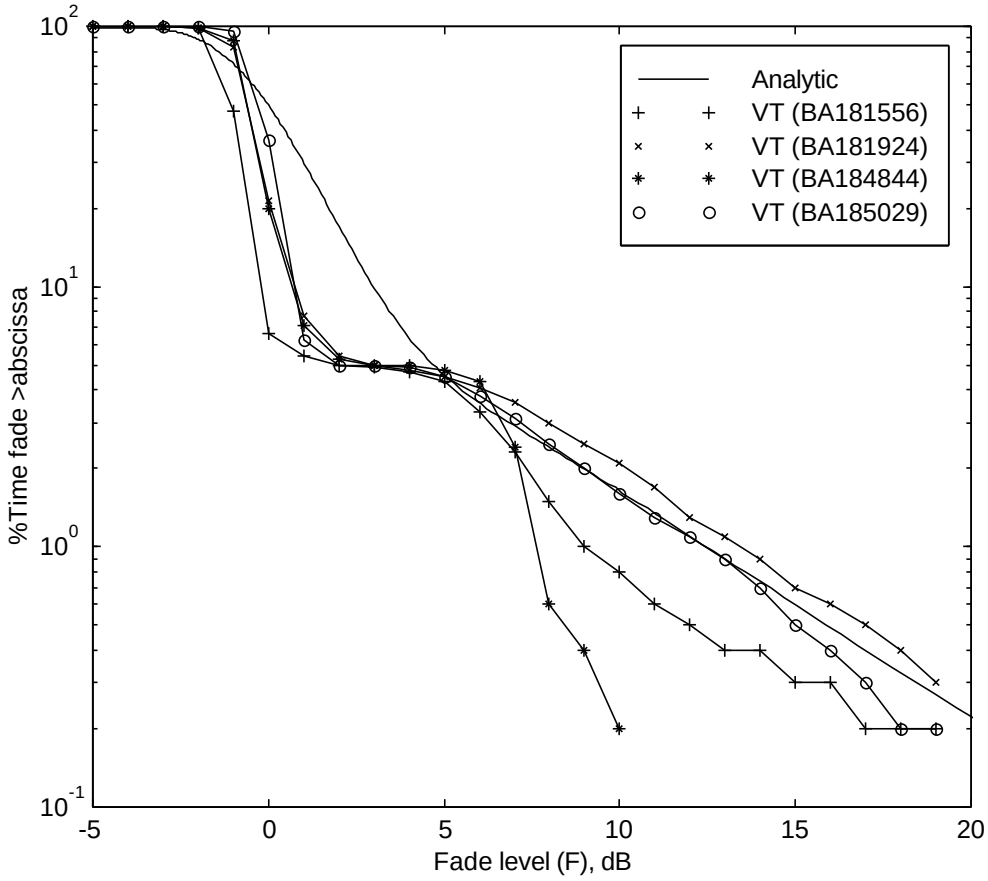

Figure 3.3-4 Comparison of fade distributions from VT simulator using the following parameters (S=5 %, K=11 dB, $\overline{K}$ =11 dB, m_{dB} =-10 dB, s_{dB} =4.0 dB)

Chapter 4. Development of a New Simulator Using a Random Number Generator

4.1 Introduction

Even though the fade distribution can be obtained by the numerical calculation with the analytical propagation model discussed in Section 2.4, the information on fade duration and level crossing rate cannot be obtained from the analytical model. The secondary statistics, AFD and LCR, can only be obtained through measurement or simulation. Measured data are preferred, but there is a limited amount available. An accurate simulator that agrees with measurement data provides a flexible resource for obtaining data for specific situations without having to perform an expensive experiment. In addition, parameter tradeoff studies can be performed with a simulator in controlled circumstances.

There have been previous efforts in hardware and software to simulate mobile satellite propagation. Hardware simulators have been built by CRC [6] and JPL [8]. The JPL hardware simulator could simulate only a Rician fading channel, but was designed to

perform evaluation of an end-to-end communication link. The CRC hardware simulator is composed of a Voltage Controlled Attenuator (VCA) to emulate lognormal distribution and a Rayleigh Fading Generator (RFG) to emulate a Rayleigh distribution. Using these components, the CRC simulator can simulate vegetative fading, but it cannot simulate accurately for the non-stationary shadowing case. The JPL software simulator can analyze much better the dynamic statistics of a fading channel than the JPL hardware simulator. The VT software simulator could simulate vegetative shadowing channel dynamically by universal data set, which is extracted from measurement data. The fade distribution from the VT simulator shows good agreement with the analytical model and measurement data for some universal input data, but it has drawbacks in that it is restricted to simulating only UHF band and L band propagation and its simulation results are not identical when different universal data are used as an input data set mentioned in Section 3.2.

In order to overcome the restriction of the VT simulator, the author, who is in the Virginia Tech Satellite Communications Group, developed a software propagation simulator using a Random Number Generator (RNG). A new simulator was developed using a basic concept of a random phasor sum and some fundamental characteristics of RNG in MATLAB, such as the mean of RNG is zero and the variance of RNG is unity. Figure 4.1-1 is the block diagram of author's propagation simulator, PROSIM. Each data set, Rayleigh, Rician, lognormal and the shadowed data set is developed by the random number generator. The shadowed data set and unshadowed data set are blended based on the fraction of shadowing, which is a simulator input parameter, S. The outputs of the simulator are plots of data samples, PDF, CFD, AFD, and LCR. In Section 4.7, we compare simulator results to those from the analytical model and measured data. All of these approaches have been integrated into one MATLAB window to facilitate computing. Table 4.1-1 describes the definition of the terms used in Figure 4.1-1.

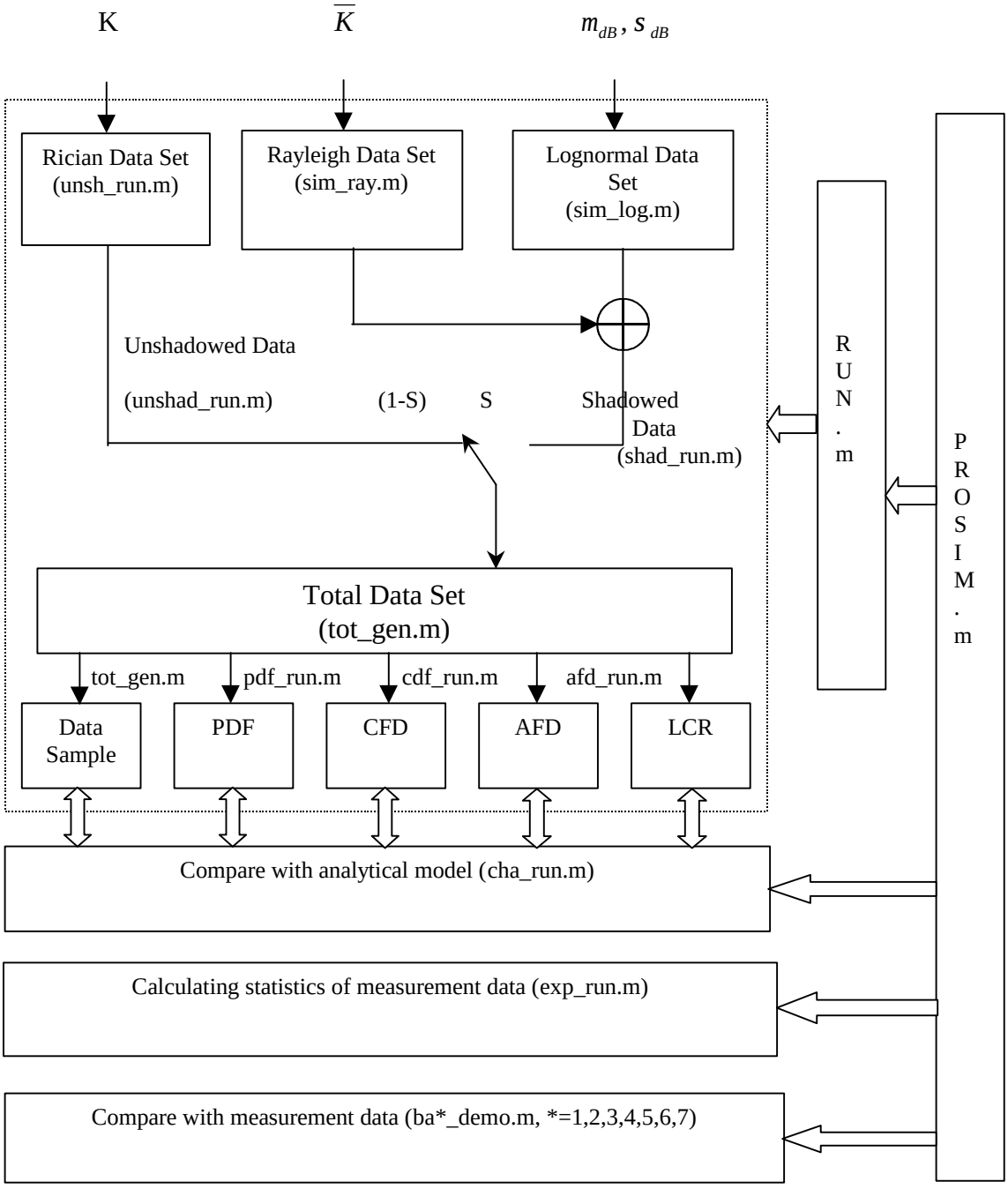

Figure 4.1-1 Block diagram of the propagation simulator, PROSIM using Random Number Generator (RNG)

Table 4.1-1 Description of terms used in Figure 4.1-1

Terms	Meaning
K	Rician carrier-to-mutipath ratio
$\overline{K}$	Rayleigh carrier-to-multipath ratio
m_{dB}	Lognormal mean in dB
s_{dB}	Lognormal standard deviation in dB
S	Percentage of shadowing
PDF	Probability density function
CFD	Cumulative fade distribution
AFD	Average fade duration
LCR	Level crossing rate

4.2 Generation of Rayleigh Data Set

4.2.1 The Fundamentals

A Rayleigh data set can be generated based on the theorem of Rayleigh random phasor sum. Figure 4.2-1 illustrates the random phasor sum in the complex plane. The mathematical expression was given (2.3-1) in Section 2.3.1. The Rayleigh complex-values data are composed of real and imaginary components having a normal distribution of zero mean and one variance, ideally, which follows from (2.3-1) as

$$X = \mathrm{Re}\left(R_{Rayleigh}\right) = r\cos q = \sum_{j=1}^{n} A_j \cos\Phi_j = \sum_{j=1}^{n} X_j \tag{4.2-1}$$

$$Y = \mathrm{Im}\left(R_{Rayleigh}\right) = r\sin q = \sum_{j=1}^{n} A_j \sin\Phi_j = \sum_{j=1}^{n} Y_j \tag{4.2-2}$$

where A_j is the j^{th} random amplitude and Φ_j is the j^{th} random phase. If n is sufficiently large, both X and Y will be normally distributed based on the Central Limit Theorem. In real simulation, if the distribution functions are smooth, values of n as low as five can be used [19]. The mean and variance values are derived by Beckmann [3]

$$\langle X\rangle = \sum_{j=1}^{n}\langle A_j\cos\Phi_j\rangle = \sum_{j=1}^{n}\langle A_j\rangle\langle\cos\Phi_j\rangle = \sum_{j=1}^{n}\langle A_j\rangle\frac{1}{2p}\int_{c}^{c+2p}\cos j_j\, dj_j = 0 \tag{4.2-3}$$

and, in the same way,

$$\langle Y\rangle = \sum_{j=1}^{n}\langle A_j\rangle\langle\sin\Phi_j\rangle = 0 \tag{4.2-4}$$

$$\left\langle X^2 - \langle X\rangle^2\right\rangle = \left\langle X^2\right\rangle = \sum_{j=1}^{n}\left\langle A_j^2\right\rangle\left\langle\cos^2\Phi_j\right\rangle = \frac{1}{2}n\left\langle A_j^2\right\rangle = s^2 \tag{4.2-5}$$

$$\left\langle Y^2 - \langle Y\rangle^2\right\rangle = \left\langle Y^2\right\rangle = \sum_{j=1}^{n}\left\langle A_j^2\right\rangle\left\langle\sin^2\Phi_j\right\rangle = \frac{1}{2}n\left\langle A_j^2\right\rangle = s^2 \tag{4.2-6}$$

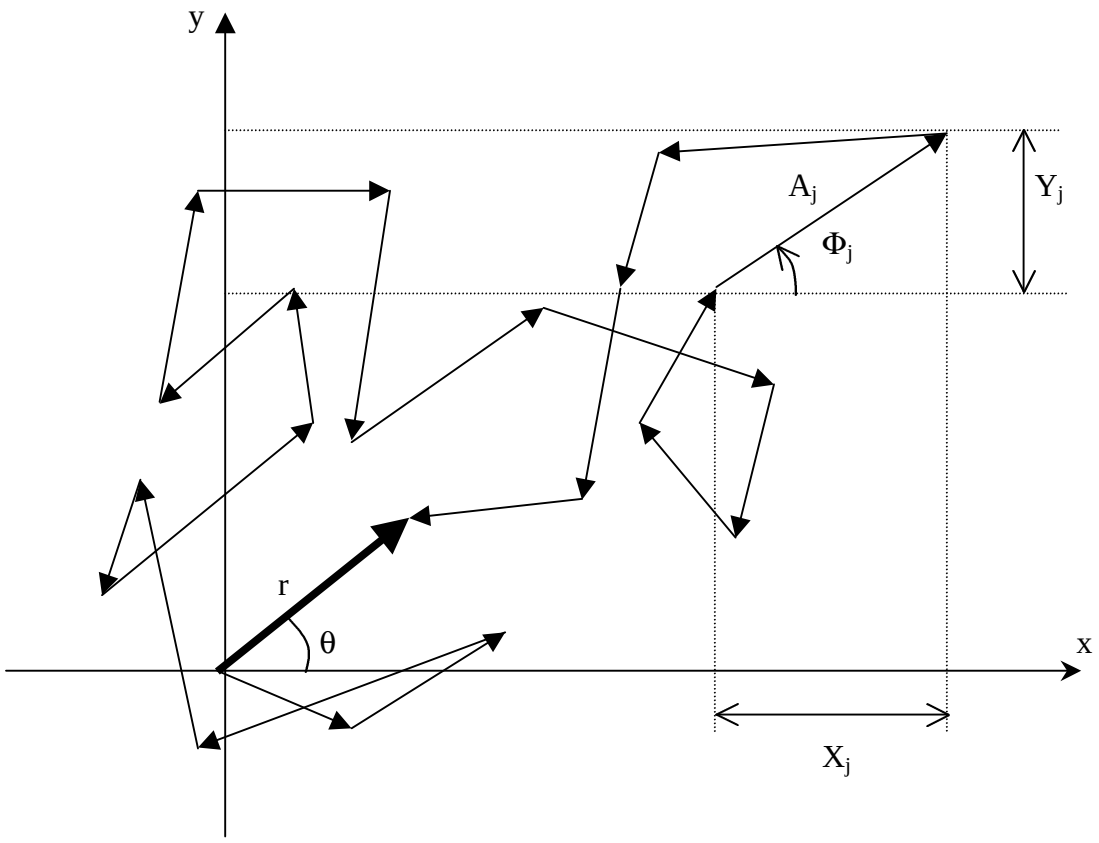

Figure 4.2-1 Illustration of a Random phasor sum in the complex plane [3]

$$\left\langle A_j^2 \right\rangle = \frac{2s^2}{n} = \frac{a}{n} \tag{4.2-7}$$

We can also determine the mean-square value of *r* given by [3]

$$\left\langle r^2 \right\rangle = \sum_{j=1}^{n} \left\langle A_j^2 \right\rangle = n\left\langle A_j^2 \right\rangle = \left\langle X^2 \right\rangle + \left\langle Y^2 \right\rangle = 2s^2 \equiv a = 10^{-\overline{K}/10} \tag{4.2-8}$$

4.2.2 Generating the Rayleigh Data Set

In order to generate the Rayleigh data set using the Random Number Generator (RNG), the characteristics of RNG in MATLAB should be employed. There are two kinds of random number generators in MATLAB. The first one, named *randn(n,m)* generates a normal distribution with mean value zero and with a variance value of unity while the second one, named *rand(n,m)* produces data with uniform distribution of one, with a mean value of 0.5 and a variance value of 0.0833 (=1/12). The parameter, *n*, represents the number of the scattered random phasor, and *m* is the number of samples to be represented in distance or time. The value of *n* should be sufficiently large to be normally distributed and can be as low as 5 based on the Central Limit Theorem. The fade distribution is a statistical representation in percentage of time or distance and it should be displayed at least 0.1 % of time or distance so that the number of sample, *m*, should be more than ten times of 1000 (=1/0.1%). However, accuracy is improved by increasing the number of samples, *m*. To avoid a time-consuming simulation, a value of *n* between 5 and 15 and *m* between 10,000 and 15,000 is recommended. Using the functions in MATLAB, we can produce the random amplitude, A_j having normal distribution with mean value zero and with a variance value of unity. However, the variance is scaled to the input value $\overline{K}$ in order to generate the Rayleigh data set having $\overline{K}$ appropriate to a Rayleigh carrier-to-multipath power ratio. Equation (4.2-8) gives the relationship between the input $\overline{K}$ and the Rayleigh mean-square value, α. The scaling

factor, α can be obtained from (4.2-7) which relates the mean-square value of A_j to $\frac{a}{n}$. The relationship between the scaling factor and the function $randn(1,m)$ is given by [18]

$$\text{var}\,iance[k \cdot randn(1,m)] = k^2 \tag{4.2-9}$$

where k is an arbitrary scaling factor. Note that (4.2-9) can be applied only to random vectors having one row and m columns in MATLAB. However, the Rayleigh data set is composed of n rows and m columns of random numbers. Hence, the variance of each row should be summed after adding the n row random vectors.

The desired data set having carrier-to multipath ratio, $\overline{K}$, can be achieved using the following relationships:

$$A_j = \sqrt{\frac{a}{n}} randn(j,m) \tag{4.2-10}$$

$$\Phi_j = 2p \cdot rand(j,m) \tag{4.2-11}$$

where function 'randn' generates the normally distributed random vector and function 'rand' produces the uniformly distributed random vector.

The following equation shows that the scaling factor $\sqrt{\frac{a}{n}}$ generates the mean-square value of r with the desired value α.

$$\left\langle r^2 \right\rangle = \sum_{j=1}^{n} \left\langle A_j^2 \right\rangle = n\left\langle \left(\sqrt{\frac{a}{n}} \cdot randn(j,m) \right)^2 \right\rangle = n \cdot \frac{a}{n} = a \tag{4.2-12}$$

Hence, the Rayleigh data set can be generated using (4.2-10) and (4.2-11) as

$$R_{Rayleigh} = r \cdot e^{jq} = \sum_{j=1}^{n} A_j \cdot e^{j\Phi_j} \tag{4.2-13}$$

where *r* is random variable for the amplitude of Rayleigh distribution and θ is the phase of the distribution having uniform PDF with $\frac{1}{2p}$.

Figure 4.2-2 is the sample of Rayleigh data set generated using the RNG with the input parameter, $\overline{K} =$ 3 dB. The figure shows that level of data samples is concentrated around -3 dB similar to the input parameter value of 3 dB. The samples represent the multipath data samples while a vehicle is traveling a road without line-of-sight. In order to eliminate the effect of vehicle speed, the abscissa of the Figure 4.2-2 is a function of distance traveled with the samples are spaced by 0.1 wavelength apart.

The data set was evaluated by comparing the PDF with the analytical PDF of Section 2.3.1.1 in Figure 4.2-3. The apogee of the Rayleigh PDF corresponds to the signal level σ, which is also described by input parameter, $\overline{K}$ as follows [20]:

$$s = \sqrt{\frac{a}{2}} = \sqrt{\frac{10^{-\overline{K}/10}}{2}} \tag{4.2-14}$$

$$p(s) = \frac{0.6065}{s} \tag{4.2-15}$$

In the Figure 4.2-3, the signal level corresponding to the apogee is about 0.56 and the PDF value is about 1.08. The values are the same with the calculation results using equation (4.2-14) and (4.2-15). The circles represent the PDF of generated data set by PROSIM while the solid line represents the PDF calculated using LMSSMOD. They are matched quite well except for the signal level from 0 to about 0.1. The very low signal levels are not easy to generate by PROSIM. The phenomenon can occur frequently in PROSIM because it generates the data samples randomly and the extremely low signals are difficult to generate statistically. The problem can be resolved by using many more input data samples (higher *m*) at the expense of simulation time.

Figure 4.2-4 is the phase distribution of the simulation results and the analytical model. The solid line represents the analytic phase PDF value of $\frac{1}{2p}$ while the circles represent the phase PDF for simulation result. The phase PDF is also matched with the analytic model. The abscissa is plotted in radians from $-\pi$ to π.

Based upon these simulation results, the Rayleigh data samples are quite satisfactory to represent the multipath signal in Land Mobile Satellite Communication.

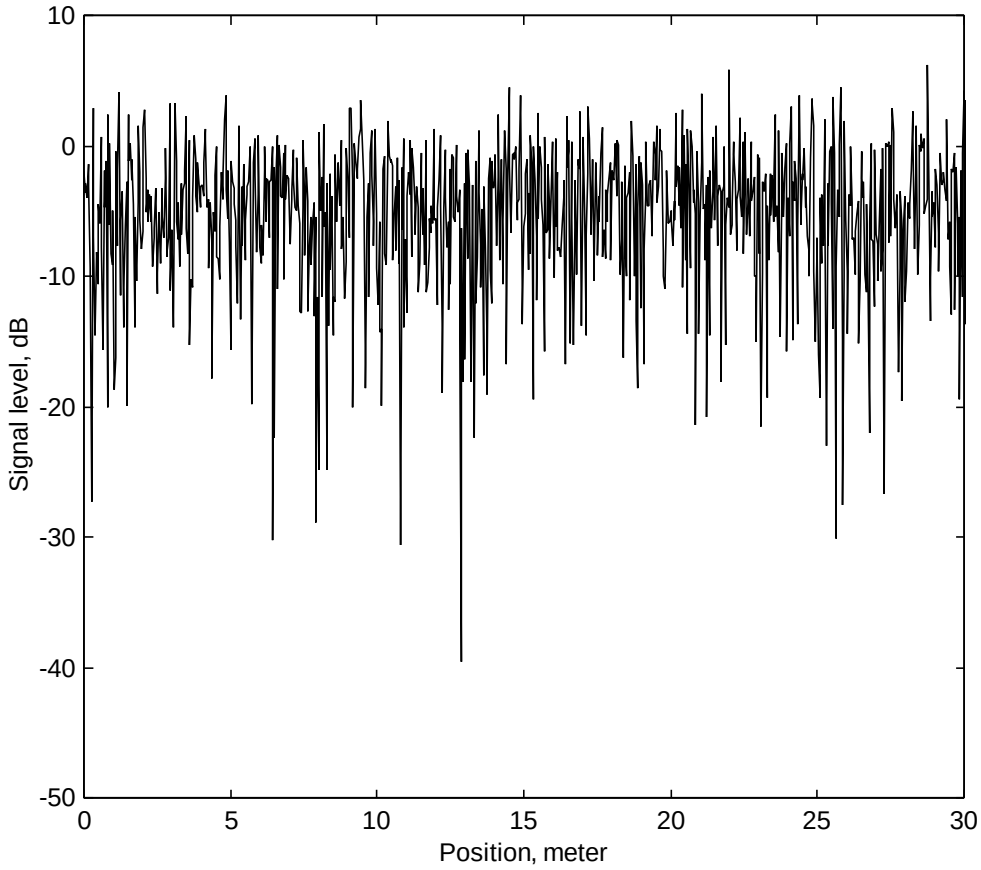

Figure 4.2-2 Samples of Rayleigh Data Set spaced 0.1 wavelength apart ($\overline{K} = 3$ dB)

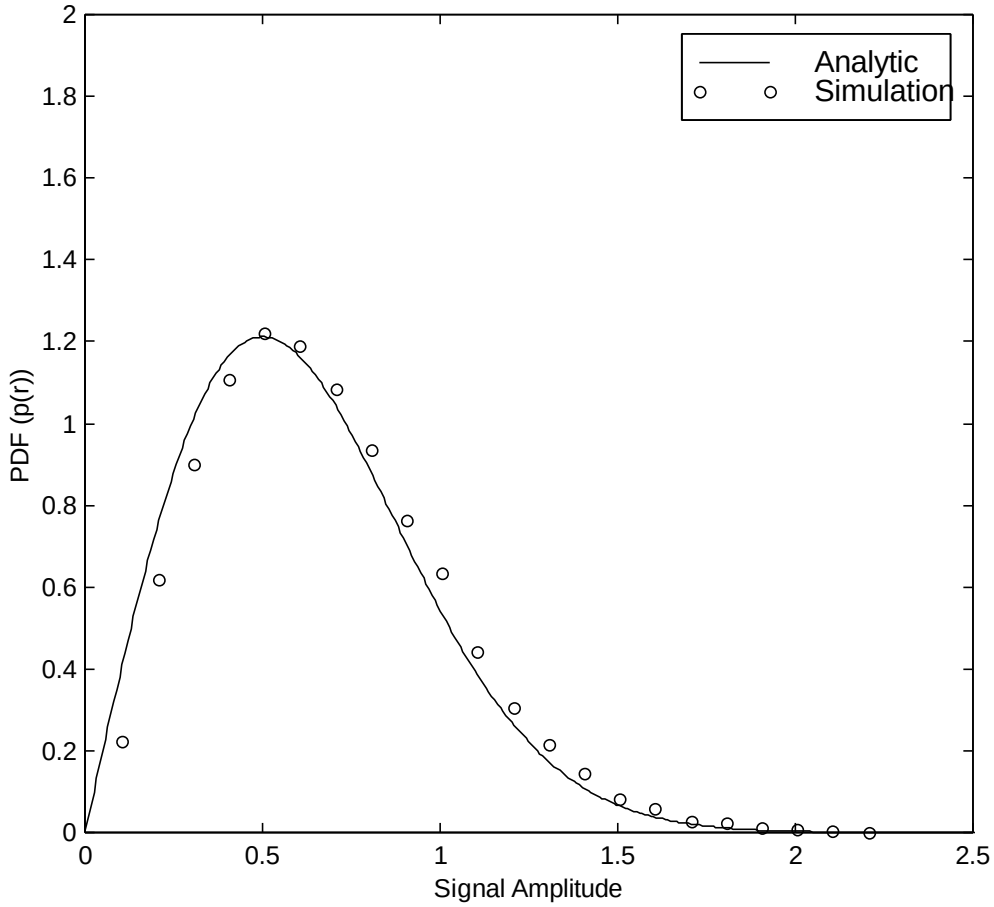

Figure 4.2-3 Comparison of Rayleigh magnitude PDF between the Simulation Data Set and the Analytical Model, equation (2.3-5) ($\overline{K} = 3$ dB)

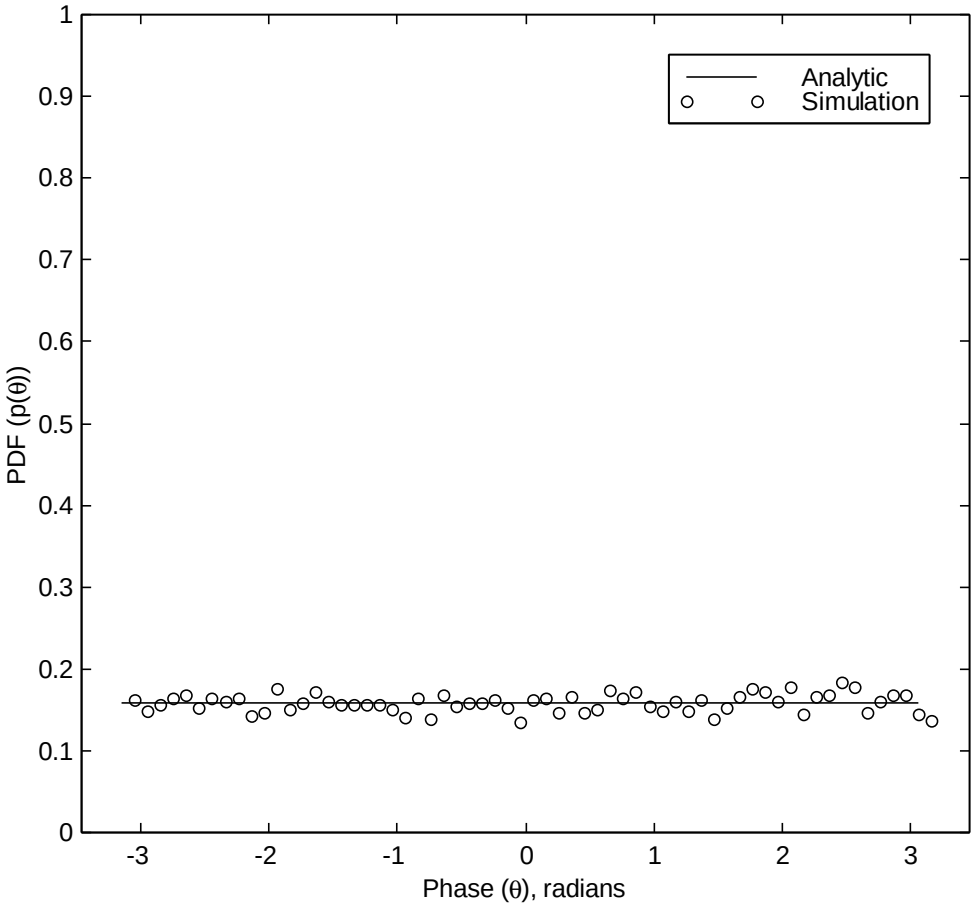

Figure 4.2-4 Comparison of Rayleigh phase PDF, p(θ) between the Simulation Data Set and the Analytical Model ($\overline{K} = 3$ dB)

4.3 Generation of Rician Data Set

The Rician data set is generated in a manner similar to that used for the Rayleigh data set, except for adding the constant LOS signal. The constant LOS signal was assumed to be unity in our study. The Rician data set can be used as data for unshadowed propagation. Figure 4.3-1 illustrates the phasor plot of a Rician model in the complex plane. The mathematical expression was given in (2.3-7) in Section 2.3.2. We note the phase distribution of Rician model is no longer uniform because the phase of the Rician data set is determined by the phase of the constant LOS signal. The phasor plot in Figure 4.3-1 illustrated the phase distribution of the Rician data set. The LOS signal, C is much larger than the Rayleigh signal, ρ. Hence, the Rayleigh phase, Ψ has little effect on the Rician phase, θ. The analytic expression for the Rician phase distribution was given also in (2.3-8) in Section 2.3.2. The Rician model is fully specified by the Rician carrier-to-mutipath power ratio *K* in dB. Using the *K* in dB, the Rician mean-square value, β, can be derived by the following relationship:

$$b = C^2 \cdot 10^{-K/10} = 10^{-K/10} \tag{4.3-1}$$

(since C is assumed to be unity)

In the same way with the Rayleigh data set, the scaling factor is obtained by

$$\text{Scaling factor} = \sqrt{\frac{b}{n}} \tag{4.3-2}$$

$$A_j = \sqrt{\frac{b}{n}} randn(1, m) \tag{4.3-3}$$

$$\Phi_j = 2p \cdot rand(1, m) \tag{4.3-4}$$

Hence, the Rician data set can be generated using (4.3-3) and (4.3-4) as

$$R_{Rician} = r \cdot e^{jq} = C + r \cdot e^{j\Psi} = C + \sum_{j=1}^{n} A_j \cdot e^{j\Phi_j} = 1 + \sum_{j=1}^{n} A_j \cdot e^{j\Phi_j} \qquad (4.3\text{-}5)$$

where r is the amplitude of Rician distribution and θ is the phase of the distribution having uniform PDF with (2.3-8).

Figure 4.3-2 is the sample of Rician Data Set generated using the RNG with the input parameter, $K = 5$ dB. Unlike the Rayleigh data set, the fade level is concentrated at the 0 dB level. This results from the dominant LOS signal, C. The peak-to-peak fade level will become larger when the value of carrier-to-multipath ratio is small. The small value, K, means that the multipath component is very large compared to the LOS signal, and, physically the vehicle should be moving along the road with potentially a large number of buildings such as in an urban area. There can be constructive multipath components in the Rician data set so that the positive fade level can exist in Figure 4.3-2. When the phase of a Rayleigh signal is between around -90° and 90°, the amplitude of these signals will be added to the LOS signal. It can be easily illustrated by the phasor plot in Figure 4.3-2. Hence, the constructive multipath component can cause signal enhancement in a Rician data set.

The Rician data set was evaluated by comparing the PDF with the analytical model of Section 2.3.1.2 in Figure 4.3-3. The signal amplitude of the Rician data set is centered around the LOS signal amplitude, C=1, but the signal amplitude is spread out due to quite low carrier-to-multipath ratio.

Figure 4.3-4 is the phase distribution of the simulation result and the analytical model in equation (2.3-9). The phase is distributed around the phase of the LOS signal, 0°. If K becomes larger, the distribution will be more concentrated into 0°. The figures show that the data set is matched well with analytical model.

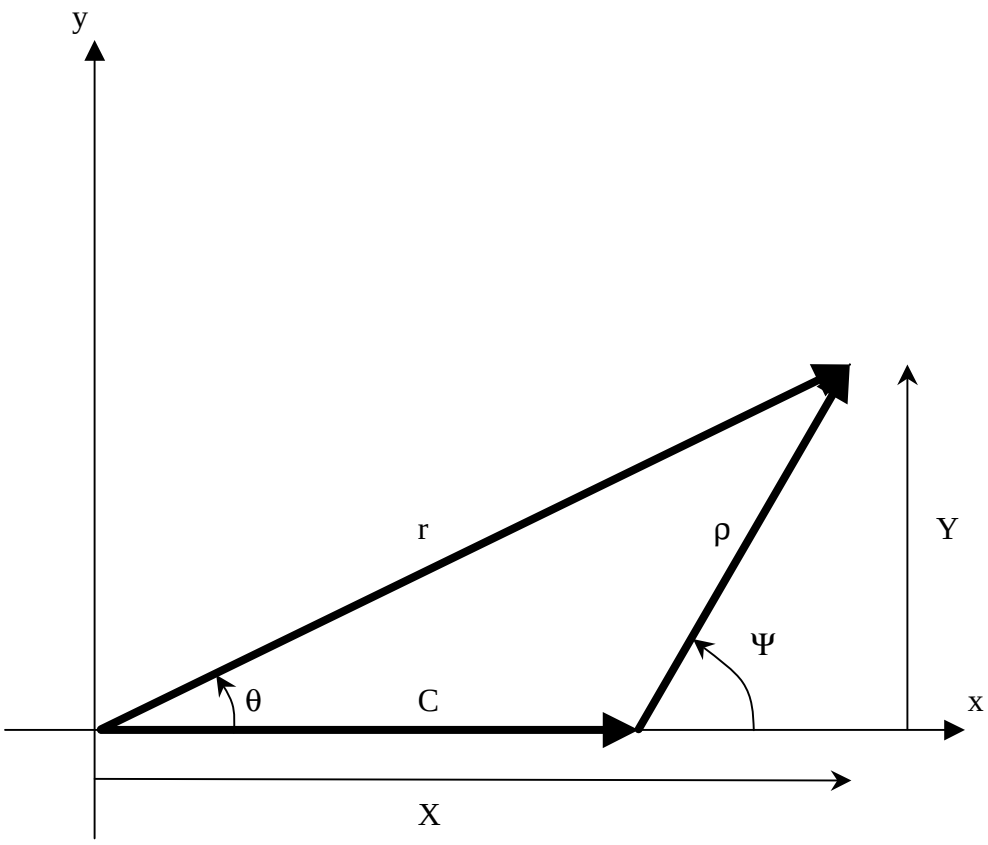

Figure 4.3-1 Illustration of a Rician phasor plot in the complex plane [3]

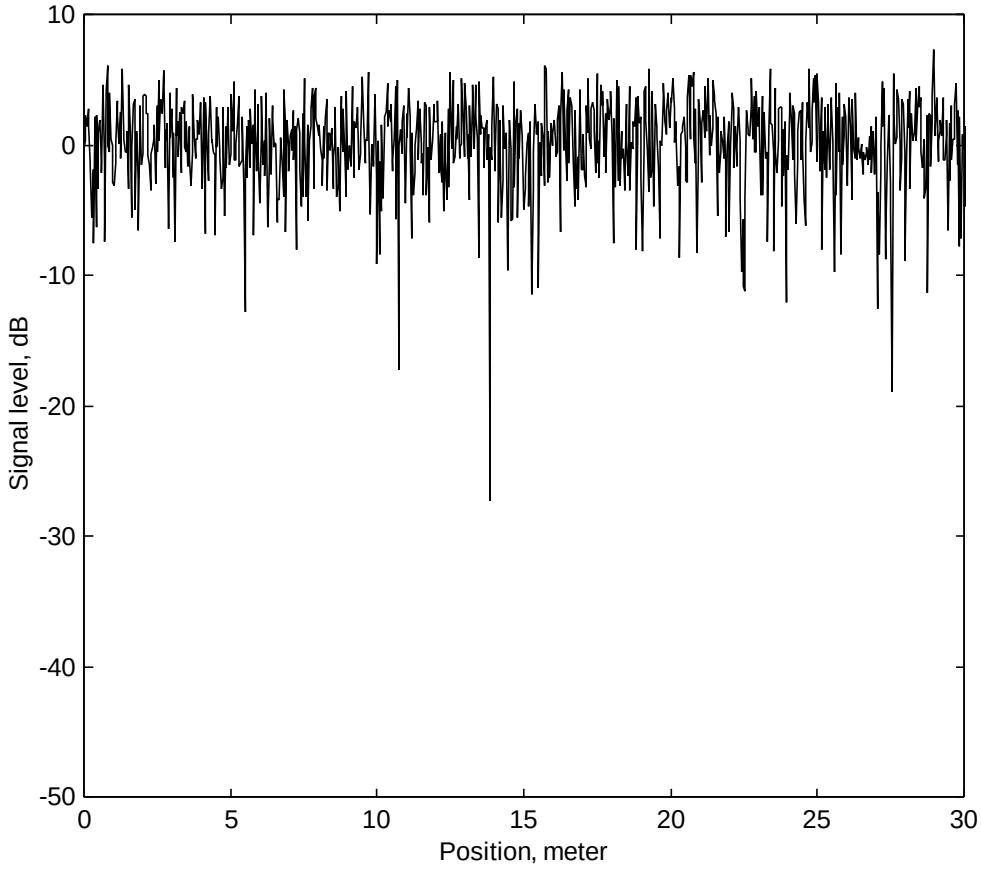

Figure 4.3-2 Samples of Rician Data Set spaced 0.1 wavelength apart ($K = 5$ dB)

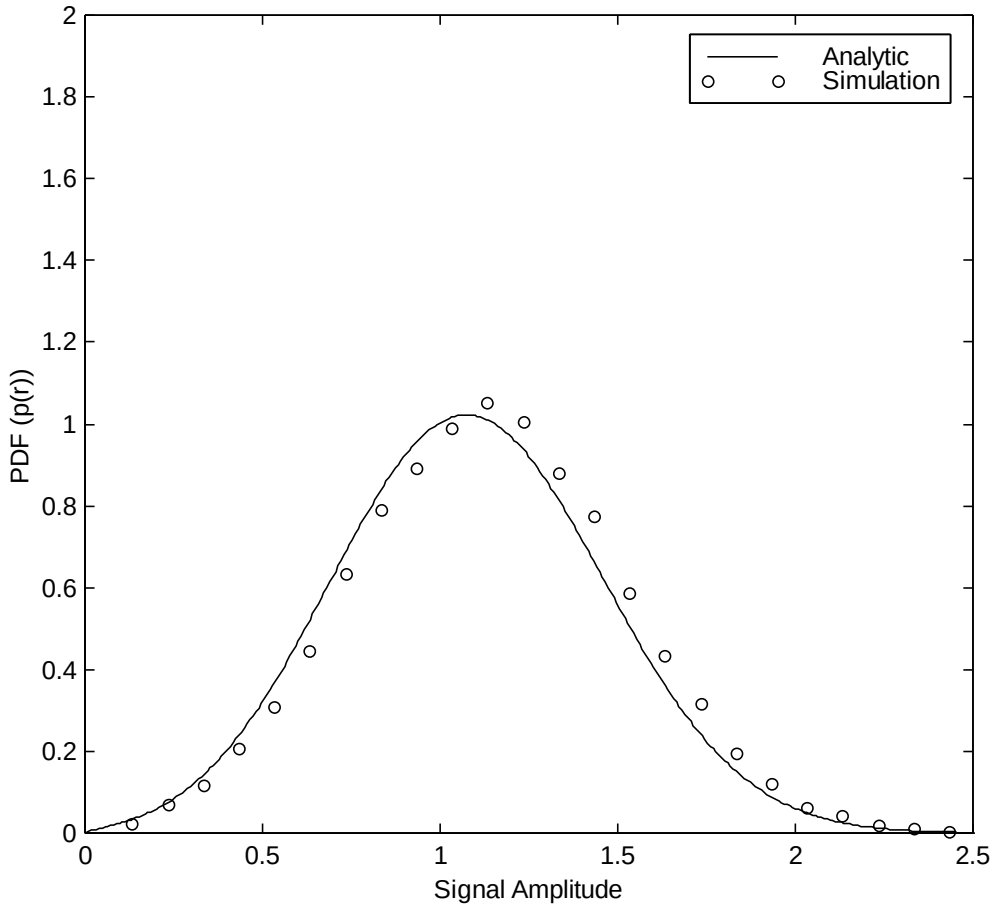

Figure 4.3-3 Comparison of a Rician magnitude PDF, $p(r)$ between the Simulation Data Set and the Analytical Model, equation (2.3-13) (K= 5 dB)

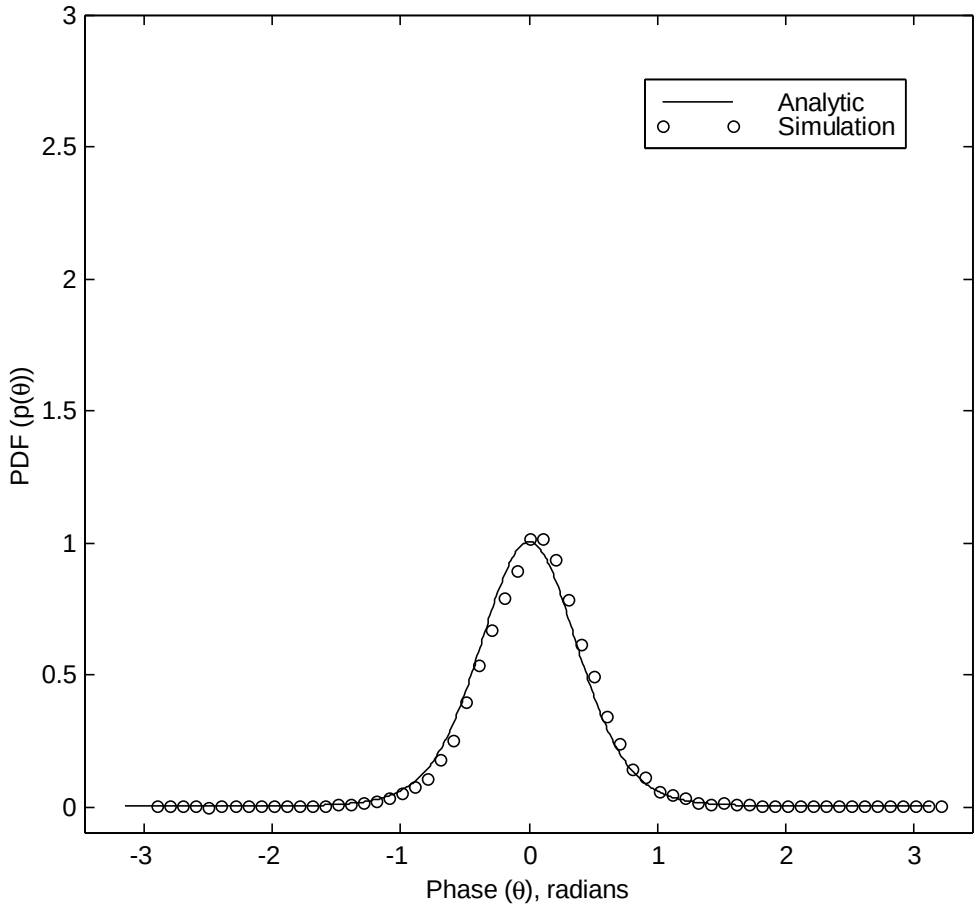

Figure 4.3-4 Comparison of a Rician phase PDF between the Simulation Data Set and the Analytical Model, equation (2.3-9) ($K = 5$ dB)

4.4 Generation of Lognormal Data Set

The lognormal data set is quite different from the Rayleigh data set and the Rician data set. The Rayleigh and Rician data sets are generated by an additive process of random variables. However, the lognormal data set is developed by a multiplicative process of random variables. The lognormal data set is combined with the lognormally distributed amplitude and the uniformally distributed phase between 0 and 2π. Note, the amplitude is a positive random variable. The author derived the following expression for a phasor plot of the lognormal model:

$$R_{\log normal} = r \cdot e^{jq} = \prod_{j=1}^{n} B_j \cdot \exp\left[j \sum_{j=1}^{n} \Phi_j \right] \tag{4.4-1}$$

$$\ln\left(R_{\log normal}\right) = \ln r + jq = \sum_{j=1}^{n} \ln B_j + j \sum_{j=1}^{n} \Phi_j = \sum_{j=1}^{n} \left(\ln B_j + j\Phi_j\right) = \sum_{j=1}^{n} H_j \cdot e^{j\Psi_j} = h \cdot e^{jj} \tag{4.4-2}$$

where $H_j = \sqrt{\left(\ln B_j\right)^2 + \Phi_j^2}$, $\Psi_j = \tan^{-1}\left(\dfrac{\Phi_j}{\ln B_j} \right)$, and the h and φ are the amplitude and the phase of the ln ($R_{lognormal}$).

If we take the natural log of the product expression, the expression changes to the sum expression. The phase term acts as an imaginary term in the phasor plot of the lognormal model, while the natural log of the amplitude acts as a real term in the complex plane. Figure 4.4-1 illustrates the phasor plot of the lognormal model derived by the author in the complex plane. The lognormal model is fully specified by the lognormal mean, μ_{dB}, and the lognormal standard deviation, σ_{dB}, in dB. Using the input μ_{dB} and σ_{dB}, the random number in MATLAB should be scaled. The function *randn*(*n*,*m*) in MATLAB includes negative values, so the random data should be shifted to positive region. Then, we can take the natural log of the random variables.

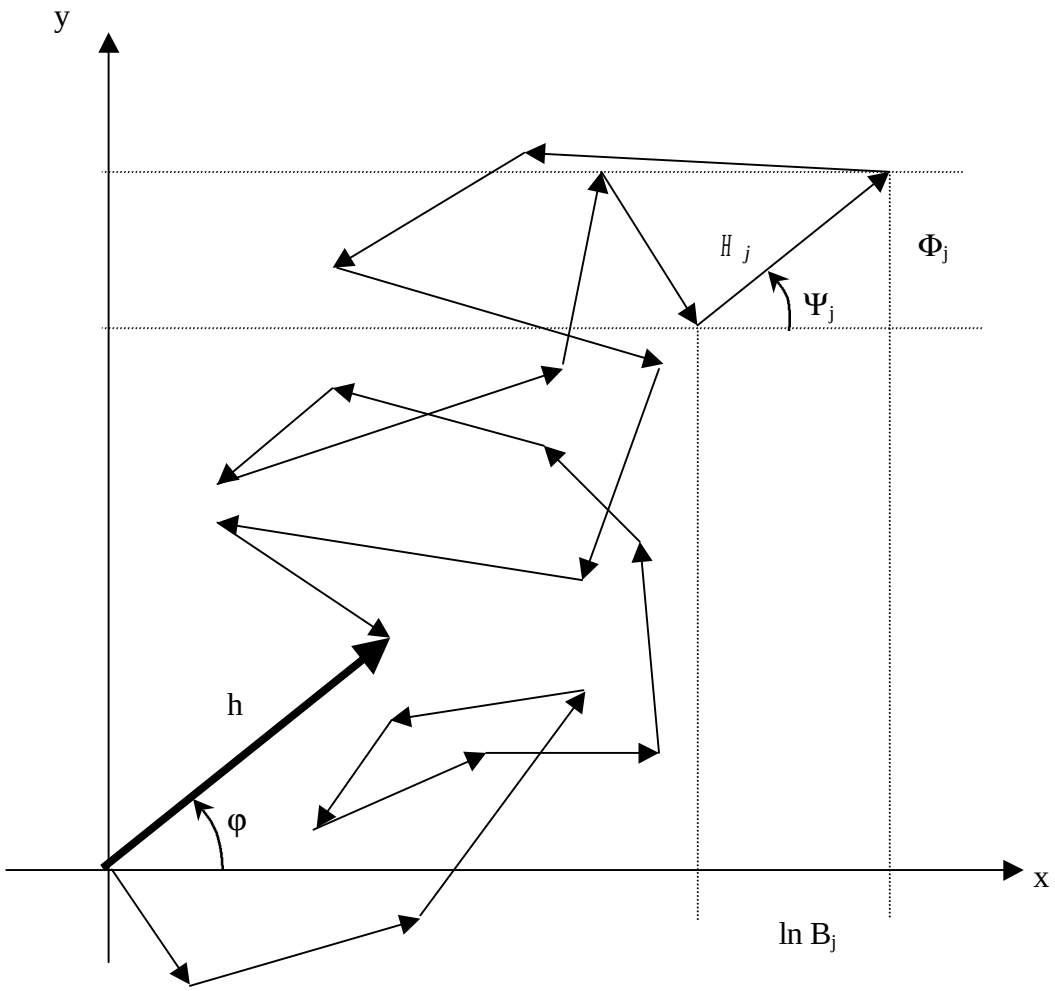

Figure 4.4-1 Illustration of a lognormal phasor plot in the complex plane

After taking the natural log of the random variable, we need to find a new relationship between the variance and the random variable. Generally we could use the relationship in the case of the Rayleigh model as follows,

$$\text{var}\, iance[k \cdot randn(1, m)] = k^2 \tag{4.4-3}$$

But (4.4-3) cannot be used anymore in the lognormal model because the random variable was shifted to the positive region. We need to find the scaling factor by including some routines in the simulation program. There cannot exist a definite value for the factor since the random number generator produces a different number for each run. The routines found the variances of the lognormal amplitude during calculation of the product with some sequential numbers, and computed the slope coefficient, *c*, corresponding to the sequential number. The slope coefficient was one in the case of the variance of the Rayleigh model. The following expressions show the statements simply.

$$\text{var}\, iance\left[k \cdot \sum_{j=1}^{n} randn(j, m) \right] = n \cdot c \cdot k^2 = n \cdot k^2 \text{ (since } c\text{=1)} \tag{4.4-4}$$

$$\text{var}\, ianc\left\{ k \cdot \sum_{j=1}^{n} \ln\left[randn_{positive}(j, m) \right] \right\} = n \cdot c \cdot k^2 = s^2 \tag{4.4-5}$$

where $randn_{positive}(j,m)$ is the j^{th} shifted random variable to positive region.

The input σ_{dB} can be achieved by applying the following scaling factor, which is derived by (2.3-19) and (4.4-5).

$$k = \sqrt{\frac{s^2}{c \cdot n}} \tag{4.4-6}$$

where *n* is the number of random variables. The input, μ_{dB} can be also found by (2.3-18) and (4.4-5).

$$M = mean\left\{ k \cdot \sum_{j=1}^{n} \ln\left[randn_{positive}(j, m) \right] \right\} = k \cdot \sum_{j=1}^{n} m_j \tag{4.4-7}$$

$$mean\left\{k \cdot \sum_{j=1}^{n} \ln\left[randn_{positive}(j,m)\right] - M + m\right\} \approx m \qquad (4.4\text{-}8)$$

Finally, the magnitude of the lognormal data set could be generated by scaling the lognormal mean and standard deviation. The phase of the lognormal data set is the sum of uniformly distributed random variables. The lognormal data set could be produced using (4.4-1) and (4.4-2).

Figure 4.4-2 is a sample of the lognormal data set generated using PROSIM with the input parameters, μ_{dB} = -0.5 dB and σ_{dB} =5 dB. The lognormal data set is concentrated around –0.5dB in Figure 4.4-2. The lognormal mean represents how much the direct signal will be attenuated through the vegetative shadowing. The higher negative value means that there should be heavier shadowing than with the lower negative value. The lognormal standard deviation can be interpreted as how much the lognormal signal will be scattered through vegetative shadowing. To represent a severely scattered situation, the high lognormal standard deviation value will be used to perform a simulation while the peak-to-peak fade level becomes large.

The data set was evaluated by comparing the PDF with the analytical model of Section 2.3.1.3 in Figure 4.4-3.

Figure 4.4-4 is the phase distribution of the simulation results and the analytical model. The phase is uniformly distributed between -π and π. The figures show that the data set is matched well with the analytical model.

Based upon these simulation results, the lognormal data samples are quite satisfactory to represent the attenuated direct signal due to vegetative shadowing in a Land Mobile Satellite Communication System.

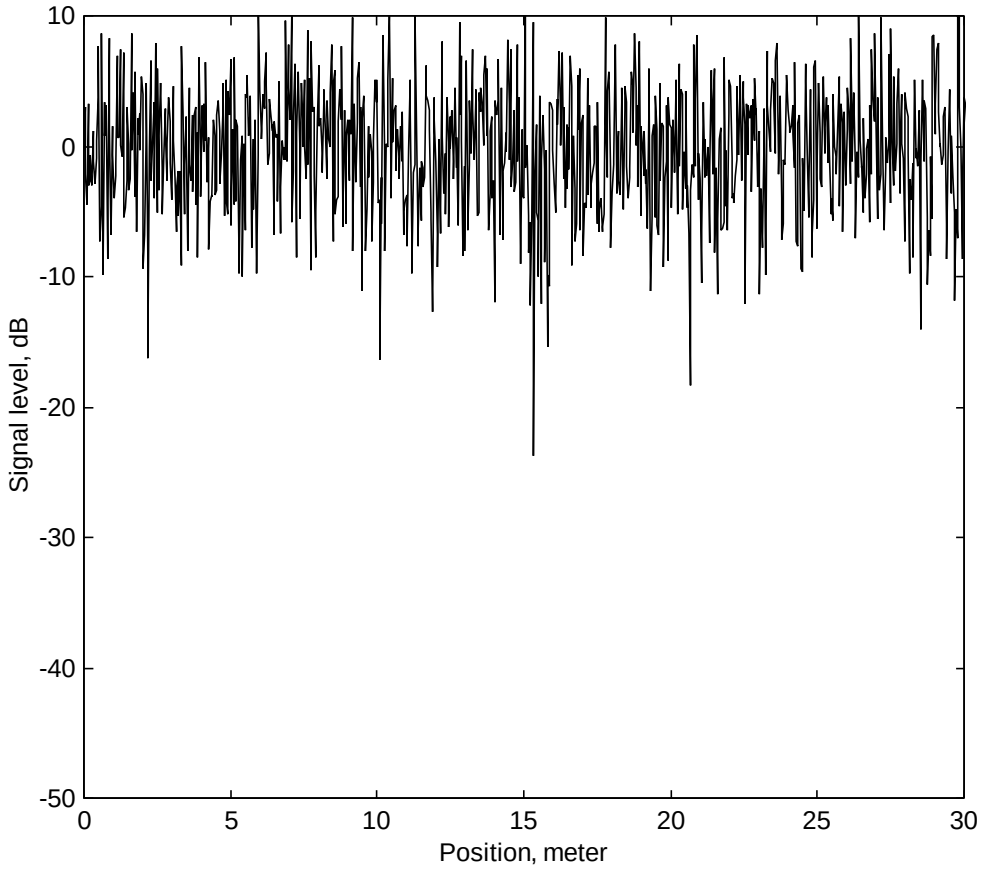

Figure 4.4-2 Samples of Lognormal Data Set spaced 0.1 wavelength apart

(μ_{dB} = -0.5 dB, σ_{dB} = 5 dB)

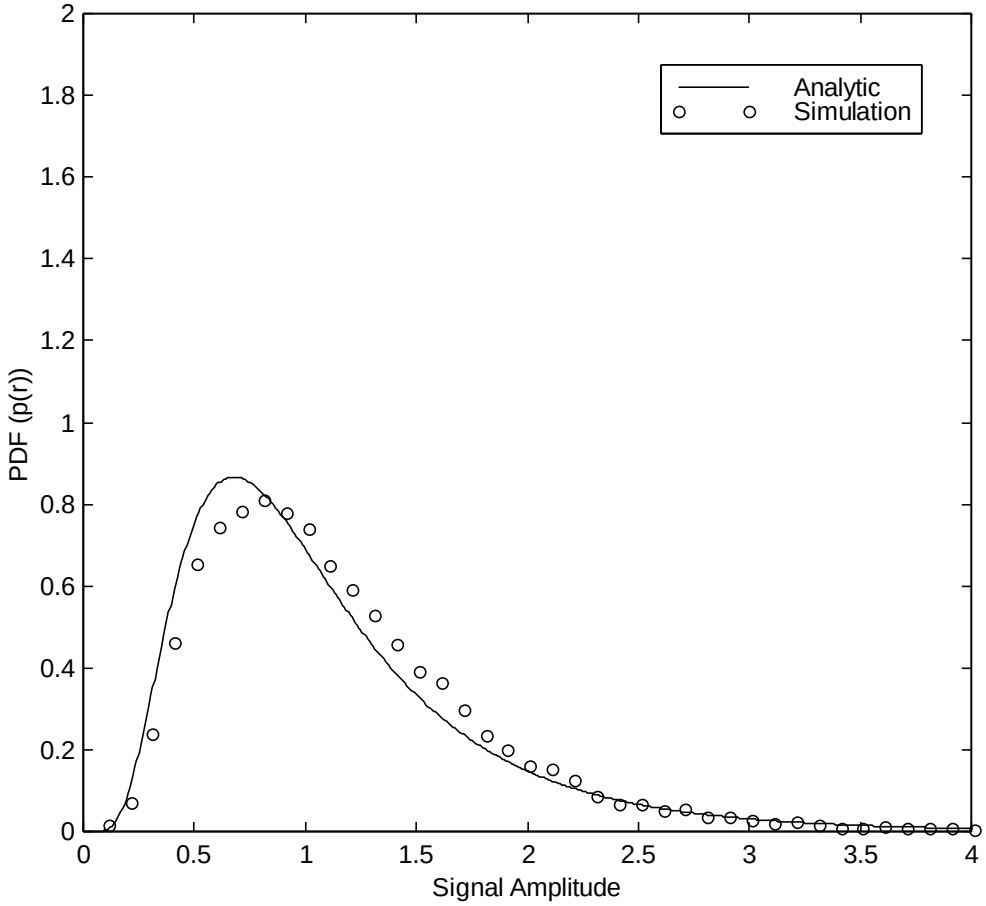

Figure 4.4-3 Comparison of lognormal magnitude PDF, $p(r)$ between the Simulation Data Set and the Analytical Model, equation (2.3-20) (μ_{dB} = -0.5 dB, σ_{dB} = 5 dB)

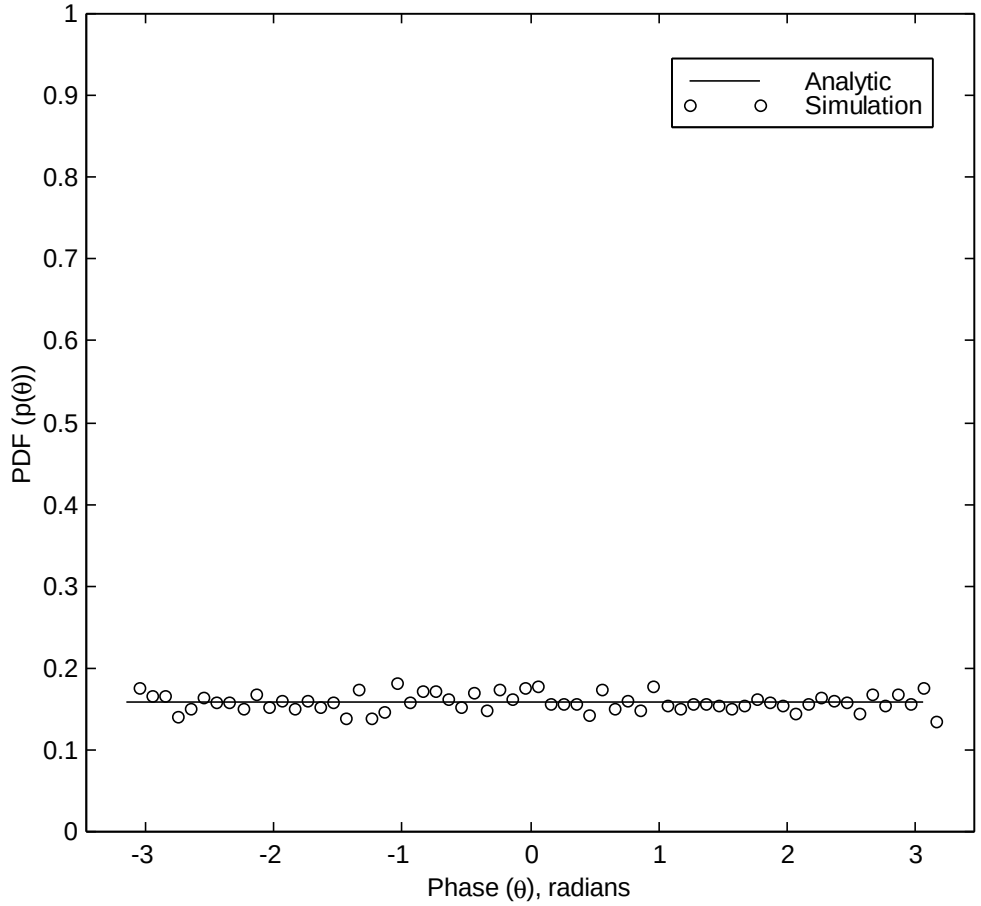

Figure 4.4-4 Comparison of lognormal phase PDF, $p(q)$ between the Simulation Data Set and the Analytical Model (μ_{dB} = -0.5 dB, σ_{dB} = 5 dB)

4.5 Generation of Shadowed Data Set

The shadowed data set is the phasor sum of the Rayleigh data set and the lognormal data set. The two data sets developed in Section 4.3 and 4.4. were used to generate the shadowed data set. The mathematical expressions for the shadowed data set are given by [3].

$$R_{shadowed} = R_{\log normal} + R_{Rayleigh} = r \cdot e^{jq} = z \cdot e^{jf} + w \cdot e^{jj} \qquad (4.5\text{-}1)$$

where the phase ϕ and φ are uniformly distributed between 0 and 2π, z is lognormally distributed, and w has a Rayleigh distribution.

The mathematical expressions represents the sum of a direct attenuated signal (log normal component) and a mutipath signal (Rayleigh component) mainly due to the vegetation shadowing and nearby buildings, etc.

Figure 4.5-1 is samples of a shadowed data set generated using RNG with the input parameter, $\overline{K}$ =3 dB, μ_{dB} = -0.5 dB and σ_{dB} =5 dB. The variation of samples is very similar to the Rayleigh data set, but the shadowed signal was enhanced due to the lognormal data set. The rapidly varying signal (Rayleigh component) and slowly varying signal (logormal component) are blended in the shadowed data set. Barts and Stutzman used these characteristics to separate the Rayleigh component and the lognormal component from the measured data in the VT simulator [2].

The data set was evaluated by comparing the PDF with the analytical model of Section 2.3.1.3 in Figure 4.5-2. The figure shows that the shadowed signal is more spread out than the one of the Rayleigh and lognormal. This was caused by the signal enhancement and signal deterioration due to the phasor sum of Rayleigh and lognormal component.

Figure 4.5-3 is the phase distribution of the simulation result and the analytical model. The phase of the shadowed data set is uniformly distributed because the phase is also the sum of two uniformly distributed phases (Rayleigh component and lognormal component).

Based on these evaluations, the shadowed data set by PROSIM is appropriate for use as a data set to simulate the shadowed propagation path.

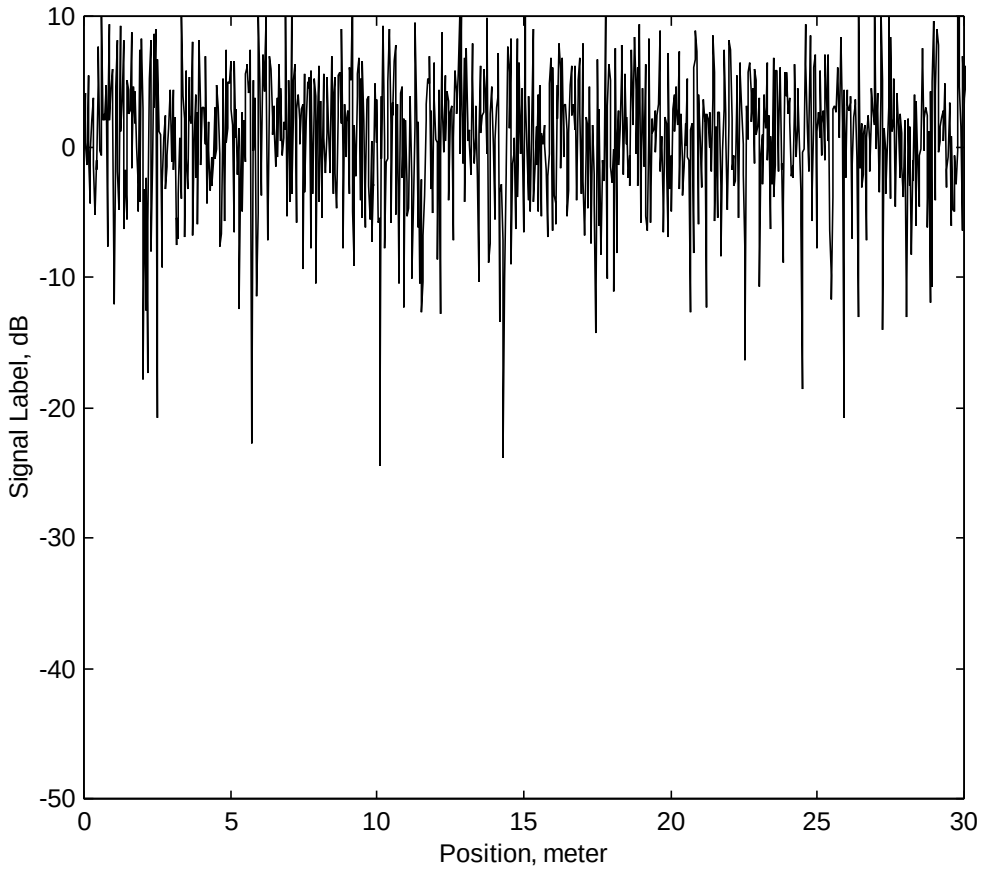

Figure 4.5-1 Samples of Shadowed Data Set spaced 0.1 wavelength apart

($\overline{K}$ = 3 dB, μ_{dB} = -0.5 dB, σ_{dB} = 5 dB)

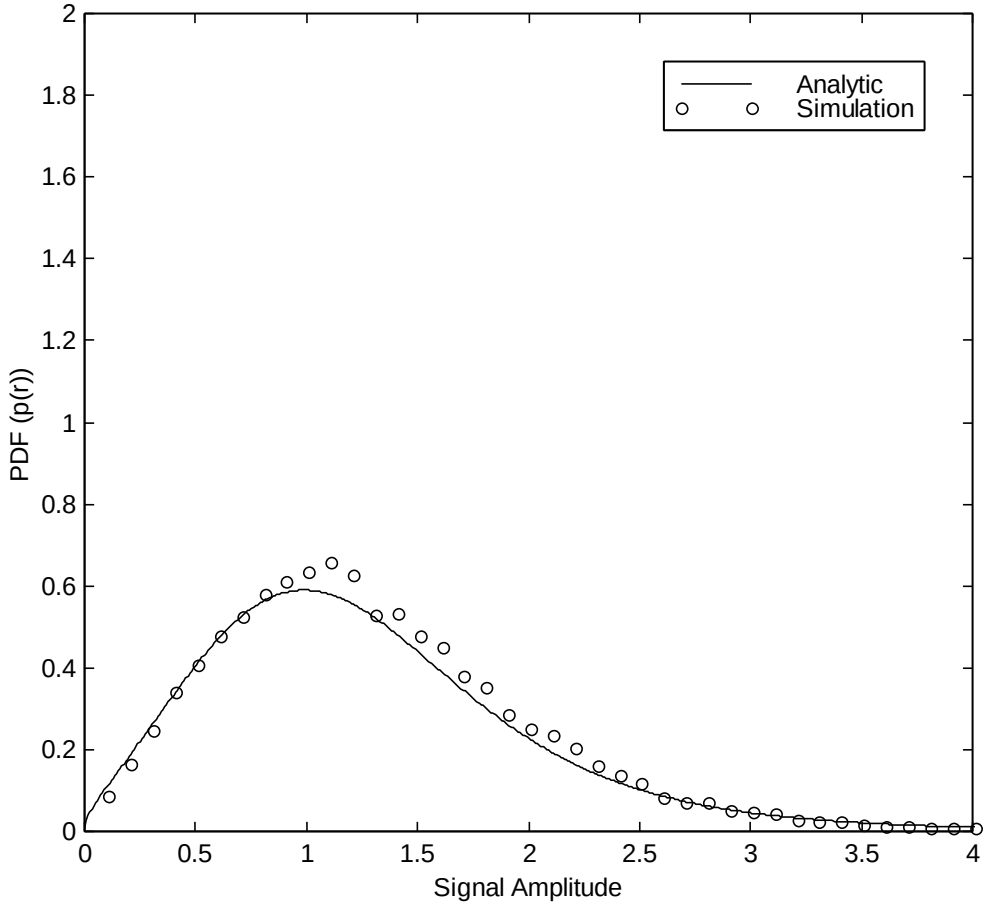

Figure 4.5-2 Shadowed magnitude PDF of the Simulation Data Set and the Analytical Model, equation (2.3-22) ($\overline{K}$ = 3 dB, μ_{dB} = -0.5 dB, σ_{dB} = 5 dB)

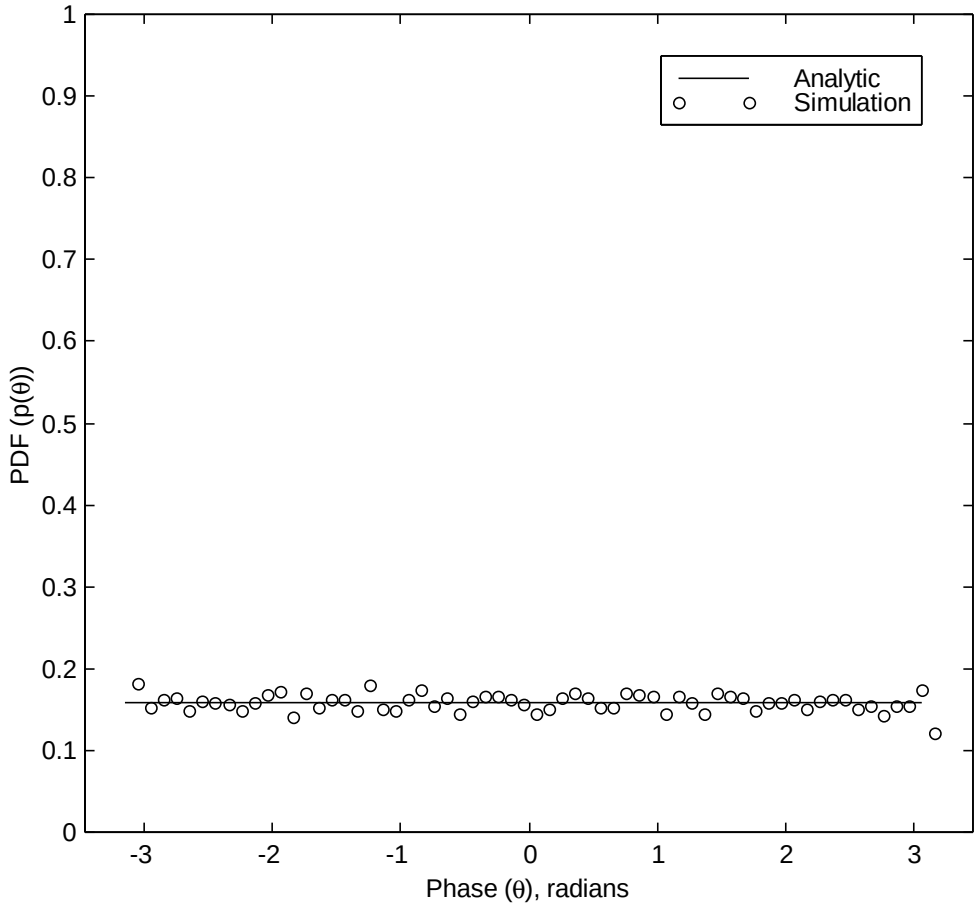

Figure 4.5-3 Shadowed phase PDF, p(θ) of the Simulation Data Set and the Analytical Model

($\overline{K}$ = 3 dB, μ_{dB} = -0.5 dB, σ_{dB} = 5 dB)

4.6 Generation of Total Data Set

A typical path for a mobile vehicle undergoes both unshadowed and shadowed propagation conditions while the percentage of shadowing varies. One of the input parameters, S (percentage of shadowing) was used to generate the total data set. The number of samples in the shadowed data set was reduced by the amount of S% time of the shadowed data set. In the same manner, the number of unshadowed data samples was collected as the amount of the (100-S)% time of the unshadowed data set. The total data set was generated by just concatenating each fraction of the data sets. Figure 4.6-1 shows the samples of the total data set. The shadowed data set lasts up to about 170 meter and after that distance the unshadowed data set was concatenated. The data set was generated using the input parameter as S=50%, K=5 dB, $\overline{K}$ =3 dB, μ_{dB} = -0.5 dB, and σ_{dB} = 5 dB. Unlike the unshadowed and shadowed data set, there is no analytic model for comparing the statistics, except for the CFD. Hence, the simulation results should be compared with the measured data to evaluate its feasibility. Section 4.7 describes the details of several simulation results and compares the results with those from Vogel's measured data.

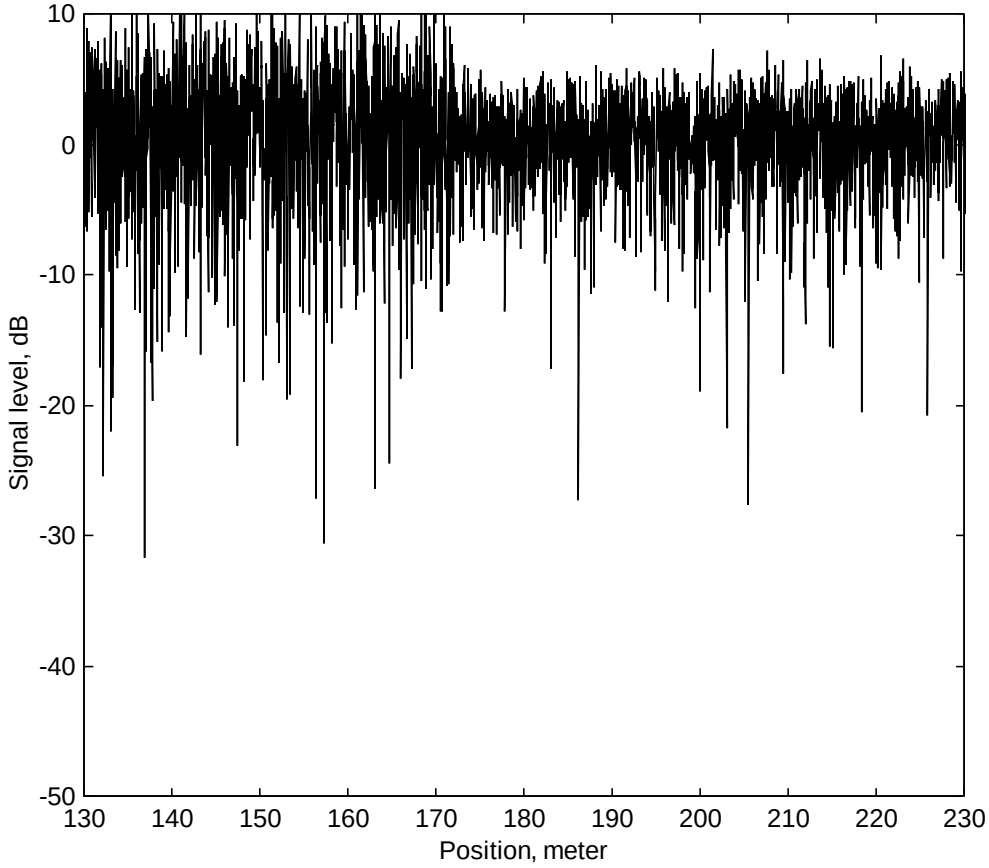

Figure 4.6-1 Samples of Total Data Set spaced 0.1 wavelength apart

(S = 50%, K = 5 dB, $\overline{K}$ = 3 dB, μ_{dB} = -0.5 dB, σ_{dB} = 5 dB)

4.7 Simulation Results

In order to evaluate the feasibility of the total data set, some statistical experiments were performed including the CFD, AFD, LCR, and phase PDF. Moreover, the results were compared with the analytic model, LMSSMOD and Vogel's measured data. In the case of the secondary statistics and phase PDF, there is no analytic model for a mixed path. Hence, the three statistics were compared with Vogel's measured data to evaluate their statistics. The index numbers of measured data and their possible parameter values used in these simulations are described in Table 4.7-1. Every sample in the Table was used to measure the statistics of the measured data and 10,000 samples were used to predict the statistics by PROSIM.

Table 4.7-1 Measured data and its parameter values

Index number	BA181556 Figure 4.7-5 to 4.7-9	BA181740 Figure 4.7-10 to 4.7-14	BA184508 Figure 4.7-15 to 4.7-19
S [%]	6	60	50
K [dB]	13	12	5
$\overline{K}$ [dB]	4.4	0.2	3
m_{dB} [dB]	-4	-2	-0.5
s_{dB} [dB]	4.9	1	5
Number of samples	57261	60040	54601

4.7.1 Comparison of CFD from PROSIM and LMSSMOD

Figure 4.7-1 through 4.7-4 show comparisons between the CFD predicted by LMSSMOD and measured from the simulated data set generated by PROSIM. In order to show the feasibility for both lightly and heavily shadowed propagation conditions, a set of input parameters representing heavy shadowing was included in this simulation. The reason is that there is no data set for representing the heavily shadowed propagation condition in Vogel's measured data. Table 4.7-2 describes the parameters used for comparing the CFD from PROSIM and LMSSMOD. The figures show excellent agreement between the predicted and simulated CFD for both lightly and heavily shadowed conditions.

Table 4.7-2 Parameter values for comparing CFD from PROSIM and LMSSMOD

	Simulation 1 (Figure 4.7-1)	Simulation 2 (Figure 4.7-2)	Simulation 3 (Figure 4.7-3)	Simulation 4 (Figure 4.7-4)
S [%]	6	60	50	92.5
K [dB]	13	12	5	21.5
$\overline{K}$ [dB]	4.4	0.2	3	9.9
m_{dB} [dB]	-4	-2	-0.5	-4.8
s_{dB} [dB]	4.9	1	5	1.7

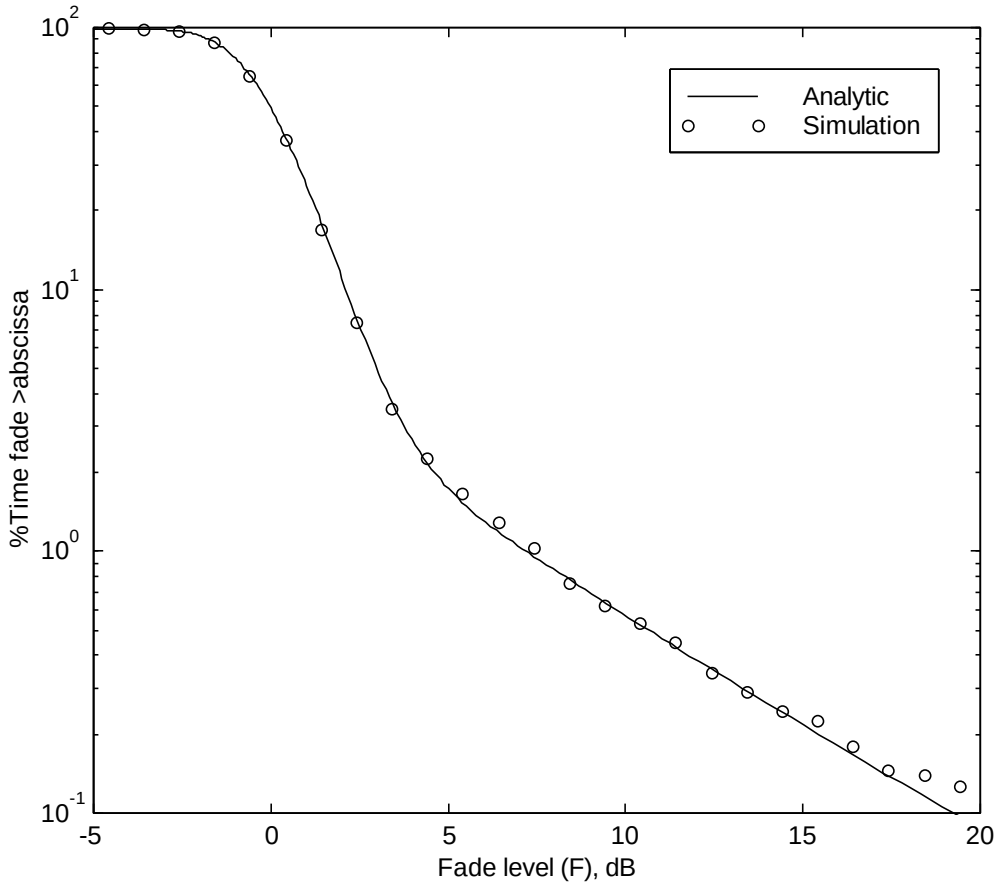

Figure 4.7-1 Comparison of CFD from PROSIM and LMSSMOD

(S = 6%, K = 13 dB, $\overline{K}$ = 4.4 dB, m_{dB} = -4 dB, s_{dB} = 4.9 dB)

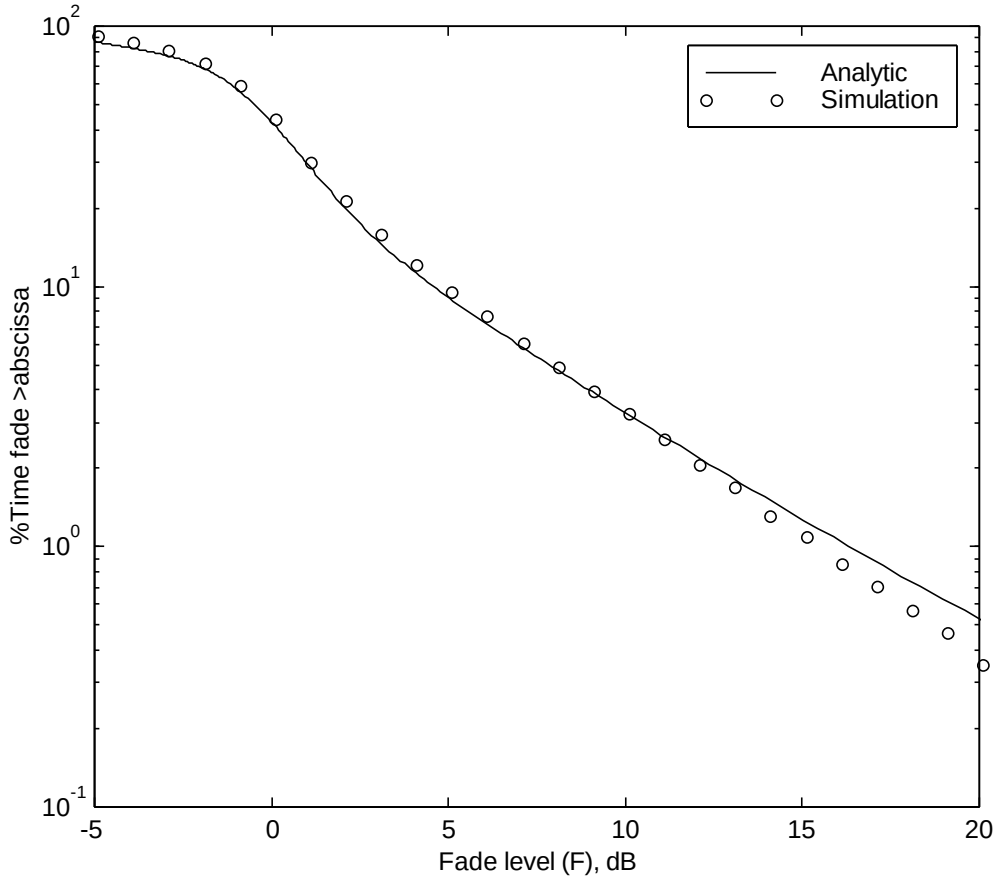

Figure 4.7-2 Comparison of CFD from PROSIM and LMSSMOD

(S = 60%, K = 12 dB, $\overline{K}$ = 0.2 dB, m_{dB} = -2 dB, s_{dB} = 1 dB)

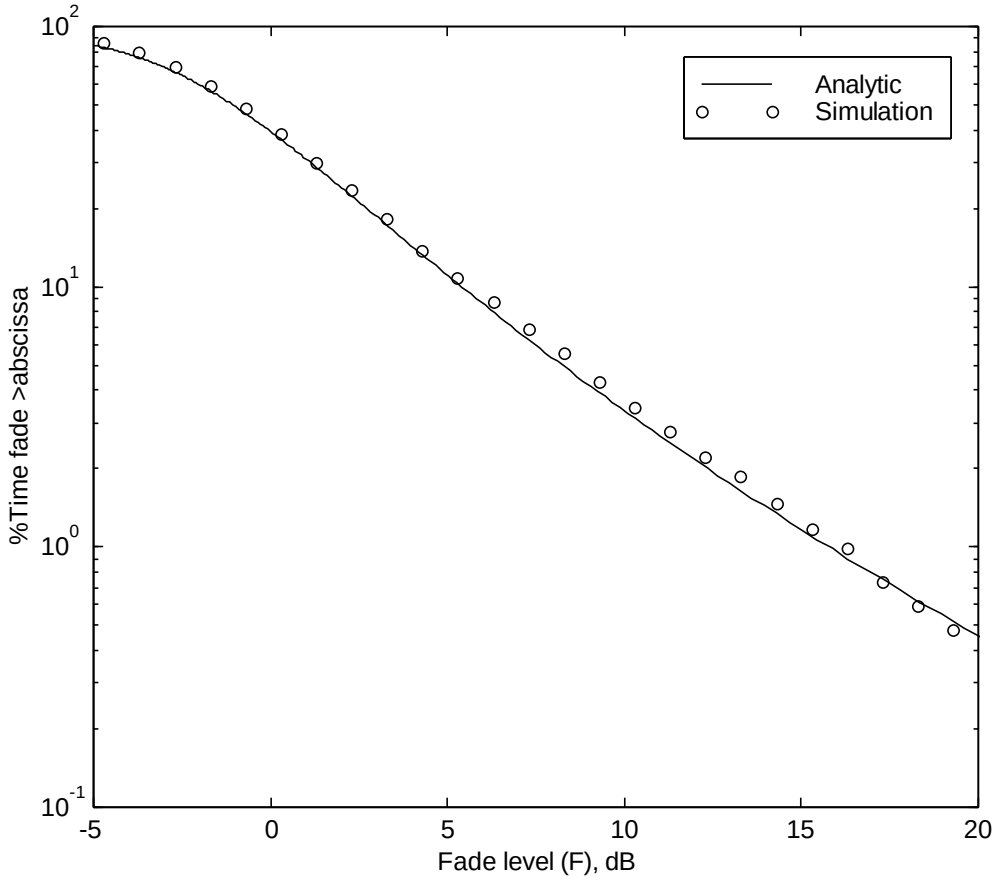

Figure 4.7-3 Comparison of CFD from PROSIM and LMSSMOD

(S = 50%, K = 5 dB, $\overline{K}$ = 3 dB, m_{dB} = -0.5 dB, s_{dB} = 5 dB)

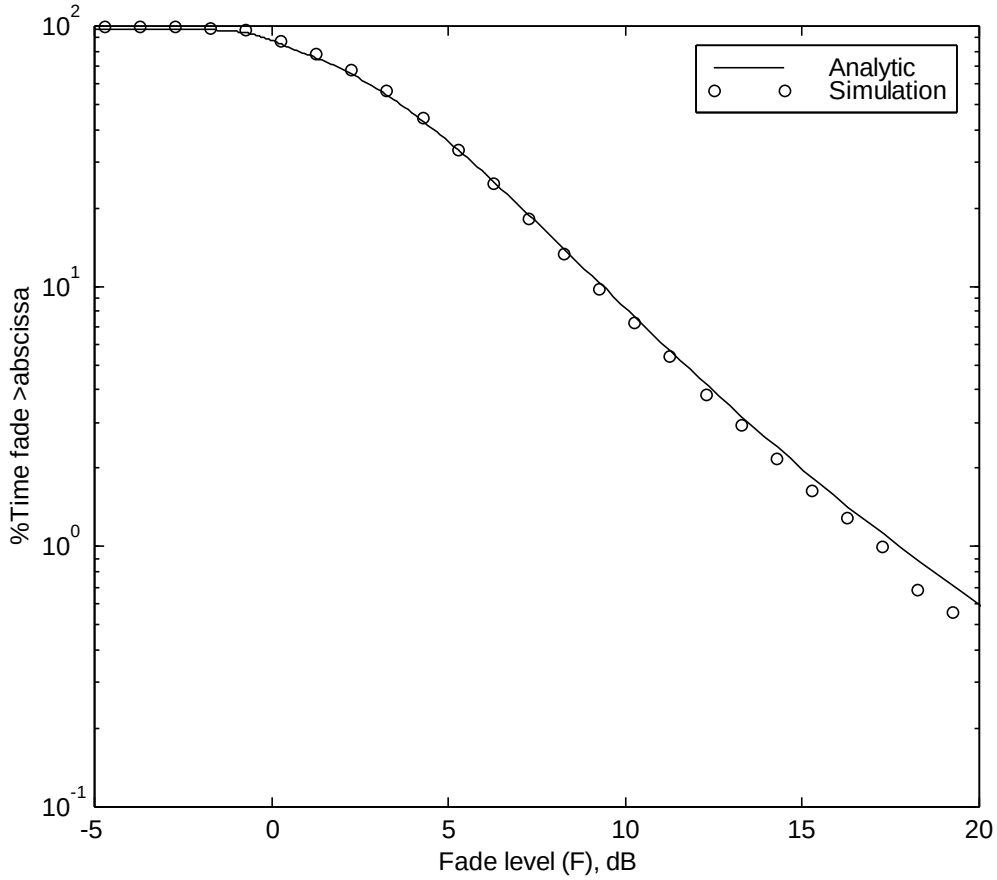

Figure 4.7-4 Comparison of CFD from PROSIM and LMSSMOD

(S = 92.5%, K = 21.5 dB, $\overline{K}$ = 9.9 dB, m_{dB} = -4.8 dB, s_{dB} = 1.7 dB)

4.7.2 Comparison of Statistics from PROSIM and Vogel's measured data

Due to the lack of an analytic model for secondary statistics and phase PDF in the total data set, the statistics of the total data set from PROSIM were compared with Vogel's measured data. Three measured data sets in Table 4.7-1 were employed in this simulation. The BA181556 data represents the lightly shadowed propagation condition, the BA181740 data has similar parameter values to those of the overall measured data through Route 108 in Central Maryland in Table 3.2-1, and the BA184508 data represents the case of very low carrier-to-multipath power ratio condition. CFD, AFD, LCR, and phase PDF from PROSIM were calculated and compared with the results from Vogel's measured data.

4.7.2.1 Comparison of Statistics from PROSIM and BA181556

Figure 4.7-5 represents typical samples of Vogel's measured data BA181556 and the corresponding simulated data. In the measured data, two large signal enhancements were found at about 480 meter and 520 meter traveling distance. The signal enhancement is about 8 dB. Except for the signal enhancement in the measured data samples, the trend of the measured data is similar to that of the simulated data from PROSIM. Figure 4.7-6 through 4.7-9 show comparisons between statistics predicted by PROSIM and extracted from Vogel's measured data. They show excellent agreement between simulated and measured statistics. The small dip at a fade level of -8 dB in the AFD and LCR plot may be caused by an 8 dB signal enhancement. The phenomenon of signal enhancement is a statistically unusual case and is hard to generate by simulator. The secondary statistics, AFD and LCR were normalized by maximum doppler frequency so the unit of the statistics is l (wavelength) for normalized AFD and is $1/l$ (crossings per wavelength) for normalized LCR. The normalized AFD can be interpreted as how much average fade occurred at the fade level and the amount is represented by multiples of the wavelength.

The normalized LCR can be interpreted as how many times the data samples cross the fade level during one wavelength traveling distance and the amount is represented by the number of crossings per wavelength. At fade level 0 dB the curve of the normalized AFD and LCR changed abruptly for both measured data and simulated data. It means that most of the signal is concentrated about 0 dB and the Rician component is dominant in the traveling path. Figure 4.7-9 shows the comparison of the phase PDF, $p(q)$ from measured data and PROSIM. They are matched well in all phase angles from -π to π. Most of the phase was distributed around 0 radians and the phase disappeared after ± 0.5 radians. The characteristics of the phase distribution are very similar to those of the Rician phase distribution in Figure 4.3-4 of Section 4.3. The phase distribution supports the assumption that the BA181556 data was collected through an almost unshadowed propagation path.

Based upon these evaluations, PROSIM works well for generating the data set, which has similar characteristics to measured data collected through lightly shadowed propagation condition.

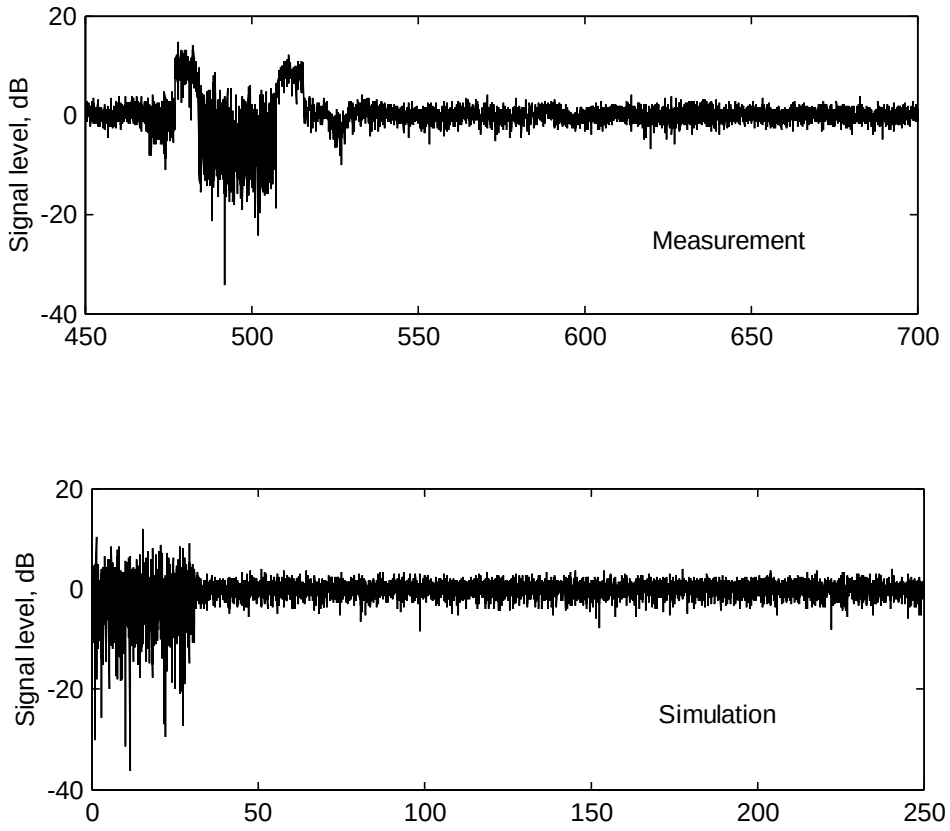

Figure 4.7-5 Comparison of data samples from PROSIM and BA181556 measured data (Simulation 1: S = 6%, K = 13 dB, $\overline{K}$ = 4.4 dB, m_{dB} = -4 dB, s_{dB} = 4.9 dB)

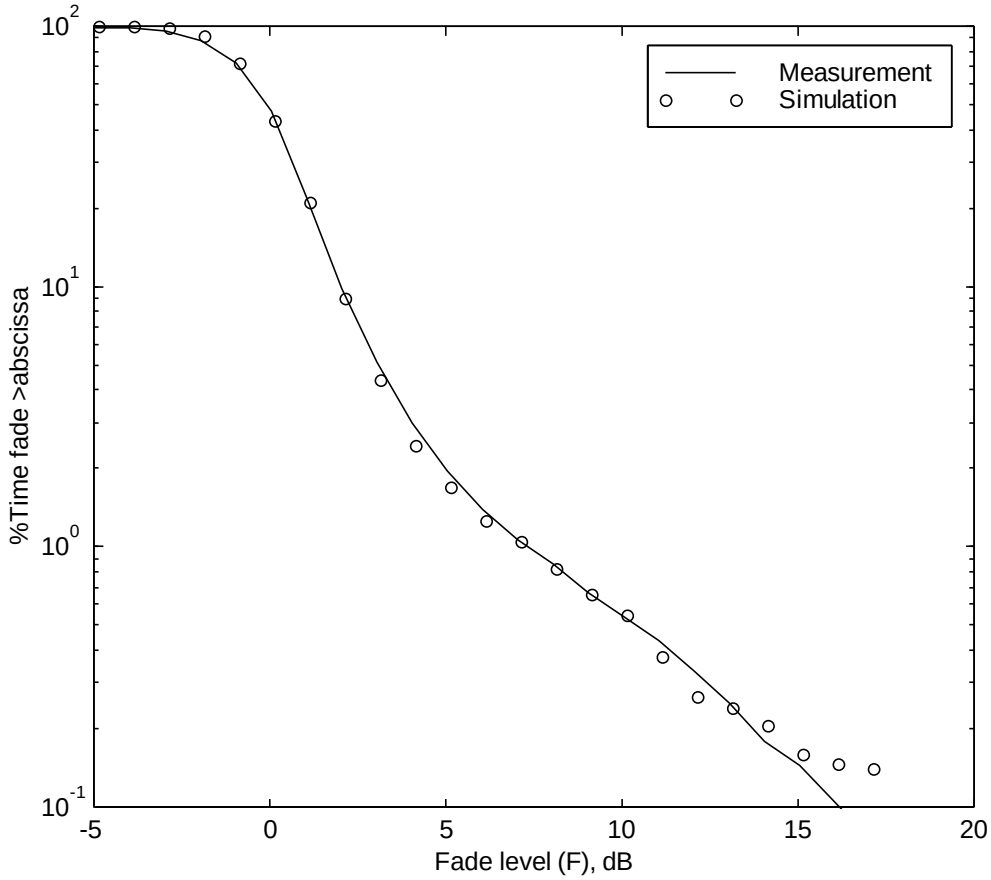

Figure 4.7-6 Comparison of CFD from PROSIM and BA181556 measured data

(Simulation 1: S = 6%, K = 13 dB, $\overline{K}$ = 4.4 dB, m_{dB} = -4 dB, s_{dB} = 4.9 dB)

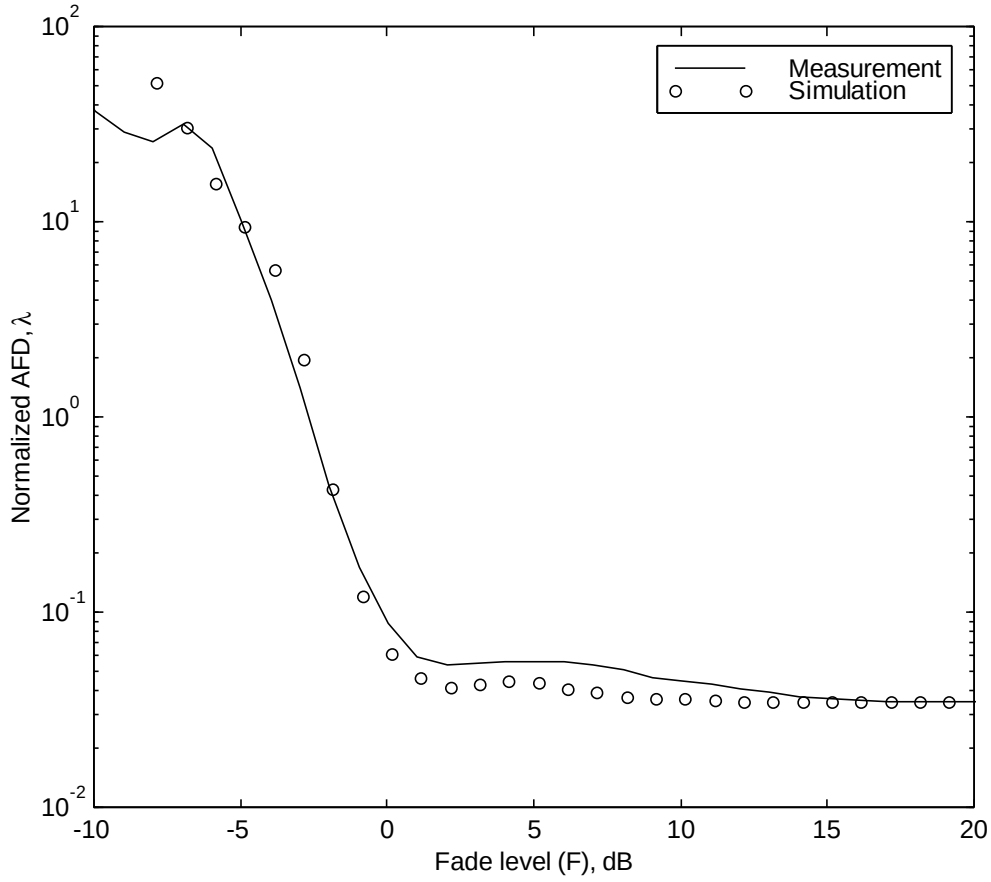

Figure 4.7-7 Comparison of normalized AFD from PROSIM and BA181556 measured data (Simulation 1: S = 6%, K = 13 dB, $\overline{K}$ = 4.4 dB, m_{dB} = -4 dB, s_{dB} = 4.9 dB)

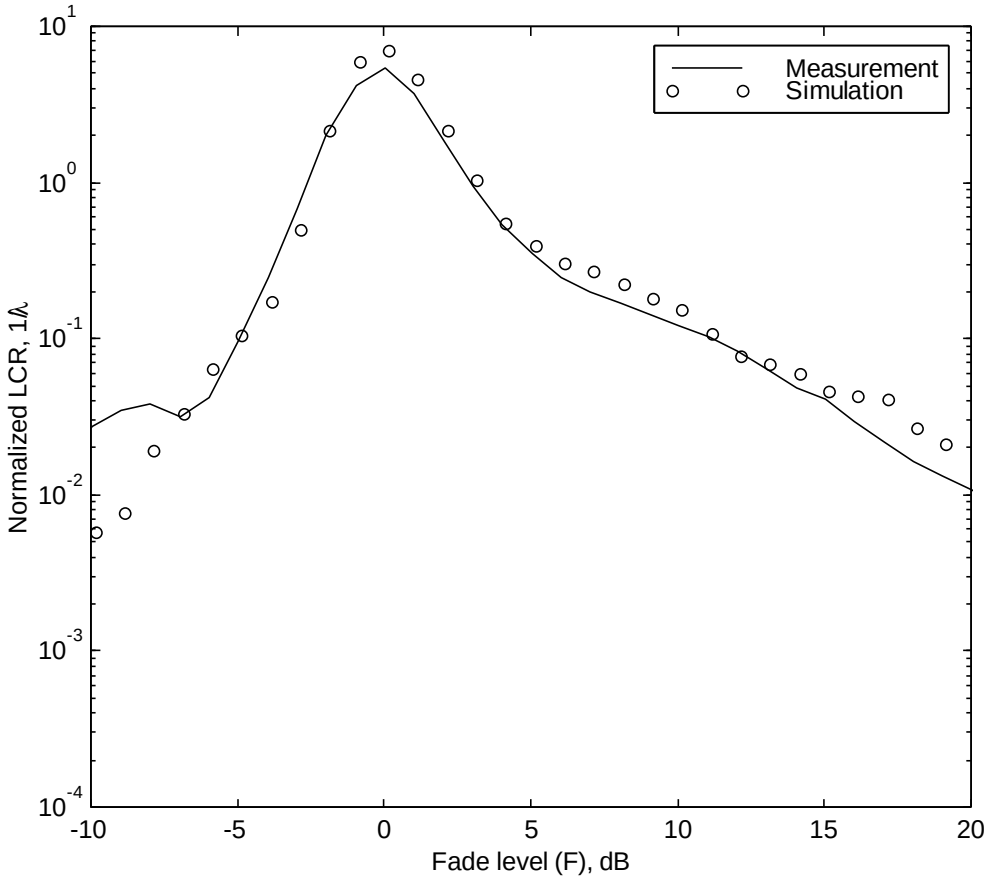

Figure 4.7-8 Comparison of normalized LCR from PROSIM and BA181556 measured data (Simulation 1: S = 6%, K = 13 dB, $\overline{K}$ = 4.4 dB, m_{dB} = -4 dB, s_{dB} = 4.9 dB)

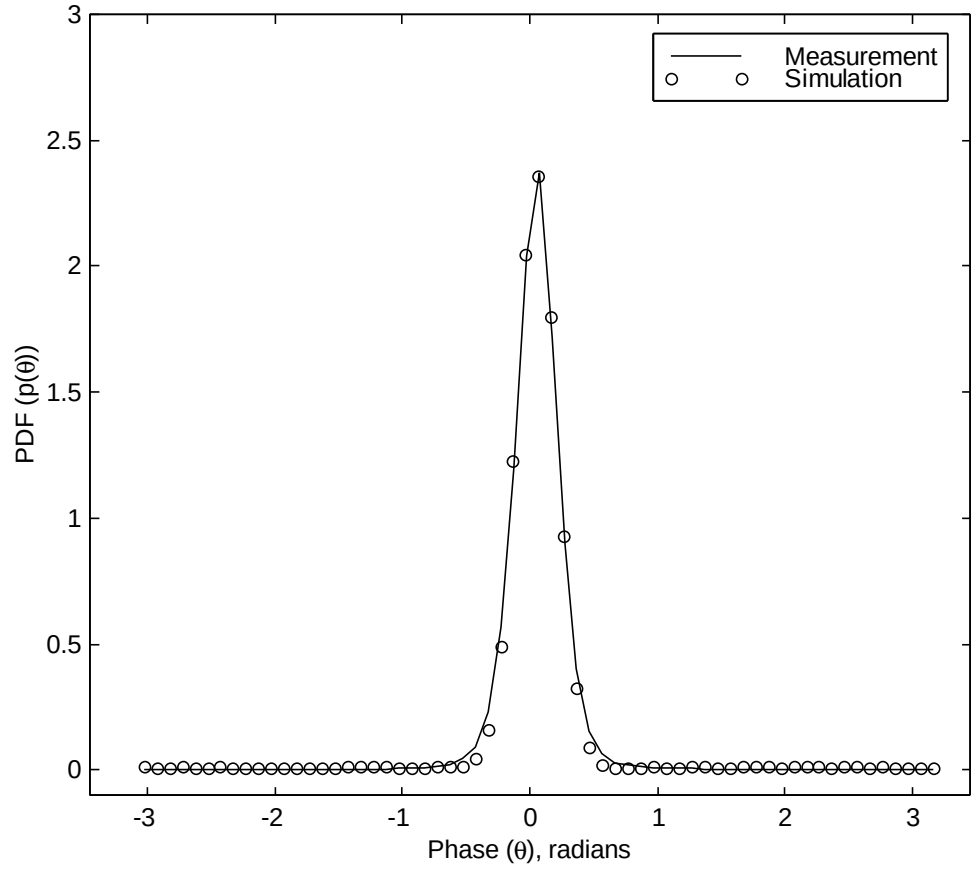

Figure 4.7-9 Comparison of phase PDF, $p(q)$ from PROSIM and BA181556 measured data (Simulation 1: S = 6%, K = 13 dB, $\overline{K}$ = 4.4 dB, m_{dB} = -4 dB, s_{dB} = 4.9 dB)

4.7.2.2 Comparison of Statistics from PROSIM and BA181740

BA181740 data was selected because its statistics are very similar to the overall statistics of the concatenated data described in Section 3.2.2. Figure 4.7-10 represents typical samples of data BA181740 and its corresponding simulated data. The trend of measured data is similar to that of simulated data from PROSIM. Figure 4.7-11 through 4.7-14 show comparisons between statistics predicted by PROSIM and extracted from Vogel's measured data. They show excellent agreement between simulated and measured statistics. The curve of the normalized AFD and LCR was more spread out than that shown in Figure 4.7-12 and 4.7-13 for both measured data and simulated data. It means that some of the shadowed data samples, which are largely composed of mutipath components, were also collected in addition to the unshadowed data samples from the traveled path. The parameters extracted from BA181740 are described in Table 4.7-1. Figure 4.7-14 shows the comparison of the phase PDF, $p(q)$ from measured data and PROSIM. They are matched well in all phase angles from $-\pi$ to π. The phase is mainly distributed around 0 radians but the small amount of phase exists all over the range. The amount of phase PDF at 0 radian is smaller than the one in Figure 4.7-9. It means that BA181740 data is blended with the shadowed components and unshadowed components by some ratio.

Based upon these evaluations, PROSIM works well for generating the data set, which has similar characteristics to measured data collected through the intermediately shadowed propagation condition.

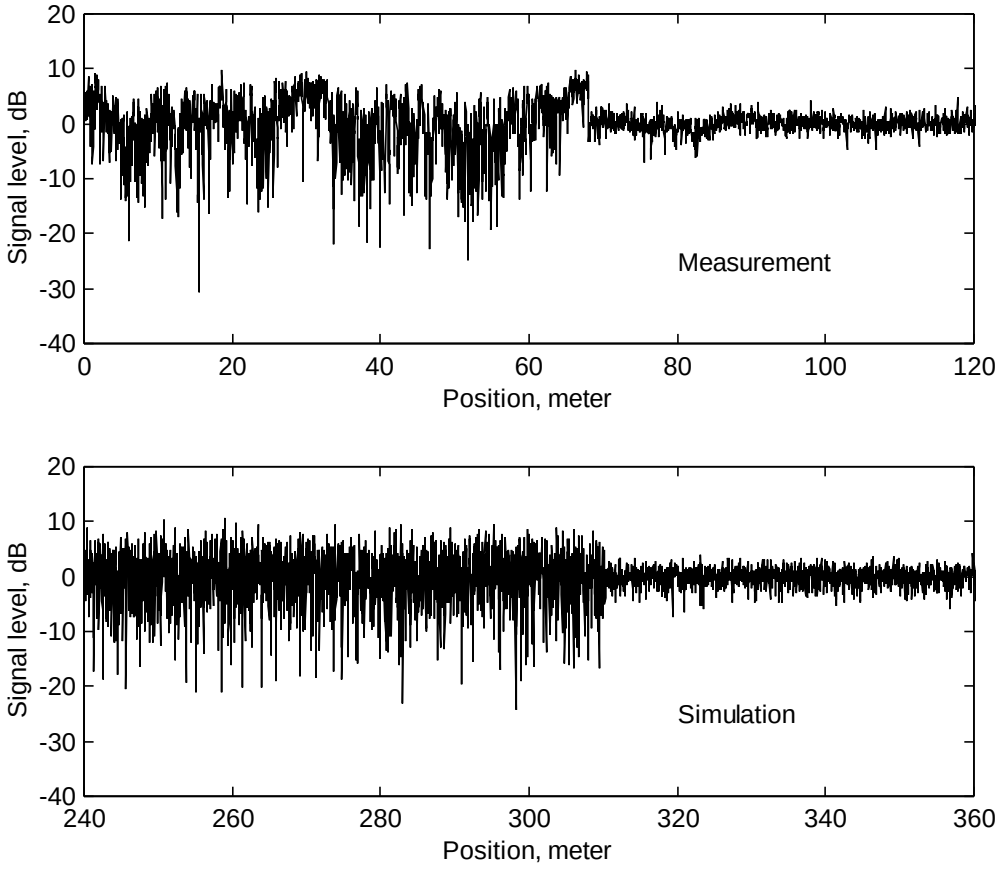

Figure 4.7-10 Comparison of data samples from PROSIM and BA181740 measured data (S = 60%, K = 12 dB, $\overline{K}$ = 0.2 dB, m_{dB} = -2 dB, s_{dB} = 1 dB)

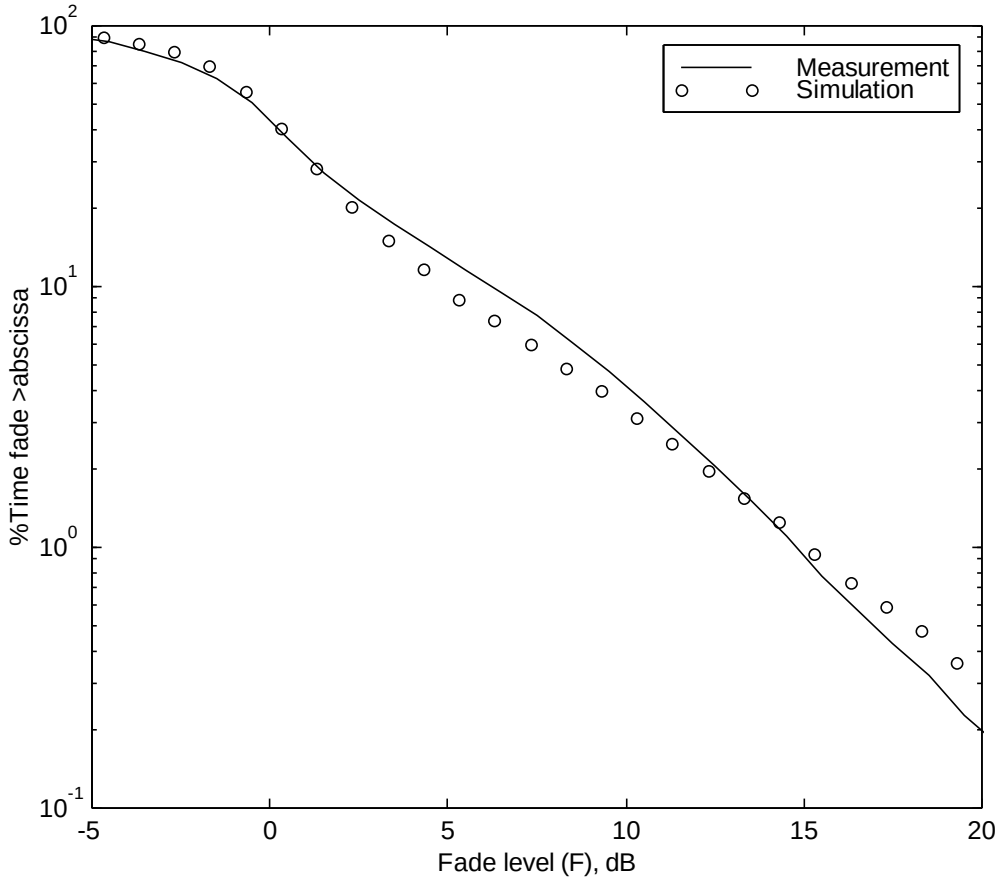

Figure 4.7-11 Comparison of CFD from PROSIM and BA181740 measured data (S = 60%, K = 12 dB, $\overline{K}$ = 0.2 dB, m_{dB} = -2 dB, s_{dB} = 1 dB)

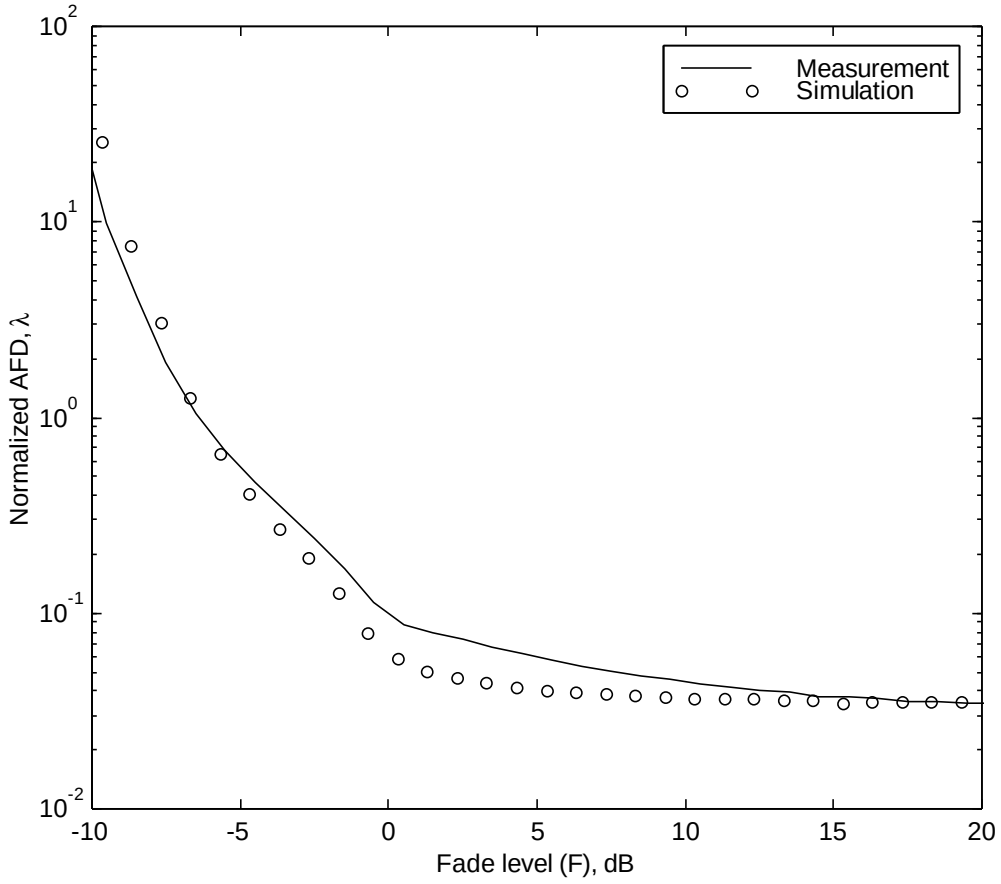

Figure 4.7-12 Comparison of normalized AFD from PROSIM and BA181740 measured data (S = 60%, K = 12 dB, $\overline{K}$ = 0.2 dB, m_{dB} = -2 dB, s_{dB} = 1 dB)

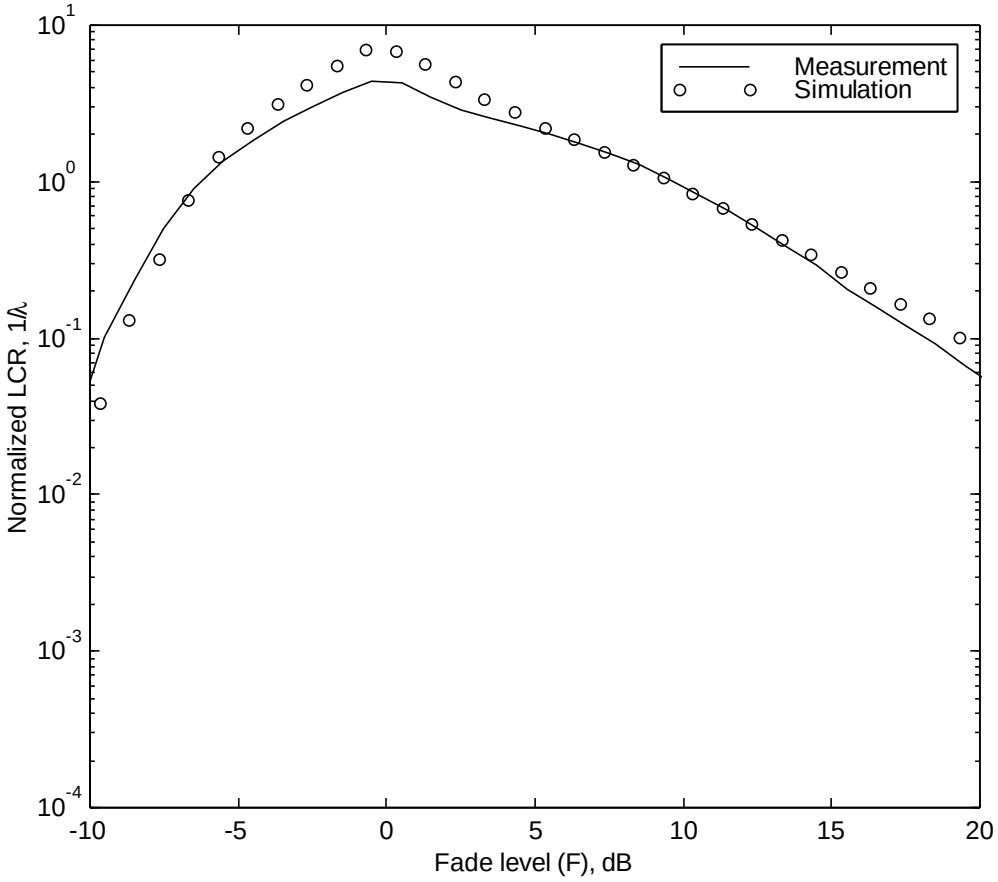

Figure 4.7-13 Comparison of normalized LCR from PROSIM and BA181740 measured data (S = 60%, K = 12 dB, $\overline{K}$ = 0.2 dB, m_{dB} = -2 dB, s_{dB} = 1 dB)

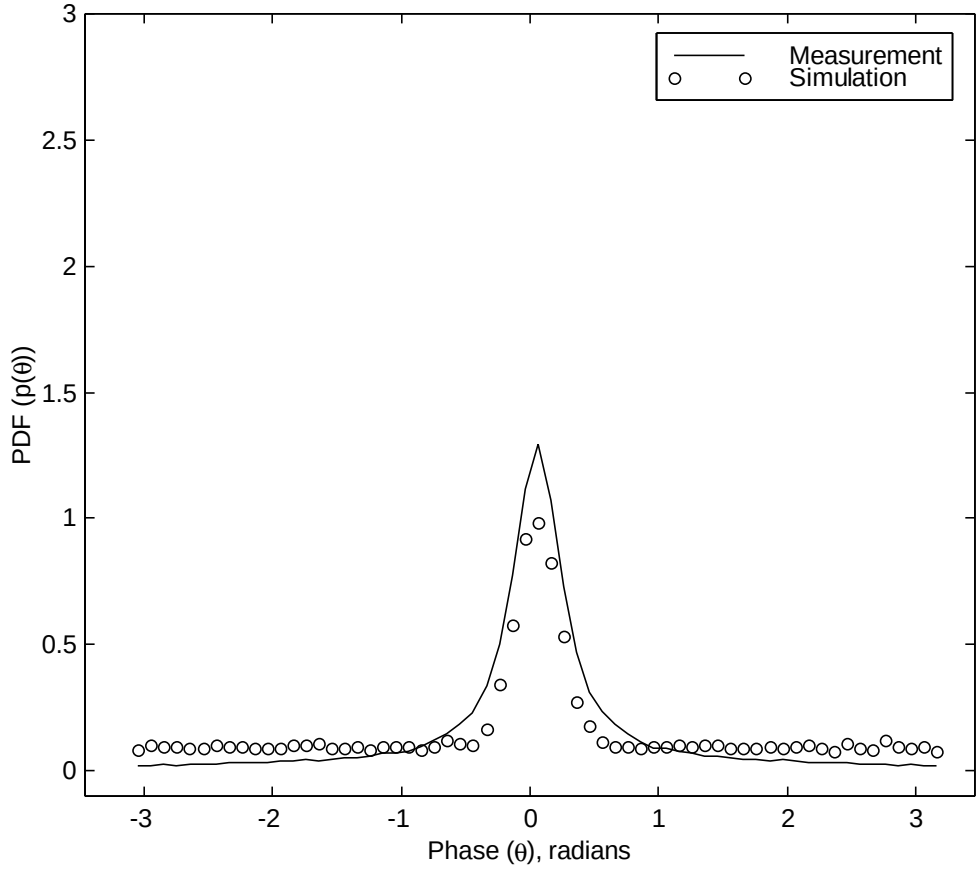

Figure 4.7-14 Comparison of phase PDF, $p(q)$ from PROSIM and BA181740 measured data (S = 60%, K = 12 dB, $\overline{K}$ = 0.2 dB, m_{dB} = -2 dB, s_{dB} = 1 dB)

4.7.2.3 Comparison of Statistics from PROSIM and BA184508

BA184508 data was selected because the phase distribution has an interesting curve, that is, the phase angles are distributed all over the 0 to 2π range with some significant quantities. Figure 4.7-15 represents typical samples of data BA184508 and its corresponding simulated data. The trend of measured data is similar to that of simulated data from PROSIM. Figure 4.7-16 through 4.7-19 show comparisons between statistics predicted by PROSIM and extracted from Vogel's measured data. They show excellent agreement between simulated and measured statistics. The normalized AFD and LCR are similar to the one of Figure 4.7-17 and 4.7-18, but the phase distribution is quite different from them. The phase PDF has significant values for all angles in BA184508 data. In the case of BA181740 described in Section 4.7.2.2, the Rician carrier-to-multipath ratio (K) was quite high (about K=12 dB), but BA184508 has quite low Rician carrier-to-multipath ratio (about K=5 dB). It means that there are a lot of high power mutipath components due to signal reflections from the surrounding environment. Hence, the LOS signal deteriorated due to the multipath component and the uniform phase distribution in multipath components became effective to total phase distribution. Figure 4.7-19 shows the phase PDF for BA184508. The peak value of phase PDF is smaller than that in Figure 4.7-14 even though the percentage of shadowing (S=50%) is smaller than that in Figure 4.7-14 (S=60%). The phase distribution is mainly determined by Rician carrier-to-multipath power ratio only if the percentage of shadowing is not significantly high or low.

Based upon these evaluations, PROSIM works well for generating the data set, which has similar characteristics to measured data collected through a severe mutipath channel. The PROSIM generated data set, which corresponds to input parameters and its primary statistics and secondary statistics were also matched well for all data set. The phase PDF was also considered to verify the feasibility of PROSIM.

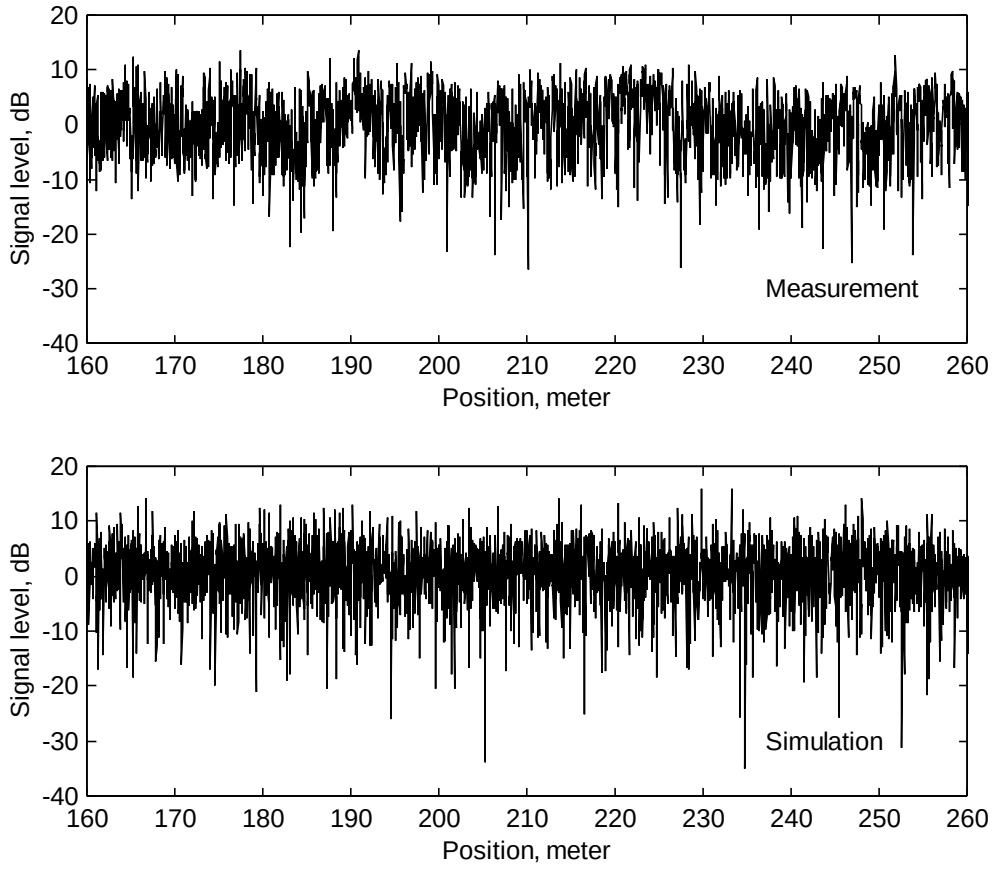

Figure 4.7-15 Comparison of data samples from PROSIM and BA184508 measured data (S = 50%, K = 5 dB, $\overline{K}$ = 3 dB, m_{dB} = -0.5 dB, s_{dB} = 5 dB)

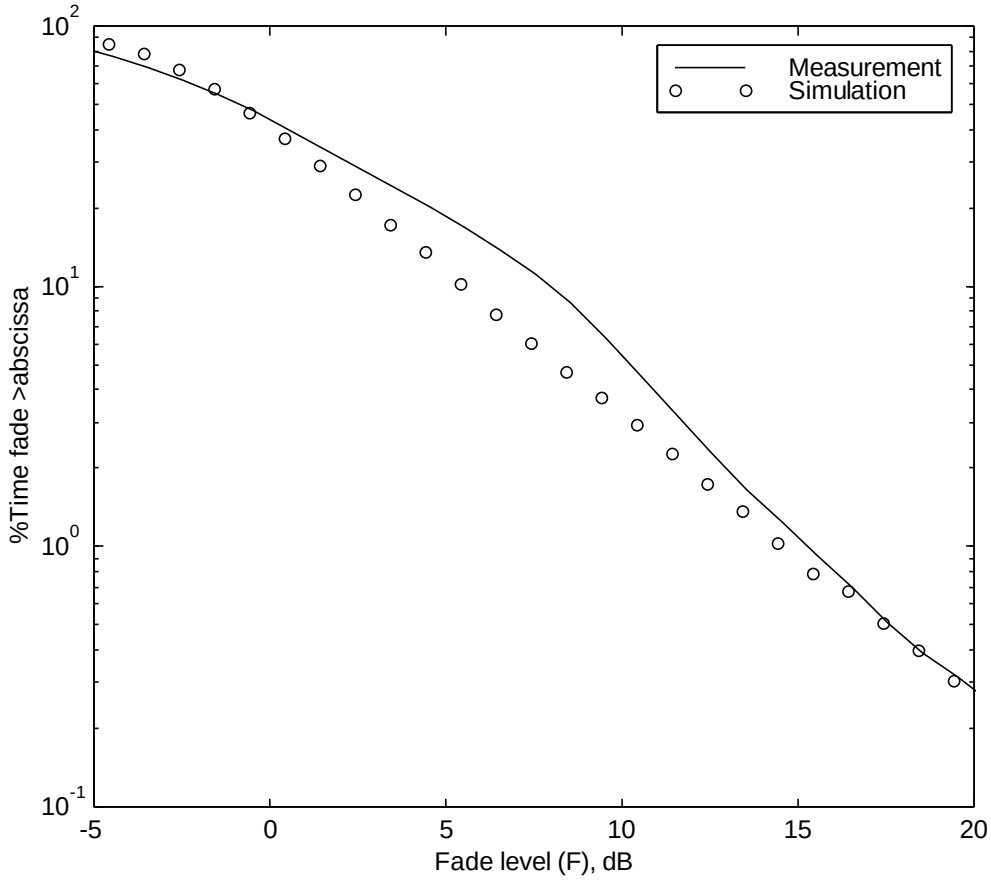

Figure 4.7-16 Comparison of CFD from PROSIM and BA184508 measured data (S = 50%, K = 5 dB, $\overline{K}$ = 3 dB, m_{dB} = -0.5 dB, s_{dB} = 5 dB)

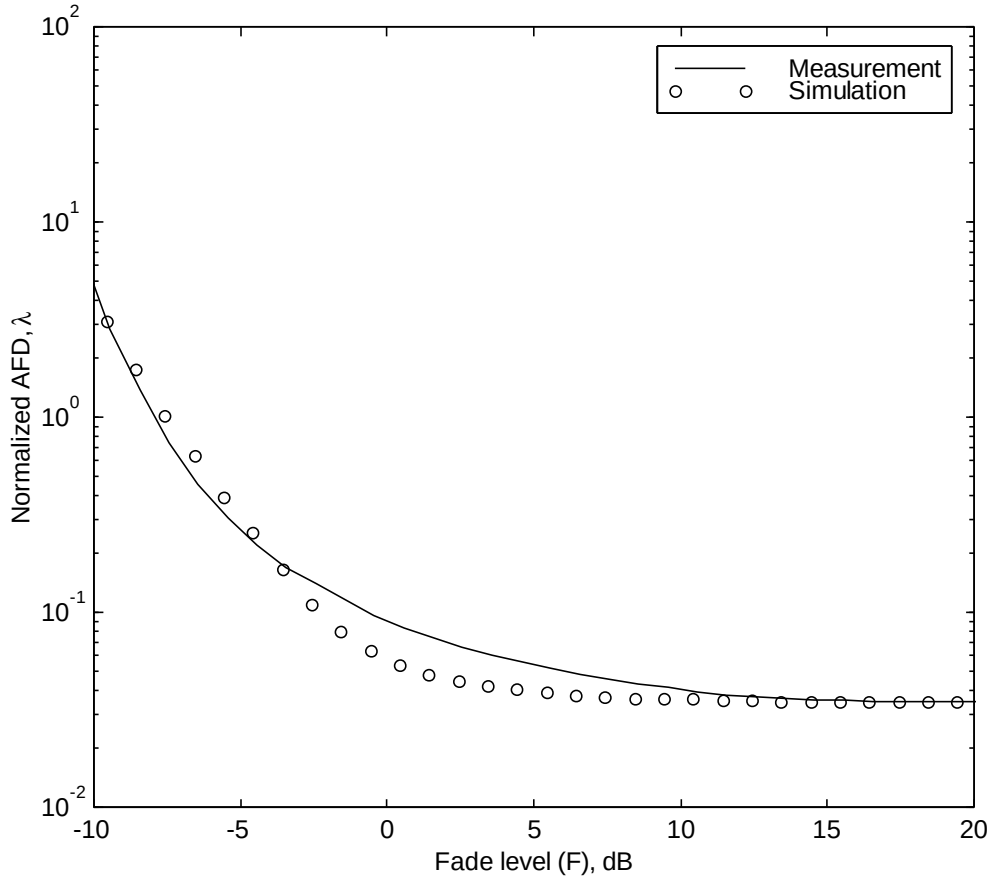

Figure 4.7-17 Comparison of normalized AFD from PROSIM and BA184508 measured data (S = 50%, K = 5 dB, $\overline{K}$ = 3 dB, m_{dB} = -0.5 dB, s_{dB} = 5 dB)

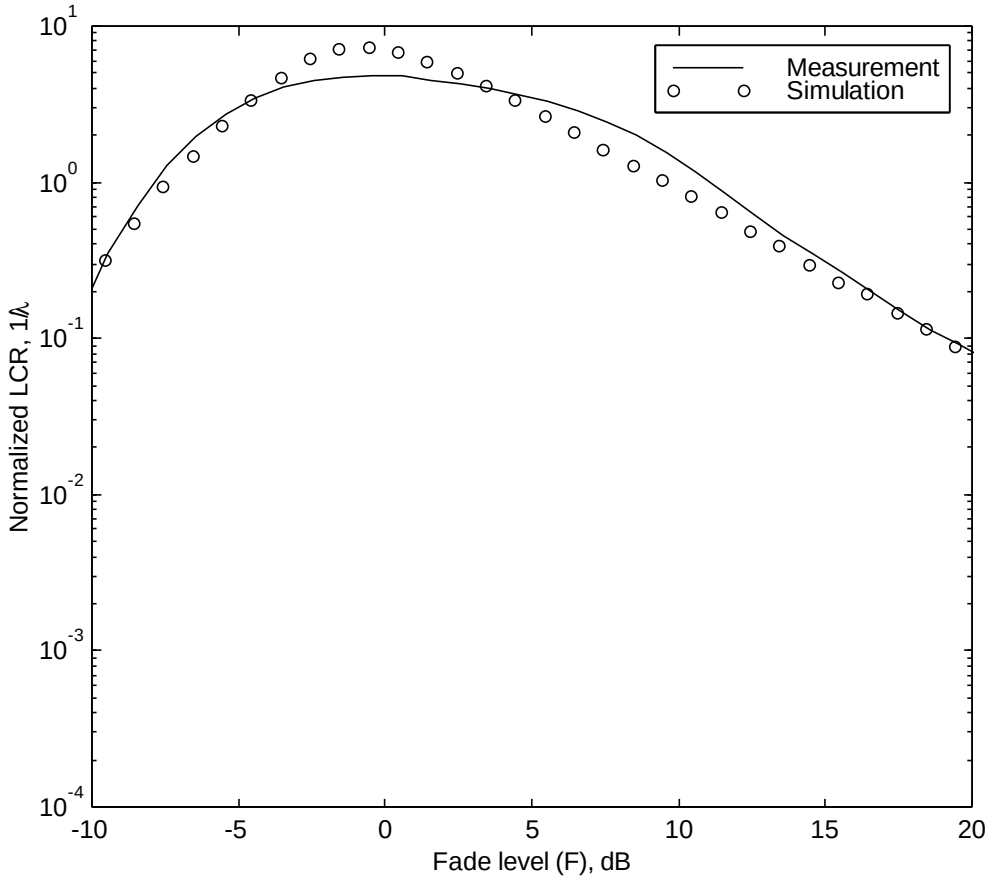

Figure 4.7-18 Comparison of normalized LCR from PROSIM and BA184508 measured data (S = 50%, K = 5 dB, $\overline{K}$ = 3 dB, m_{dB} = -0.5 dB, s_{dB} = 5 dB)

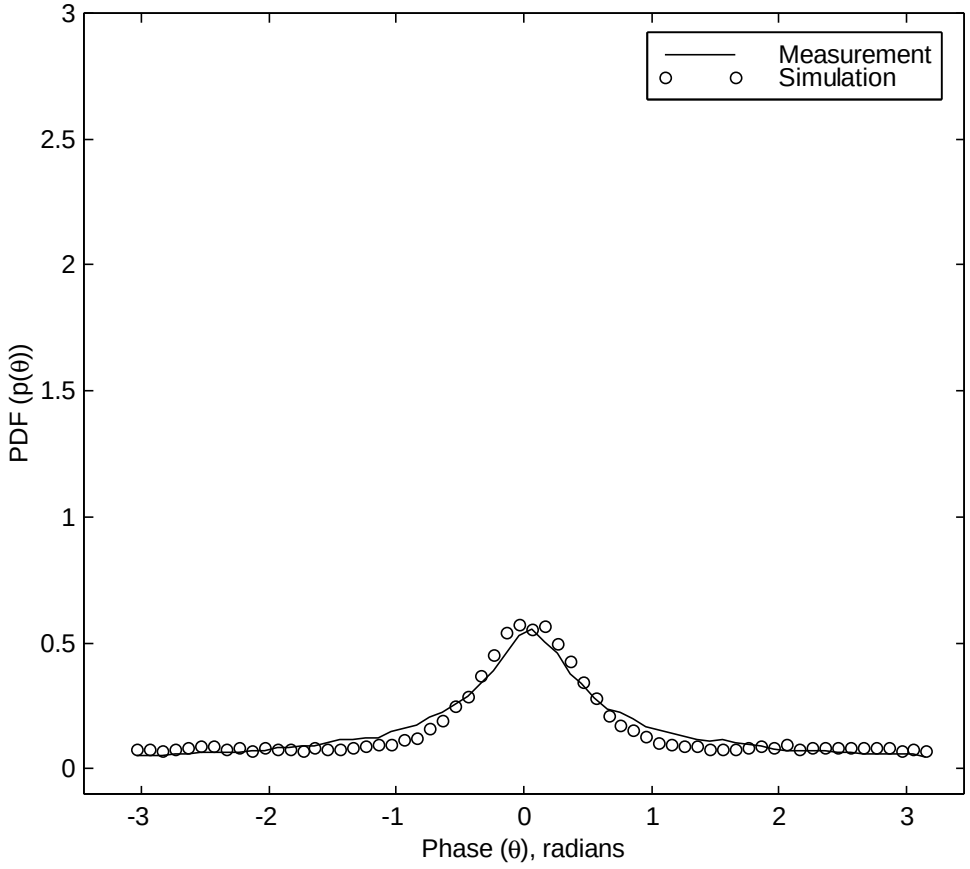

Figure 4.7-19 Comparison of phase PDF, $p(q)$ from PROSIM and BA184508 measured data (S = 50%, K = 5 dB, $\overline{K}$ = 3 dB, m_{dB} = -0.5 dB, s_{dB} = 5 dB)

Chapter 5. Conclusions and Recommendations

In this report, we discussed a software simulator, called PROSIM, that uses a random number generator to generate a data set for predicting statistics of a propagation path. The corresponding propagation path statistics were also extracted and were compared with analytical model, LMSSMOD and Vogel's measured data. The data set was produced by combining data sets such as Rayleigh, Rician, lognormal, and a shadowed data set. In order to get each data set corresponding input parameters, a proper scaling operation of the random numbers was performed.

The most significant results of this study are:

1. PROSIM generates an excellent data set for predicting statistics of a propagation path between a satellite and a mobile user in that the statistics used in evaluating the performance of PROSIM are matched well both with the analytical model, LMSSMOD and Vogel's measured data. The statistics include CFD, AFD, LCR, and phase PDF. In the previous VT simulator, only the CFD was matched well with LMSSMOD and measured data. For secondary statistics, AFD and LCR, the VT simulator was not satisfactory to predict the dynamics of the propagation path. Moreover, in the VT simulator, no attempt was made to evaluate the phase PDF.

2. Even though PROSIM uses different random numbers for each individual simulation, the simulation results are almost identical for the same input parameters. (Generally, it was hard to discern the difference when we used several different random numbers generated in MATLAB.) However, the VT simulator provides quite different simulation results with different universal data sets.

3. While the operating frequency band of VT simulator is limited within UHF and L band, PROSIM is not restricted to any particular frequency band because random number used in PROSIM is not a function of frequency.

4. A lognormal phasor plot in the complex plane and its mathematical expression was derived in Section 4.4 (Equation (4.4-2) and Figure 4.4-1). It is very helpful to understand, to model, and to simulate the lognormal channel because the lognormal channel is the most significant channel among LMSS propagation paths in determining the whole statistics. A good lognormal data set will provide a good total data set. If we use the lognormal phasor plot and its mathematical expression, a good lognormal data set will be obtained, just as we get Rayleigh and Rician data sets using phasor plots in Section 4.2 and 4.3.

Recommendations for future study follows.

1. A program for estimating the parameters from measured data should be developed to predict the real propagation situation. The extracted parameters must be used as an input of PROSIM and its simulation results such as CFD, AFD, LCR, and phase PDF are to be matched well with the statistics of measured data. The author developed the initial version of the parameter-estimating program and used some results in this study. However, it needs to be modified to estimate proper parameters automatically.

2. The results here were all for an omnidirectional mobile antenna. Reliability of the LMSS is also determined by performance of antenna and terminal. Inclusion of the antenna patterns through a propagation condition will be a good project.

3. In order to improve the performance of a communications system, a diversity technique such as spatial diversity or polarized diversity is often employed. Simulation of the diversity gain using the simulated data set by PROSIM will also be a good project.

4. Development of software for a Mobile Satellite Channel Simulator will be a promising project. It will evaluate the bit-error-rate (BER) performance of new modulation and coding schemes for use in mobile satellite systems through certain propagation conditions, integrating PROSIM into a channel simulator to produce a realistic signal path so that the modulation and coding schemes can be evaluated for performance under realistic conditions

References

1. J. Aichison and J. A. C. Brown, *The Lognormal Distribution*, Cambridge University Press, London, 1957.
2. R. M. Barts, W. L. Stutzman, "Modeling and simulation of mobile satellite propagation," IEEE Trans. On Antenna and Propagation, vol. AP-40, no.4, April 1992.
3. P. Beckmann, *Probability in Communication Engineerings*, Harcourt, Brace &World, NY, 1967.
4. P. Beckmann and A. Spizzichino, *The Scattering of Electromagnetic Waves from Rough Surfaces*, Pergamon Press, NY, 1963.
5. W. S. Bradley and W. L. Stutzman, "Propagation modeling for land mobile satellite communications," Virginia Tech Report EE Satcom 85-3, performed for JPL sponsored by NASA under contract 956512, August 1985.
6. J. S. Butterworth, "The description and evaluation of a mobile satellite communications channel simulator," Proceedings of the Propagation Workshop in support of MSAT-X, JPL, Pasadena, CA, Jan. 1985.
7. R. L. Campbell and R. Estus, "Attenuated direct and scattered wave propagation on simulated land mobile satellite service paths in the presence of trees," *Proceedings of the Mobile Satellite Conference*, JPL Publication 88-9, Pasadena, CA, May 3-5, 1988.
8. F. Daravian, "Channel simulation to facilitate mobile-satellite communications research," IEEE Trans. on Communications, vol. COM-35, no. 1,Jan. 1987.

9. W. L. Flock, *Propagation Effects on Satellite Systems at Frequencies Below 10 GHz*, NASA Reference Publication 1108(02), 1987
10. J. G. Gardiner, "Satellite services for mobile communication," Telecommunications, North American Edition, vol. 20, no 8, pp. 34-41, Aug. 1986.
11. J. Goldhirsh and W. J. Vogel, "Roadside Tree Attenuation Measurements at UHF for Land Mobile Satellite Systems" IEEE Trans. On Antenna and Propagation, vol. AP-35, no.5, May 1987.
12. W. C. Jakes, *Microwave Mobile Communication*, John Wiley & Sons, NY, 1974.
13. V. Jamnejad, " Ground Multi-path in TOPEX's precisio orbit determination tracking system," JPL Interoffice Memorandum 3365-84-003, Jet Propulsion Lab., Pasasdena, CA, Jan. 9, 1985.
14. A. Kumar, *Fixed and Mobile Terminal Antennas*, Boston, Artech, 1991.
15. C. Loo, "A statistical model for a land mobile satellite link," IEEE Trans. Vech. Technol., vol VT-34, pp. 122-127, Aug. 1985.
16. E. Lutz, et al., "Land mobile satellite communications – channel model, modulation, and error control," Proceedings of 7th International Conference on Digital Satellite Communications, Munich, May 12-16, 1986.
17. E. Lutz, et al., "The Land Mobile Satellite Communication Channel-Recording, Statistics, and Channel Model," IEEE Trans. on Vehicular Technology, vol. 40, no. 2, pp.375-386, May 1991.
18. Mathworks Inc., *MATLAB manual*, ver 4.2c,
19. A. Papoulis, *Probability Random Variables and Stochastic Processes*, 3rd edition, McGraw Hill, NY 1991.
20. T. S. Rappaport, *Wireless Communications*, Prentice Hall, NJ, 1996.
21. R. G. Schmier, "Fade Durations in Satellite-Path Mobile Radio Propagation," M.S. Thesis of Virginia Tech, Dec. 1986.
22. W. T. Smith and W. L. Stutzman, "Statistical modeling for land mobile satellite communications," Virginia Tech Report EE Satcom 86-3, performed for JPL sponsored by NASA under contract 956512, Aug. 1986.

23. W. L. Stutzman, *Polarization in Electromagnetic Systems*, Artech, Boston, 1992.
24. W. J. Vogel and E. K. Smith, “Propagation Considerations in land-mobile satellite transmission,” MSAT-X Report No. 105, NASA-JPL, Pasadena, CA.
25. B. Vucetic and J. Du, “Channel Modeling and Simulation in Satellite Mobile Communication Systems,” IEEE Journal of Selected Areas in Communications, vol. 10, no. 8, pp. 1209-1218, Oct. 1992.

Appendix A. Computer Programs

All programs are coded using MATLAB ver 4.2c.

Contents of programs

1. sim_ray.m (A program for generation of Rayleigh data set)
2. unsh_run.m (A program for generation of Rician data set)
3. sim_log.m (A program for generation of lognormal data set)
4. shad_run.m (A program for generation of shadowed data set)
5. tot_gen.m (A program for generation of total data set)
6. cdf_run.m (A program for calculation of CFD statistics)
7. pdf_run.m (A program for calculation of magnitude PDF statistics)
8. pdf_phs.m (A program for calculation of phase PDF statistics)
9. afd_run.m (A program for calculation of AFD and LCR statistics)
10. run.m (A program for simulating those programs from 1 to 9)
11. channelf.m (A program for numerical calculation of analytic model, LMSSMOD)
12. rici_ph.m (A program for calculation of analytic Rician phase distribution)
13. cha_run.m (A program for comparing the analytic model and the simulation result)
14. exp_run.m (A program for calculating statistics of the experimental data)
15. pro_run2.m (A program for running Graphic User Interface (GUI))
16. prog_run.m (A program for running GUI)
17. prosim.m (A program for running PROSIM using GUI)

1. sim_ray.m

```
%sim_ray.m
%A program for generation of Rayleigh data set

function [R_ray,Kbar,r_ray,P_ray,r_ray_ph,P_ray_ph]= sim_ray(sample,Kbar_expr,fd)

%     Sample is N by M matrix. N represents number of independent random variable and
%     M represents number of sample in the variable
%     Kbar_expr is carrier to multipath ratio in dB.
%     fd is used to determine the interval of sorted signal level

%     Written by Seong-Youp Suh
%     Jan.8. 1998


%Simulation for Rayleigh
alpha_expr=10^(-Kbar_expr/10); %Converting Kbar to natural scale
K_ray=sqrt(alpha_expr/sample(1)); %Getting Multiplier to get desired variance
A=K_ray*randn(sample); %Generation of NxM randomly distributed magnitude using
scaler
PI=rand(sample)*2*pi; %Generation of NxM Uniformly Distributed phase

R_ray=sum(A.*exp(j*PI)); %Phasor sum in complex form
R_env_ray=abs(R_ray); %Getting magnitude of Rayleigh data
theta_ray=angle(R_ray); % Getting phase of Rayleigh data

alpha_ray=mean(R_env_ray.^2); %Calculation of mean squared signal in natural form
Kbar=10*log10(1/alpha_ray); %Calculation of Kbar in dB using simulated data set

%Magnitude
r_rays=sort(R_env_ray); %Soting the signal
r_ray_dB=20*log10(r_rays); %Converting to dB scale
R_entry=[min(r_rays):fd:max(r_rays)+fd];
R_entrydB=20*log10(R_entry);

%PDF
[r_ray,P_ray]=pdf_run(R_env_ray,fd); %Getting magnitude PDF
[r_ray_ph,P_ray_ph]=pdf_phs(theta_ray,fd); %Getting phase PDF
```

2. unsh_run.m

```
%unsh_run.m
%A program for generation of Rician data set

function [R_rice,K_rice,r_rice,P_unshd,r_rice_ph,P_rice_ph]=
        unsh_run(sample,C,K_exprc,fd)

%   Sample is N by M matrix. N represents number of
%   independent random variable and M represents number
%   of sample in the variable
%   C is amplitude of LOS signal.
%   Kbar_expr is carrier to multipath ratio in dB.
%   fd is used to determine the interval of sorted signal level

%   Written by Seong-Youp Suh
%   Jan.8. 1998

alpha_expr=C^2*10^(-K_exprc/10); %Converting K to natural scale
K=sqrt(alpha_expr/sample(1)); %Getting Multiplier to get desired variance
A=K*randn(sample); %Generation of NxM randomly distributed magnitude using scaler
PI=rand(sample)*2*pi;%Generation of NxM Uniformly Distributed phase
[a,b]=size(A);
R=sum(A.*exp(j*PI)); %Phasor sum in complex form
R_rice=C+R;% Summing the LOS signal and Rayligh signal in complex form
R_ray=abs(R);%Getting magnitude of Rayleigh data
R_env_rice=abs(R_rice); % Getting magnitude of Rician data
theta_rice=angle(R_rice); % Getting phase of Rayleigh data

alpha_rice=mean(R_ray.^2); %Calculation of mean squared signal in natural form
K_rice=10*log10(C^2/alpha_rice);%Calculation of K in dB using simulated data set

%Magnitude
r_rices=sort(R_env_rice); %Soting the signal
r_rice_dB=20*log10(r_rices); %Converting to dB scale
R_entry=[min(r_rices):fd:max(r_rices)+fd];
R_entrydB=20*log10(R_entry);

%PDF

[r_rice,P_unshd]=pdf_run(R_env_rice,fd); %Getting magnitude PDF
[r_rice_ph,P_rice_ph]=pdf_phs(theta_rice,fd); %Getting phase PDF
```

3. sim_log.m

```
%sim_log.m
%A program for generation of lognormal data set

function [R_log,u2_dB,std2_dB,r_log,P_log,r_log_ph,P_log_ph]=
          sim_log(sample,u_dBl,std_dBl,fd)

%     Sample is N by M matrix. N represents number of independent random variable and
%     M represents number of sample in the variable.
%     u_dBl and std_dBl are mean and stadard deviation in dB.
%     fd is used to determine the interval of sorted signal level

%     Written by Seong-Youp Suh
%     Jan.8. 1998

u_natl=u_dBl/20/log10(exp(1)); %Converting the input lognormal mean and standard
                                %deviation in dB to natural scale
std_natl=std_dBl/20/log10(exp(1));
var_natl=std_natl^2;

A_log=randn(sample); %Generating of random variable
PI_log=rand(sample)*2*pi; %Generating the UDP phase distribution

for i=1:sample(1) %Loop for getting the indepedent positive variable
   A_min_log(i)=abs(min(A_log(i,:)));
   A_log(i,:)=A_log(i,:)+1.001*A_min_log(i);
   A_var_log(i)=std(A_log(i,:)).^2;
   A_log(i,:)=A_log(i,:)/A_var_log(i);
end

A_ln=log(A_log); %Converting to natural log random variable

k=[1:100];

for h=1:sample(1)
  for i=1:length(k) %Getting the relations between the variance and multiplier k
    var_k(h,i)=std(A_ln(h,:)*k(i)).^2;
  end
c(h)=var_k(h,length(k))/length(k)^2; %Desired Var=c*k^2
end

K=sqrt(var_natl/sample(1)./c); %Getting Multiplier corresponding to desired variance
```

```
for m=1:sample(1) %Calculating each random variable to get proper variance
   A_old_a(m,:)=A_ln(m,:)*K(m);
   ui_old(m)=mean(A_old_a(m,:));
   A_old(m,:)=A_old_a(m,:)-ui_old(m)+u_natl/sample(1);
   vari_old(m)=std(A_old(m,:)).^2;
   ui_old_n(m)=mean(A_old(m,:));
end

u_sum_n=sum(ui_old_n); %Summing each mean value = total mean value
var_sum=sum(vari_old); %Summing each variance = total variance

R_log_old=sum(A_old+j*PI_log); %Summing the magnitude and phasor based on the
                               % lognormal phasor plot and its mathematical relationship
R_log=exp(R_log_old); %Convert to natural scale
R_env_log=abs(R_log); %Getting magnitude
theta_log=angle(R_log); %Getting phase

%Computation of mean and variance of simulated data
u2=mean(log(R_env_log));
u2_dB=20*log10(exp(1))*u2;
R_env_ln=log(R_env_log);
std2=std(R_env_ln);
std2_dB=20*log10(exp(1))*std2;

r_logs=sort(R_env_log);%Sorting the signal
r_log_dB=20*log10(exp(1))*log(r_logs);
R_entry=[min(r_logs):fd:max(r_logs)+fd];
R_entrydB=20*log10(exp(1))*log(R_entry);

%PDF
[r_log,P_log]=pdf_run(R_env_log,fd);%Getting magnitude PDF
[r_log_ph,P_log_ph]=pdf_phs(theta_log,fd); %Getting phase PDF
```

4. shad_run.m

```
%shad_run.m
%A program for generation of shadowed data set

function [R_shad_sim,res_sim,r_sim,P_shad_sim,r_shad_ph,P_shad_ph]=
        shad_run(sample,Kbar_expr,u_dBl,std_dBl,fd)

%   Sample is N by M matrix. N represents number of
%   independent random variable and M represents number
%   of sample in the variable
%   Kbar_expr is carrier to multipath ratio in dB.
%   u_dBl and std_dBl are mean and stadard deviation in dB.
%   fd is used to determine the interval of sorted signal level

%   Written by Seong-Youp Suh
%   Jan.8. 1998

%Getting lognormal data set
[R_log,u2_dB,std2_dB,r_log,P_log]=sim_log(sample,u_dBl,std_dBl,fd);

%Getting Rayleigh data set
[R_ray,Kbar,r_ray,P_ray]=sim_ray(sample,Kbar_expr,fd);

alpha_ray=10^(-Kbar_expr/10);
res_sim=[Kbar,u2_dB,std2_dB];

%Simulation of Shadowed Signal
R_shad_sim=R_log+R_ray;  %Adding lognormal and Rayleigh data set
R_shad_sim_env=abs(R_shad_sim);  %Envelope
theta_shad=angle(R_shad_sim);%Phase
r_sims=sort(R_shad_sim_env);
r_sim_dB=20*log10(r_sims);

R_entry=[min(r_sims):fd:max(r_sims)+fd];
R_entrydB=20*log10(R_entry);

%PDF
[r_sim,P_shad_sim]=pdf_run(R_shad_sim_env,fd); %Getting magnitude PDF
[r_shad_ph,P_shad_ph]=pdf_phs(theta_shad,fd); %Getting phase PDF
```

5. tot_gen.m

```
%tot_gen.m
%A program for generation of total(Shadow+Unshadow) data set

function [R_tot,R_entrydB]=tot_gen(S,R_rice,R_shad_sim,sample,fd_cdf)

%     S is percentage of shadowing.
%     R_rice is an Unshadowed data set in complex form.
%     R_shad_sim is a Shadowed data set in complex form.
%     Sample is N by M matrix. N represents number of
%     independent random variable and M represents number
%     of sample in the variable.
%     fd_cdf is used to determine the interval of sorted signal level.

%     Written by Seong-Youp Suh
%     Jan.8. 1998

%Rounding the number of samples for input S
shapt=round(S*sample(2));
unshapt=round((1-S)*sample(2));

%Determining the number of samples for each data set (Unshadowed and Shadowed)
r_shadow=R_shad_sim(1:shapt);
r_unshadow=R_rice(1:unshapt);

R_tot=[r_shadow,r_unshadow]; %Concatenating each data set

R_tot_dB=20*log10(abs(R_tot));  %Converting the envelop of total data set to log scale

%Sorting the total signal with interval fd_cdf dB
R_entrydB=[min(R_tot_dB):fd_cdf:max(R_tot_dB)+fd_cdf];
```

6. cdf_run.m

```
%cdf_run.m
%A program for calculating Cumilative Fade Distribution

function [F,CDF]=cdf_run(R_tot_dB,R_entrydB)

%      R_tot_dB is envelop of total data set in dB
%      R_entrydB is sorted total sigal with interval fd_cdf dB

%     Written by Seong-Youp Suh
%     Jan.8. 1998

index=0;

for m=1:length(R_entrydB)

   index=index+1;

   occur=length(find(R_tot_dB<R_entrydB(m)));

   CDF(index)=occur/length(R_tot_dB)*100;

   F(index)=-R_entrydB(m);

end
```

7. pdf_run.m

```
%pdf_run.m
%A program for calculating magnitude Probability Density Function

function [R_envl,PDF]=pdf_run(r_env,fd)

%     r_env is envelope of signal.
%     fd is interval of signal envelope. It determines the resolution of PDF.

%     Written by Seong-Youp Suh
%     Jan.8. 1998


%PDF

index=0;

r_sort=sort(r_env);
r_entry=[min(r_sort):fd:max(r_sort)+fd];

%Calculating CFD

for m=1:length(r_entry)

   index=index+1;

   occur=length(find(r_env<r_entry(m)));

   CDF(index)=occur/length(r_env)*100;

end

%Derivating the CDF in order to get PDF

for n=1:length(CDF)-1

   PDF(n)=(CDF(n+1)-CDF(n))/(r_entry(n+1)-r_entry(n))/100;

end

R_envl=r_entry(2:length(r_entry));
```

8. pdf_phs.m

```
%pdf_phs.m
%A program for calculating phase Probability Density Function

function [theta_entry,PDF]=pdf_phs(theta,fd)

%     theta is phase of signal in radians.
%     fd is interval of signal phase. It determines the resolution of PDF.

%     Written by Seong-Youp Suh
%     Jan.8. 1998


%phase PDF

index=0;

theta_sort=sort(theta);%finding minimum and maximum signal variation

theta_entry=[min(theta_sort):fd:max(theta_sort)+fd];

for m=1:length(theta_entry)

   index=index+1;

   occur=length(find(theta<theta_entry(m)));

   CDF(index)=occur/length(theta)*100;

   F(index)=theta_entry(m);

end

for n=1:length(CDF)-1

   PDF(n)=(CDF(n+1)-CDF(n))/(theta_entry(n+1)-theta_entry(n))/100;

end

theta_entry=theta_entry(2:length(theta_entry));
```

9. afd_run.m

```
%afd_run.m
%A program for calculating Average Fade Duration and Level Crossing Rate

function [F,AFD,LCR]=afd_run(R_tot_dB,R_entrydB,li,lf,freq,speed)

%     R_tot_dB is envelop of total data set in dB
%     R_entrydB is sorted total sigal with interval fd_cdf dB
%     li is interval of position in meter.
%     lf is the final position traveled in meter.
%     freq is operating frequency in MHz.
%     speed is average vehicle speed in mile per hour.

%     Written by Seong-Youp Suh
%     Jan.8. 1998


index=0;
speed=speed*1.604*1000; %Convering the speed in mph to the one in m/hour
V=speed/3600; %Converting the speed in m/hour to one in m/sec
lambda=300/freq; %Calculating wavelength
N0=V/lambda; %Calculating maximum Doppler frequency

for m=1:length(R_entrydB)

   index=index+1;
   fade=find(R_tot_dB <= R_entrydB(m));  %finding index of faded signal

  for k=1:length(fade)-1;  %Evaluating of continuity

      decision(k)=fade(k+1)-fade(k);

   end

   N=length(find(decision~=1))+1;  %Getting number of faded interval
   LCR(index)=N/lf; % Calculating LCR
   occur=length(fade); % Getting number of faded signal in a signal level
   AFD(index)=li*occur/N; %Calculating AFD
   F(index)=-R_entrydB(m);

end
```

10. run.m

```
tic
%run.m
%A program for running whole program

%    Written by Seong-Youp Suh
%    Jan.8. 1998

disp('          ##########################################')
disp('          ###  Running Propagation Simulator  !!! ###')
disp('          ##########################################')

%Getting Input parameters
S=input('Percentage of Shadowing in % = ');
K_exp=input('K(Rice) in dB = ');
Kbar_expr=input('Kbar(Rayleigh) in dB = ');
u_dBl=input('Lognormal mean in dB= ');
std_dBl=input('Lognormal standard deviation in dB = ');
N=input('How many random variable do you want (5<N<15, recommend) = ');
M=input('How many sample do you want (10000<M<15000, recommend) = ');
fd_cdf=input('How many BIN size do you want (generally "1") = ');
freq=input('Input operating frequency in MHz = ');
speed=input('Input average vehicle speed in miles per hour = ');

S=S/100; %Scaling S in percentage to one in natural scale
sample=[N,M]; % Integrating the N and M in a variable, sample.


disp('          ##########################################')
disp('          ### Wait a moment, it is running now !!!###')
disp('          ##########################################')

alpha=10.^(-Kbar_expr/10);
C=1;
fd=0.1;

%Getting lognormal data set and its corresponding PDF
[R_log,u2_dB,std2_dB,r_log,P_log,r_log_ph,P_log_ph]=
                    sim_log(sample,u_dBl,std_dBl,fd);
%Getting Rayleigh data set and its corresponding PDF
[R_ray,K_bar,r_ray,P_ray,r_ray_ph,P_ray_ph]= sim_ray(sample,Kbar_expr,fd);
```

```
%Getting shadowed data set and its corresponding PDF
[R_shad_sim,res_sim,r_sim,P_shad_sim,r_shad_ph,P_shad_ph]=
                    shad_run(sample,Kbar_expr,u_dBl,std_dBl,fd);
%Getting unshadowed (Rician) data set and its corresponding PDF
[R_rice,K_rice,r_rice,P_unshd,r_rice_ph,P_rice_ph]= unsh_run(sample,C,K_exp,fd);

%Comparing the parameters from input and simulation result
disp('The parameters, [K, Kbar, u, sigma] of INPUT and SIMULATION are')
INPUT=[K_exp,Kbar_expr,u_dBl,std_dBl]
SIMULATION=[K_rice,res_sim]
comp=[INPUT;SIMULATION];

%Plotting
ti=0.001;
tf=ti*sample(2);
lambda=300/freq;
li=0.1*lambda;
lf=li*sample(2);
dist=[0:li:lf-li];
t=[0:ti:tf-ti];

%Getting total data set
[R_tot,R_entrydB]=tot_gen(S,R_rice,R_shad_sim,sample,fd_cdf);
R_tot_dB=20*log10(abs(R_tot));

%Claculating phase PDF of total data set
theta_tot=angle(R_tot);
[r_tot_ph,P_tot_ph]=pdf_phs(theta_tot,fd);

%Claculating CFD, AFD, and LCR of total data set
[F,CDF]=cdf_run(R_tot_dB,R_entrydB);
[F,AFD,LCR]=afd_run(R_tot_dB,R_entrydB,li,lf,freq,speed);

figure(2),clf
subplot(221),plot(dist,20*log10(exp(1))*log(abs(R_log)))
title('Lognormal data set')
ylabel('Signal level (R), dB')
axis([0,lf,-50,10])

subplot(222),plot(r_log,P_log)
title('Lognormal PDF')
ylabel('PDF (p(r))')
```

```
subplot(223),plot(dist,20*log10(abs(R_ray)))
title('Rayleigh data set')
xlabel('Position, meter')
ylabel('Signal level (R), dB')
axis([0,lf,-50,10])

subplot(224),plot(r_ray,P_ray)
title('Rayleigh PDF')
xlabel('Signal Amplitude (r)')
ylabel('PDF (p(r))')

figure(3),clf
subplot(221),plot(dist,20*log10(abs(R_rice)))
title('Unshadowed data set')
ylabel('Signal level (R), dB')
axis([0,lf,-50,10])

subplot(222),plot(r_rice,P_unshd)
title('Unshadowed PDF')
ylabel('PDF (p(r))')

subplot(223),plot(dist,20*log10(abs(R_shad_sim)))
title('Shadowed data set')
xlabel('Position, meter')
ylabel('Signal level (R), dB')
axis([0,lf,-50,10])

subplot(224),plot(r_sim,P_shad_sim)
title('Shadowed PDF')
xlabel('Signal Amplitude (r)')
ylabel('PDF (p(r))')

figure(4)
subplot(221),plot(dist,R_tot_dB)
title('Total Signal')
xlabel('Position, meter')
ylabel('Signal level (R), dB')
axis([0,lf,-50,10])

subplot(222),semilogy(F,CDF)
title('CFD')
xlabel('Fade level (F), dB')
ylabel('%Time fade >abscissa')
axis([-5,20,0.1,100])
```

```
subplot(223),semilogy(F,AFD)
title('AFD')
xlabel('Fade level (F), dB')
ylabel('Normalized AFD')
axis([-10,40,0.01,100])

subplot(224),semilogy(F,LCR)
title('LCR')
xlabel('Fade level (F), dB')
ylabel('Normalized LCR')
axis([-10,40,1e-4,10])

figure(5)
plot(r_tot_ph,P_tot_ph,'w:')
title('A phase PDF for total data set')
xlabel('Phase, radians')
ylabel('Phase PDF')
axis([-1.1*pi 1.1*pi 0 2])

toc
```

11. channelf.m

```
%channelf.m
%A program, LMSSMOD for calculating Analytical Model

function [F_ana,CDF_ana,r,Q_log,Q_ray,Q_rice,Q_shad,Q_tot]= channelf(Kbar,K,u,a,S)

%     Kbar is Rayleigh carrier-to-multipath power ratio in dB
%     K is Rician carrier-to-multipath power ratio in dB
%     u is lognormal mean in dB
%     a is lognormal standard deviation in dB
%     S is pecentage of shadowing in %

%     Written by Seong-Youp Suh
%     Jan.8. 1998

%Parameter
r=[0.001:0.01:5]; %Signal level in natural scale
R=length(r); %Length of signal to be calculated
alpha=10.^(-Kbar/10); %Rayleigh Mean square value
C=1; %LOS signal
beta=10.^(-K/10); %Rician Mean square value
%Converting the lognormal mean and standard deviation in dB to natural scale
Log_mean=u/20/log10(exp(1));
Log_stad=a/20/log10(exp(1));

%Calculating Probability Density Distribution (PDF)

Q_ray=2*r/alpha.*exp(-r.^2/alpha);%Rayleigh PDF

%Lognormal PDF
Q_log=20*log10(exp(1))*exp(-(20*log10(r)-u).^2/(2*a^2))./(sqrt(2*pi)*a*r);

%Unshadowed(Rician) PDF
theta_R=[0:0.01:2*pi];
Ini=2*r*C/beta;
Q_rice=log(2*r/beta)-(r.^2+C^2)/beta+Ini-log((2*pi*Ini).^.5);
Q_rice=exp(Q_rice);

%Shadowed PDF
z=[0:0.01:10]+1e-10;
for k=1:R
  Ini_z=2*r(k)*z/alpha;
```

```
  Q_shad_1(k)=8.686*2*r(k)/(sqrt(2*pi)*alpha*a);
  Q_shad_2(k,:)=log(1./z)+Ini_z-log(sqrt(2*pi*Ini_z))+(-(20*log10(z)-u).^2./(2*a^2)-
                    (r(k)^2+z.^2)/alpha);
  Q_shad_3(k)=trapz(z,exp(Q_shad_2(k,:)));
  Q_shad(k)=Q_shad_1(k).*Q_shad_3(k);
end

%Calculating CFD
for i=2:R
  G_unshad(i-1)=1-trapz(r(1:i),Q_rice(1:i));
  G_shad(i-1)=1-trapz(r(1:i),Q_shad(1:i));
end

G_tot=G_shad*S+G_unshad*(1-S);
CDF=1-G_tot;

for k=1:R-2
   Q_tot(k)=(CDF(k+1)-CDF(k))/(r(k+1)-r(k));
end
Q_tot=[Q_tot,Q_tot(k),Q_tot(k)];

F_ana=-20*log10(r(1:R-1));
CDF_ana=CDF*100;
```

12. rici_ph.m

```
%rici_ph.m
%A program for calculating analytical phase PDF for Unshadowed(Rician) Channel

function [ph_rice_ana,theta]=rici_ph(C,K)

%     C is amplitude of LOS signal.
%     K is Rician carrier to multipath ratio in dB.

%     Written by Seong-Youp Suh
%     March. 1. 1998

beta=10^(-K/10);

theta=[-pi:0.01:pi-0.01];

G=C*cos(theta)/sqrt(beta);

ph_rice_ana=1/2/pi*exp(-C^2/beta)*(1+G.*sqrt(pi).*exp(G.^2).*(1+erf(G)));
```

13. cha_run.m

```
tic
%cha_run.m
%A program for comparing the analytical model and the simulation result

%    Written by Seong-Youp Suh
%    Jan.8. 1998

clear

disp('          ##########################################')
disp('          ### Comparing with Analytic Solution !!!###')
disp('          ##########################################')

%Getting Input parameters
S=input('Percentage of Shadowing in % = ');
K_exp=input('K(Rice) in dB = ');
Kbar_expr=input('Kbar(Rayleigh) in dB = ');
u_dBl=input('Lognormal mean in dB= ');
std_dBl=input('Lognormal standard deviation in dB = ');
N=input('How many random variable do you want (5<N<15, recommend) = ');
M=input('How many sample do you want (8000<M<15000, recommend) = ');
fd_cdf=input('How many BIN size do you want (generally "1") = ');
freq=input('Input operating frequency in MHz = ');
speed=input('Input average vehicle speed in miles per hour = ');

S=S/100; %Scaling S in percentage to one in natural scale
sample=[N,M]; % Integrating the N and M in a variable, sample.

disp('          ##########################################')
disp('          ### Wait a moment, it is running now !!!###')
disp('          ##########################################')

alpha=10.^(-Kbar_expr/10);
C=1;

fd=0.1;
%Getting lognormal data set and its corresponding PDF
[R_log,u2_dB,std2_dB,r_log,P_log,r_log_ph,P_log_ph]=
                                    sim_log(sample,u_dBl,std_dBl,fd);
%Getting Rayleigh data set and its corresponding PDF
[R_ray,K_bar,r_ray,P_ray,r_ray_ph,P_ray_ph]= sim_ray(sample,Kbar_expr,fd);
```

```
%Getting shadowed data set and its corresponding PDF
[R_shad_sim,res_sim,r_sim,P_shad_sim,r_shad_ph,P_shad_ph]=
                                    shad_run(sample,Kbar_expr,u_dBl,std_dBl,fd);
%Getting unshadowed (Rician) data set and its corresponding PDF
[R_rice,K_rice,r_rice,P_unshd,r_rice_ph,P_rice_ph]= unsh_run(sample,C,K_exp,fd);

%Comparing the parameters from input and simulation result
disp('The parameters, [K, Kbar, u, sigma] of INPUT and SIMULATION are')
INPUT=[K_exp,Kbar_expr,u_dBl,std_dBl]
SIMULATION=[K_rice,res_sim]
comp=[INPUT;SIMULATION];

%Plotting
ti=0.001;
tf=ti*sample(2);
lambda=300/freq;
li=0.1*lambda;
lf=li*sample(2);
dist=[0:li:lf-li];
t=[0:ti:tf-ti];

%Claculating phase PDF of total data set
theta_tot=angle(R_tot);
[r_tot_ph,P_tot_ph]=pdf_phs(theta_tot,fd);

%Calculating CFD and PDF of Analytical Model
[F_ana,CDF_ana,r_ana,Q_log,Q_ray,Q_rice,Q_shad,Q_tot]=
                                    channelf(Kbar_expr,K_exp,u_dBl,std_dBl,S);
[ph_rice_ana,theta]=rici_ph(C,K_exp); %Calculating analytical Rician Phase PDF

%Getting total data set
[R_tot,R_entrydB]=tot_gen(S,R_rice,R_shad_sim,sample,fd_cdf);
R_tot_dB=20*log10(abs(R_tot));

%Claculating CFD, AFD, and LCR of total data set
[F,CDF]=cdf_run(R_tot_dB,R_entrydB);
[F,AFD,LCR]=afd_run(R_tot_dB,R_entrydB,li,lf,freq,speed);

%Generating Uniformly Phase Distribution
r_ana_ph=[-pi:0.1:pi];
pr_ana=1/2/pi*ones(1,length(r_ana_ph));
```

```
figure(2),clf
subplot(221),plot(dist,20*log10(exp(1))*log(abs(R_log)))
title('Lognormal data set')
ylabel('Signal level (R), dB')
axis([0,lf,-50,10])

subplot(222),plot(r_log,P_log,r_ana,Q_log,'r')
title('Lognormal PDF')
ylabel('PDF (p(r))')
legend('Simulation','Analytic')

subplot(223),plot(dist(1:1000),20*log10(abs(R_ray(1:1000))),'w')
title('Rayleigh data set')
xlabel('Position, meter')
ylabel('Signal level (R), dB')
axis([0,lf,-50,10])

subplot(224),plot(r_ray,P_ray,'w:',r_ana,Q_ray,'w')
title('Rayleigh PDF')
xlabel('Signal Amplitude (r)')
ylabel('PDF (p(r))')
legend('Simulation','Analytic')

figure(3),clf
subplot(221),plot(dist,20*log10(abs(R_rice)))
title('Unshadowed data set')
ylabel('Signal level (R), dB')
axis([0,lf,-50,10])

subplot(222),plot(r_rice,P_unshd,r_ana,Q_rice,'r')
title('Unshadowed PDF')
ylabel('PDF (p(r))')
legend('Simulation','Analytic')

subplot(223),plot(dist,20*log10(abs(R_shad_sim)))
title('Shadowed data set')
xlabel('Position, meter')
ylabel('Signal level (R), dB')
axis([0,lf,-50,10])
```

```
subplot(224),plot(r_sim,P_shad_sim,r_ana,Q_shad,'r')
title('Shadowed PDF')
xlabel('Signal Amplitude (r)')
ylabel('PDF (p(r))')
legend('Simulation','Analytic')

figure(4),clf
subplot(221),plot(dist,R_tot_dB)
title('Total Signal')
xlabel('Position, meter')
ylabel('Signal level (R), dB')
axis([0,lf,-50,10])

subplot(222),semilogy(F_ana,CDF_ana,F,CDF,'ro')
title('CFD')
xlabel('Fade level (F), dB')
ylabel('%Time fade >abscissa')
axis([-5,20,0.1,100])

subplot(223),semilogy(F,AFD)
title('AFD')
xlabel('Fade level (F), dB')
ylabel('Normalized AFD')
axis([-10,40,0.01,100])

subplot(224),semilogy(F,LCR)
title('LCR')
xlabel('Fade level (F), dB')
ylabel('Normalized LCR')
axis([-10,40,1e-4,10])

figure(5),clf
subplot(221),plot(r_log_ph,P_log_ph,':',r_ana_ph,pr_ana)
title('Lognormal phase PDF')
xlabel('Phase, radians')
ylabel('PDF')
axis([-1.1*pi 1.1*pi 0 0.5])
legend('Simulation','Analytic')
```

```
subplot(222),plot(r_ray_ph,P_ray_ph,':',r_ana_ph,pr_ana)
title('Rayleigh phase PDF')
xlabel('Phase, radians')
ylabel('PDF')
axis([-1.1*pi 1.1*pi 0 0.5])
legend('Simulation','Analytic')

subplot(223),plot(r_rice_ph,P_rice_ph,':',theta,ph_rice_ana)
title('Unshadowed phase PDF')
xlabel('Phase, radians')
ylabel('PDF')
axis([-1.1*pi 1.1*pi -1 8])
legend('Simulation','Analytic')

subplot(224),plot(r_tot_ph,P_tot_ph,'w:')
title('A phase PDF for total data set')
xlabel('Phase, radians')
ylabel('Phase PDF')
axis([-1.1*pi 1.1*pi 0 2])

toc
```

14. exp_run.m

```
tic
%exp_run.m
%A program for calculating statistics of Experimental data

%     Written by Seong-Youp Suh
%     Jan.8. 1998

clear

fd=0.1;

%Selecting experimental data
disp('1 = BA181556 MEASUREMENT DATA')
disp('2 = BA181924 MEASUREMENT DATA')
disp('3 = BA184844 MEASUREMENT DATA')
disp('4 = BA185029 MEASUREMENT DATA')
disp('5 = BA181412 MEASUREMENT DATA')
disp('6 = BA181740 MEASUREMENT DATA')
disp('7 = BA184508 MEASUREMENT DATA')

n=input('Select an index number = ');
fd_cdf=input('Input BIN size you want (generally "1") = ');
freq=input('Input operating frequency in MHz = ');
speed=input('Input average vehicle speed in miles per hour = ');

file=['e:\lmss\output\ba' int2str(n)];
file_name=[file '.tim'];

%In case wrong input number
if ~exist(file_name)
   disp('There is no file you selected')
   disp(' ')
   disp('Please try again')
   break
end

%File open and read the data
fid_tim=fopen(file_name,'r');
[A_exp, countr1]=fscanf(fid_tim,'%f');
fid_tim=fopen(file_name,'r');
[A_exp, countr2]=fscanf(fid_tim,'%f',[4,countr1/2]);
```

```
A_exp=A_exp(1,:)+A_exp(2,:)*j; %Converting the imported data to complex form
A_env_exp=abs(A_exp); %Envelop of the data
A_phase_exp=angle(A_exp); %Phase of the data

R_tot=A_env_exp;
R_tot_dB=20*log10(R_tot);
R_entry=[min(R_tot):fd:max(R_tot)+fd];
R_entrydB=[min(R_tot_dB):fd_cdf:max(R_tot_dB)+fd_cdf];

%basic parameters
ti=0.001;
tf=ti*countr2/4;
lambda=300/freq;
li=0.1*lambda;
lf=li*length(R_tot_dB);
dist=[0:li:lf-li];
t=[0:ti:tf-ti];

%Calculating Statistics including PDF, CFD, AFD, LCR and phase PDF
[R,PDF]=pdf_run(R_tot,fd);
[F,CDF]=cdf_run(R_tot_dB,R_entrydB);
[F,AFD,LCR]=afd_run(R_tot_dB,R_entrydB,li,lf,freq,speed);
[theta,PDF_ph]=pdf_phs(A_phase_exp,fd);

%Plotting

figure(1),clf
subplot(221),plot(dist,R_tot_dB)
title('Experimental data set')
xlabel('Position, meter')
ylabel('Signal level (R), dB')
axis([0,max(dist),0.9*min(R_tot_dB),1.1*max(R_tot_dB)])

subplot(222),semilogy(F,CDF)
title('CFD')
xlabel('Fade level (F), dB')
ylabel('%Time fade >abscissa')
axis([-5,20,0.1,100])
```

```
subplot(223),semilogy(F,AFD)
title('AFD')
xlabel('Fade level (F), dB')
ylabel('Normalized AFD')
axis([-10,40,0.01,100])

subplot(224),semilogy(F,LCR)
title('LCR')
xlabel('Fade level (F), dB')
ylabel('Normalized LCR')
axis([-10,40,1e-4,10])

figure(2)
plot(theta,PDF_ph)
title('A measured phase PDF')
xlabel('Phase, radians')
ylabel('PDF')
axis([-1.1*pi 1.1*pi -0.1 3])

toc
```

15. pro_run2.m

```
%pro_run2.m
%A program for running ba*_demo in Graphic User Interface
%(*=1,2,3,4,5,6,7)

%     Written by Seong-Youp Suh
%     Jan.8. 1998

function pro_run2(program)

global BA181556
global BA181924
global BA184844
global BA185029
global BA181412
global BA181740
global BA184508

if (program==BA181556)

     ba1_demo
elseif (program==BA181924)
     ba2_demo
elseif (program==BA184844)
     ba3_demo
elseif (program==BA185029)
     ba4_demo
elseif (program==BA181412)
     ba5_demo
elseif (program==BA181740)
     ba6_demo
elseif (program==BA184508)
     ba7_demo

end
```

16. prog_run.m

```
%prog_run.m
%A program for running ba*_demo and cha_run in Graphic User Interface
%(*=1,2,3,4,5,6,7)

%     Written by Seong-Youp Suh
%     Jan.8. 1998


function prog_run(program)

global ANALYTIC
global SIMPLE
global BA181556
global BA181924
global BA184844
global BA185029
global BA181412
global BA181740
global BA184508

if (program==ANALYTIC)

     cha_run
elseif (program==SIMPLE)
     sim_run
elseif (program==BA181556)
     ba1_demo
elseif (program==BA181924)
     ba2_demo
elseif (program==BA184844)
     ba3_demo
elseif (program==BA185029)
     ba4_demo
elseif (program==BA181412)
     ba5_demo
elseif (program==BA181740)
     ba6_demo
elseif (program==BA184508)
     ba7_demo

end
```

17. prosim.m

```
%prosim.m
%A program for running Propagation Simulator, PROSIM in GUI

%====================================
% Handle INITIALIZATION
%====================================

   % Make sure the window is big enough
   figurePos=[320,35,450,280];
   figNumber=figure( ...
      'Name','Welcome to LMSS Propagation Simulator ver.1.0!', ...
      'NumberTitle','off', ...
      'Visible','on', ...
      'Resize','off', ...
      'Colormap',[], ...
      'Position',figurePos);
   set(gca,'Position',[0 0 1 1]);

   axis off;

%====================================
% SIMULATOR Menu
%====================================

h=uicontrol(gcf,...
      'Style','push',...
      'String','SIMULATION',...
      'Position',[50,100,100,100],...
      'Callback','run');

%====================================
% COMPARING WITH ANALYTIC SOLUTION Menu
%====================================

global ANALYTIC ; ANALYTIC=1;
global SIMPLE  ; SIMPLE=2;
global program1
global popupprog1

h=uicontrol(gcf,...
      'Style','push',...
      'String','COMPARING DATA',...
```

```
    'Position',[210,200,200,30],...
    'Callback','disp(" ");');

popupprog1=uicontrol(gcf,...
    'Style','popup',...
    'String','ANALYTIC SOLUTION|SIMPLE  MODEL',...
    'Position',[210, 180, 200,30],...
    'Callback',['program1=[ANALYTIC,SIMPLE];',...
    'pro_run1(program1(get(popupprog1,"Value")));']);

%=======================================
% EXPERIMENTAL DATA Menu
%=======================================

global BA181556 ; BA181556=1;
global BA181924 ; BA181924=2;
global BA184844 ; BA184844=3;
global BA185029 ; BA185029=4;
global BA181412 ; BA181412=5;
global BA181740 ; BA181740=6;
global BA184508 ; BA184508=7;

global program2
global popupprog2

h=uicontrol(gcf,...
    'Style','push',...
    'String','MEASUREMENT DATA',...
    'Position',[210,100,200,30],...
    'Callback','disp(" ");');

popupprog2=uicontrol(gcf,...
    'Style','popup',...
    'String','BA181556|BA181924|BA184844|BA185029|BA181412|BA181740| BA1845
08',...
    'Position',[210, 80, 200,30],...
    'Callback',['program2=[BA181556,BA181924,BA184844,BA185029,BA181412,BA
181740,BA184508];',...
    'pro_run2(program2(get(popupprog2,"Value")));']);
```

Vita

Seong-Youp Suh

Seong-Youp Suh was born in Chonbuk, Korea on February 17, 1968. He received the B.E. degree from the Chonbuk National University, Korea, in 1990. From 1990 to 1996 he was employed as a researcher for Agency for Defense Development in Daejeon, Korea. In August, 1996, he joined with the Virginia Tech Satellite Communications Group. His research interests are radio wave propagation, channel modeling and simulation, antenna design, and satellite communications.